APPLICATION OF FULL FACTORIAL DESIGN TO CONTROL THE SIZE OF BISPHENOL A MOLECULAR IMPRINTED POLYMER

NURUL SHAREENA AQMAR BINTI MOHD SHARIF

MASTER OF ENGINEERING（CHEMICAL）

UNIVERSITI MALAYSIA PAHANG

APPLICATION OF FULL FACTORIAL DESIGN TO CONTROL THE SIZE OF BISPHENOL A MOLECULAR IMPRINTED POLYMER

NURUL SHAREENA AQMAR BINTI MOHD SHARIF

Thesis submitted in fulfillment of the requirements

for the award of the degree of

Master of Engineering (Chemical)

Faculty of Chemical and Natural Resources Engineering

UNIVERSITI MALAYSIA PAHANG

MAY 2013

THESIS CONFIDENTIAL STATUS

UNIVERSITI MALAYSIA PAHANG

DECLARATION OF THESIS AND COPYRIGHT

Author's full name : NURUL SHAREENA AQMAR BINTI MOHD SHARIF

Date of birth : 8 SEPTEMBER 1986

Title : APPLICATION OF FULL FACTORIAL DESIGN TO CONTROL THE SIZE OF BISPHENOL A MOLECULAR IMPRINTED POLYMER

Academic Session : SEMESTER 2 SESSION 2012/2013

I declare that this thesis is classified as :

☐ **CONFIDENTIAL** (Contains confidential information under the Official Secret Act 1972)*

☐ **RESTRICTED** (Contains restricted information as specified by the organization where research was done)*

☐ **OPEN ACCESS** I agree that my thesis to be published as online open access (Full text)

I acknowledge that Universiti Malaysia Pahang reserve the right as follows:

1. The thesis is the Property of Universiti Malaysia Pahang
2. The library of Universiti Malaysia Pahang has the right to make copies for the purpose of research only.
3. The library has the right to make copies of the thesis for academic exchange.

Certified By:

(Student's Signature)	(Signature of Supervisor)
860908-52-5844	Profesor Madya Dr. Che Ku Mohammad Faizal Bin Che Ku Yahya
Date: 25 July 2013	Date: 25 July 2013

NOTES :*If the thesis is CONFIDENTIAL or RESTRICTED, please attach with the letter from the organization with period and reasons for confidentiality or restriction

SUPERVISORS' DECLARATION

We hereby declare that we have checked this thesis and in our opinion, this thesis is adequate in terms of scope and quality for the award of the degree of Master of Engineering (Chemical).

Signature :

Name of Supervisor: PROFESOR MADYA DR. CHE KU MOHAMMAD FAIZAL BIN CHE KU YAHYA

Position: DEPUTY DEAN OF FACULTY OF CHEMICAL AND NATURAL RESOURCES ENGINEERING.

Date: 25 JULY 2013

Signature :

Name of Co-supervisor: DR. SYED MOHD SAUFI BIN TUAN CHIK

Position: SENIOR LECTURER OF FACULTY OF CHEMICAL AND NATURAL RESOURCES ENGINEERING.

Date: 25 JULY 2013

STUDENT'S DECLARATION

I hereby declare that the work in this thesis is my own except for the quotations and summaries which have been duly acknowledged. The thesis has not been accepted for any degree and is not concurrently submitted for the award of any other degree.

Signature :

Name : NURUL SHAREENA AQMAR BINTI MOHD SHARIF

ID Number : MKC 10006

Date : 25 JULY 2013

DEDICATION

Dedicated especially to:

My superb parents,
my wonderful siblings,
my incredible family,
my amazing fiancé,
and my fabulous friends,
for all your love and care for me.

Million thanks for everything.

ACKNOWLEDGEMENTS

In the name of Allah, the most gracious and merciful;

Praise and gratitude to Allah SWT, the Almighty, for with His willing that I successfully complete this research thesis and be granted a Master scroll.

First and foremost, I would like to extent my deepest thanks to my respected supervisors, Dr. Che Ku Mohammad Faizal and Dr. Syed Mohd Saufi for their relentless support, encouragement and guidance throughout my study since from the beginning of experiments until the end of thesis writing. Their constant support has helped so much in making this research an accomplishment.

The financial aid and grants provided from Kementerian Pengajian Tinggi and Universiti Malaysia Pahang in supporting this study is highly acknowledge. Furthermore, many thanks to all individual involved in assisting this research including professors, lecturers, colleagues and laboratory instructors of Chemical and Natural Resources Engineering Faculty. The knowledge and experience I gained along the process of completing this project would prove to be invaluable for the better to guide me in the challenges that lies ahead. Also, thank you to Centre of Graduate Studies department for their continual efforts in ensuring a smooth progress of this project.

And last but not least, to all my loving family members and devoted fiancé, I can never thank you enough for your everlasting love, sacrifice, patience, and prayers throughout the ups and downs during my study. I'm overwhelmed with gratitude for all your faith and support in me to achieve my dream. This thesis is simply impossible without you. Only Allah SWT can repay all your kindness.

ABSTRACT

Molecular imprinted polymer (MIP) has caught the attention of many researchers in recent years as a great tool for molecular recognition and other applications. However, the main issue in the synthesis of MIP nanoparticles is the identification and optimization of the main factors affecting the particle size. This study described two objectives; first, to control the particle size of MIP using an experimental design analysis, secondly to synthesize MIP nanoparticles with recognition of Bisphenol A (BPA). Sixteen sets of BPA-MIP particle with three center point replications were produced according to factor combination set by Design Expert Software. The analysis was aimed at the relationship of four selected parameters: the polymerisation temperature, agitation rate, solvent to crosslinker ratio, and percentage of initiator. Almost all obtained particle sizes were in the range of 90 to 160 nm, but the smallest size obtained was 30nm, and the largest size was 2 µm. Polymerization temperature was the most significant factor, followed by solvent to crosslinker ratio, agitation rate and percentage of initiator. Two-way interaction of polymerization temperature and solvent to crosslinker ratio was also found to be highly significant in affecting BPA-MIP. An acceptable value for R^2 presented from ANOVA analysis is 0.9770. The characterization studies also support a good rigidity and stable thermal properties of BPA-MIP particles. Resultant BPA-MIP copolymers had BPA binding capacity ranging from 77.74 to 102.26 µmol/g. The highest binding of BPA was MIP 15 at 100 nm particle size, with 102.26 µmol/g, while the lowest BPA binding of 77.74 µmol/g was achieved from MIP 16 with the same size. It can be concluded that the smaller the size of imprinted polymer, does not necessarily improved its binding ability. The selected optimum condition of BPA-MIP synthesis was MIP 15 due to its highest binding capacity, which was synthesized at 45 ^{o}C, no agitation, 50 % of solvent to crosslinker ratio and 1% of initiator. In overall, experimental design approach used in this study could, overcome tedious procedure involves in controlling the size of BPA-MIP within the nano size. Nano size BPA-MIP is required to produce high performance hybrid MIP membrane that can be easily handle and operate. This MIP technique can be further extended to any other template for different applications.

ABSTRAK

Sejak beberapa tahun kebelakangan ini, polimer molekul yang dicetak (MIP) telah menarik ramai perhatian pengkaji sebagai satu alat untuk pengenalpastian molekul dan untuk kegunaan lain. Walaubagaimanapun, isu utama dalam sintesis zarahnano MIP ialah pengenalpastian dan pengoptimuman faktor-faktor utama yang berkaitan saiz zarah. Kajian ini menjelaskan dua objektif ; pertama, mengawal saiz zarah MIP dengan menggunakan rekabentuk analisis ujikaji, kedua, sintesis zarahnano MIP yang dapat mengenalpasti Bisphenol A (BPA). 16 set zarah BPA-MIP dengan 3 titik pusat replikasi telah dihasilkan dengan menggunakan kombinasi faktor yang telah ditetapkan oleh Design Expert Software (DOE). Analisis ini memfokuskan kesinambungan antara 4 parameter yang dipilih: suhu pempolimeran, kadar pengadukan, nisbah pelarut kepada pemautsilang, dan peratus pemula. Hampir semua saiz zarah berada di antara 90 – 160 nm, tetapi saiz zarah paling kecil ialah pada 30 nm, dan paling besar pada 2 µm. Suhu pempolimeran merupakan faktor yang paling penting, diikuti oleh nisbah pelarut kepada pemautsilang, kadar pengadukan dan peratus pemula. Interaksi antara 2 faktor iaitu suhu pempolimeran dan nisbah pelarut kepada pemautsilang didapati sangat penting dalam mempengaruhi BPA-MIP. Jumlah nilai R^2 bersamaan dengan 0.9770 yang diperolehi dari analisis ANOVA berada dalam jumlah yang diterima. Hasil dari kajian pencirian menunjukkan zarah BPA-MIP berada dalam ketegaran yang baik dan mempunyai ciri ketahanan haba yang baik. BPA-MIP polimer yang terhasil mempunyai kapasiti pengikatan BPA dari 77.74 hingga 102.26 µmol/g. Pengikatan BPA yang paling tinggi diperolehi oleh MIP 15 pada 100 nm saiz zarah, dengan 102.26 µmol/g, manakala yang paling rendah diperolehi oleh MIP16 pada saiz zarah yang sama. Kesimpulannya, saiz polimer yang dicetak tidak semestinya menambahbaik kebolehan ia untuk mengikat. Kondisi optimum yang dipilih untuk sintesis BPA-MIP ialah MIP 15 kerana mempunyai kebolehan mengikat yang terbaik, dimana ia disintesis pada 45^{o}C, tiada pengadukan, 50% nisbah pelarut kepada pemautsilang, dan 1% pemula. Hasil dari keseluruhannya, pendekatan reka bentuk ujikaji yang digunakan dalam kajian ini mampu mengatasi prosedur yang remeh dalam mengawal saiz BPA-MIP dalam saiz nano. BPA-MIP dalam saiz nano amat penting dalam penghasilan membran hibrid MIP yang berprestasi tinggi yang sangat mudah beroperasi serta digunakan. Teknik MIP boleh juga dikembangkan dalam pelbagai jenis acuan dalam pelbagai aplikasi.

TABLE OF CONTENTS

LIST OF TABLES

LIST OF FIGURES

LIST OF ABBREVIATIONS

ACN	Acetonitrile
AlBN	2,2,-Azobis(2-methylpropionitrile)
BADM	Bisphenol A Dimethacrylate
BET	Brunaer Emmet and Teller Method
BPA	Bisphenol A
DMAC	Dimethyl Acetamide
FTIR	Fourier Transform Infra Red
HMIP	Hybrid Molecular Imprinted Polymers
HPLC	High Performance Liquid Chromatography
MIP	Molecular Imprinted Polymer
MIM	Molecular Imprinted Membrane
NIP	Non-Imprinted Polymer
NMP	N-methyl-prryolidone
NaOH	Sodium Hydroxide
PES	Polyethersulfone
PSf	Polysulfone
SURFER	Surface Area Analyzer
SEM	Scanning Electron Microscope
TEM	Transmission Electron Microscope
TGA	Thermogravimetric Analyzer
THF	Tetrahydrofuran
TRIM	Trimethylolpropane Trimethacrylate

LIST OF NOMENCLATURES

µm	Micrometers
µM	Micromole
µmol	Micromol
^{o}C	Degree Celsius
%	Percentage
g	Gram
h	Hour
L	Liter
M	Mole
min	Minutes
ml	Milliliters
nm	Nanometers
pH	Potential Hydrogen
S	Binding capacity
WL	Weight loss
wt %	Weight per weight percent

CHAPTER 1

INTRODUCTION

1.1 INTRODUCTION

The evolution of mankind has brought extensive growth of technologies and facilities. Many more improvements are undergoing rapidly and keep expending incredibly in the purpose of assisting nowadays hectic lifestyle. In between these progressions, the use of chemicals have risen in order to meet increasing demand without realizing the exposure of chemicals little by little inducing toxicity build up in bodies of human and wildlife which consequently bring adverse health effects that includes obesity, diabetes, and even worse, cancer (Newbold and Liehr, 2000; Grande, 2008).

These diseases could be severe, acute, short-term and long-term effect that would result in less productivity of the lifestyle which leads to lack of responsibility, negativity, poor judgments, and so forth. Because of this, the campaign for greener technologies – using less chemicals, producing less toxic waste, are quite intense nowadays, promoting the best solution to save mankind and mother nature.

Aside from that, waste and water treatment industries team up to work out more effective clean-up technology in the effort to remove all the toxics left in the environment. Newly preferred removal technique is by using molecular imprinted polymers (MIP) technology. The MIP is presented as an effective adsorbent where it mimics specifically to the structure of the molecule to be removed and increasing the

removal efficiency (Ikegami et al., 2004; Piletsky et al, 2001; Faizal et al., 2008; Zhang et al., 2009). It was first successfully attempted by Wulff and coworkers in the late 80's (Wulff and Sarhan, 1972), where they prepared organic material that was able to recognize selectively towards a target molecule. Over time, researches showed much interest of the MIP and its flexibility is evidently where nowadays, the MIP based technique has been expanded in many field of applications such as chromatography (Castro Lopez et al., 2012), sensor (Zhang et al., 2008), drug delivery (Suedee et al., 2010), medicinal (Byun et al., 2010), and magnetic (Luo et al., 2011).

1.2 BACKGROUND OF STUDY

In this modernized era, more chemicals and compounds were released into environment everyday, which consequently it could interfere the normal functioning endocrine system in human bodies and wildlife creatures. This increasing number of chemical compounds is not metabolized, also known as the emerging contaminants. They are mainly discharged in water sources such as sewers, rivers and lakes, cause's risks of environmental hazard to all the livings. Endocrine disruptors compounds (EDC), such as estradiol, nonylphenol, bisphenol A, pharmaceuticals, and some pesticides that mostly present in food, water, and soil at concentrations of sub µg/L have become a crucial environmental problem (Zhang et al., 2006; Yoon et al., 2006). EDCs are active even at low concentrations and could disturb hormone activities (Zhao et al., 2004). This phenomenon has raised consciousness among consumers and researchers about the risks of toxic exposure and harm to human health and wildlife.

One of these EDCs, particularly Bisphenol A (BPA), is used extensively in industrial chemical, as an intermediate to manufacture epoxy, polycarbonate, polyester resins, and numerous plastic articles (Lyons, 2000; Zhang et al., 2006; Bing-zhi et al., 2009). BPA also present in various consumer products as the interior coatings of food cans, milk containers, and baby formula bottles, as well as in dental sealants. Although the toxicity of BPA towards humans is fairly low, but with having characteristic of highly water soluble, researches showed that it can easily eluted and leached out from our everyday used products (Lyons, 2000; Ikegami et al., 2004).

Several techniques have been used to remove the BPA contamination from breaching into living bodies since the past decades (Gunnet et al., 1987; Georgellis and Rydstrom, 1989). Coagulation/ flocculation were used by Khiari, (2007) and Vieno et al. (2006), but they concluded that the BPA cannot be removed entirely from water by coagulation alone. An advanced oxidative technique was used by Gunten et al. (2005) but at the same time it produces other harmful by-products. This byproduct could be removed by adsorptions which eventually increase the cost of BPA removal. Various types of membrane adsorbents such as microfiltration (MF), ultrafiltration (UF), nanofiltration (NF), and reverse osmosis (RO) were modified to construct adsorptive surface layer on the membrane in order to remove the BPA (Liu et al., 2009; Su-hua et al., 2010; Bing-zhi et al., 2009). However, these filtrations are not very selective and not able to recognize specific molecule of BPA. RO and NF have shown a significant performance for EDCs removal, but they required very high driving force to operate and not cost-effective (Bing-zhi et al., 2009; Liu et al., 2009).

In the current study, MIP based separation was used to remove BPA contamination in water (Ikegami et al., 2004; Piletsky et al., 2001; Faizal et al., 2008; Zhang et al., 2009). MIP particle show many advantages for contaminant removal such as stable at low or high pressure, pH, and temperature (<180 ^{o}C), relatively inexpensive, easier to obtain and can be synthesized for a wide range of substances (Poma et al., 2010). It is also proven that it has been a very useful alternative method to separate specific desired template recognition (Ikegami et al., 2004).

The molecular imprinting technique is used to develop adsorbents for removal of BPA due to its various applications and unique characteristics. However, imprinted polymers with highly selective and largely adsorbed abilities to such endocrine disruptor are yet to be improvised. The help of experimental design approach will narrow down the key factors that affect MIP preparation thus will allow the control of its fabrication, specifically on its particle sizes (Koohpaei et al., 2008). The aim of this study is to synthesize molecular imprinted polymers nanoparticles with specific recognition of bisphenol A and to control the MIP particle size with the application of full factorial design method.

1.3 PROBLEM STATEMENT

Bisphenol A (BPA) is one of known endocrine disruptor compound (EDC) that can affects the reproduction and development of human and animal body in the ppb concentration range. The ability of BPA to leach out from our daily used foods and drinks products has risen up concerns among all consumers, scientists and researchers. What's more upsetting is that the toxicity of BPA molecules is very discreet and the effects are mostly long-term. Therefore, it is very critical to efficiently remove BPA contamination from our water sources.

Conventional approach used to synthesize nano-size MIP mainly involves trial and error because of the monomer and chemical complexity used. The ability to control uniform particle size of MIP is still a challenge due to the different properties of monomers and chemicals utilized for specific MIP template and application. However with the assists of experimental design approach, a better understanding of each factors involve in preparing MIP particle could be realized.

The nanoparticle MIP would result in a powder form polymers. This limits its application because there are high possibility that it could be lost during handling, and restoring. Hence, the MIP is attempted to modify by hybridization with membrane scaffold to maximize its uses and making it more user-friendly.

The aim of this study is to synthesize MIP particles that show specific recognition of BPA within nano-size range using experimental design approach. With the advance and feasible MIP particles and by having the ability in controlling the fabrication to achieve high BPA recognition and enhancing its performance, will provide a straight forward, proper and time saving method in performing another successful removal technology, and of course, may help to position this technology to reach market confidence.

1.4 RESEARCH OBJECTIVES

The aim of this study is to synthesize nanoparticles BPA-MIP using multivariate analysis with selected factors. The objectives are:

i) To control MIP particle size using Full Factorial Design (FFD) method from the Design of Experimental (DOE) software.
ii) To synthesize MIP nanoparticles that recognizes Bisphenol A (BPA).
iii) To develop hybrid MIP nanoparticles membrane and its performance.

1.5 SCOPE OF STUDY

In order to achieve the stated objectives, the following scopes have been identified, consisting of three (3) phases:

Phase 1: Synthesis of MIP Nanoparticles

i) Synthesize BPA MIP particles using covalent polymerization method.
ii) Selection of cross-linker, functional monomer, suitable solvent and initiator.
iii) Determine major factors affecting MIP synthesis – polymerization temperature, agitation rate, solvent to cross-linker ratio and initiator percentage.
iv) Apply experimental design analysis to study effect of selected factors on particle size and its distribution.

Phase 2: Physical, Chemical and Characterizations Of MIP Particles

i) Physical and chemical characterizations – Fourier Transform Infra Red (FTIR), Scanning Electron Microscope (SEM), Transmission Electron Microscope (TEM), Optical Microscope, Mastersizer Particle Size Analyzer, Thermal Gravimetric Analyzer (TGA), Surface Area Analyzer (SURFER).
ii) Performance characterization – Template removal using UV-Visible Spectrophotometer (UV-Vis).

Phase 3: Performance Testing, Optimization and Modification

i) Studying the binding capacity of the MIPs.

ii) Validation – Comparison between predicted value by DOE and actual experimental value.

iii) Prepare hybrid MIP (HMIP) membrane using different scaffold polymer of polyethersulfone (PES) and polysulfone (PSf).

iv) Testing and determination of BPA binding capacity by HMIP membrane.

1.6 THESIS ORGANIZATION

In overall, this thesis consists of 5 chapters as followed. Chapter 1 is outline of the study of molecular imprinting in general. For chapter 2, will be describing the literature reviews of every scope covered in this study. Then, chapter 3 explains in detail the materials, methodology, experimental design analysis, and instrumentation used in preparing covalent imprinted polymer as well as the hybrid MIP membrane application. Chapter 4 will focus on the results which consist of discussing the experimental design analysis data thoroughly, MIP particles morphology, characterization, binding capacity, and performance of MIP and hybrid MIP membrane. Lastly, chapter 5 concludes this study and also consists of suggestions on furthering the research for future development.

CHAPTER 2

LITERATURE REVIEW

2.1 ENDOCRINE DISRUPTOR COMPOUNDS

The endocrine system is one of the body's main communication networks that are responsible for controlling and coordinating numerous body functions. The word endocrine is from the Greek word "endo" which means within or inside and "crisis" for secrete. The endocrine system has a similar function as an information signal to the nervous system but using different mechanism. The nervous system exerts point-to-point control through nerves but endocrine system broadcasts messages through blood and extracellular fluid in the body. Hormones are first produced by the endocrine tissues, such as the ovaries, testes, pituitary, thyroid and pancreas. These tissues will produce the body hormonal messages, which then secreted into the blood stream and be delivered to essentially all cells where they direct communicate and coordinate among other tissues throughout the body (NIEHS, 2007). The messages or signal send by endocrine system initiate is rather slow, but their response could last from a few hours up to weeks. In contrast, nervous system sends messages very fast and responses are short-lived (NIEHS, 2007; Bowen et al., 2002)

Endocrine disruptors compounds (EDC) are group of chemical compounds that will interfere with the endocrine tissues by generating hormonal messages in humans and animals. EDC can disrupt any system in the body controlled by hormone. Growing cells require specific hormone balances to mature, enough to perform a healthy and normal cell metabolism. However, these disruptions interfere with synthesis, transport

or action in the body that are responsible for development, behavior and fertility. EDC have also been labeled as emerging contaminants in drinking water. Generally, the term "emerging contaminant" refers either to contaminant recently introduced into the environment that can potentially poses emergent threat, or can contaminate the environment even at such low levels which have not been able to detect its presence with common analytical techniques. Some of these EDCs were detected in waterways as early as the 1970's, but more recently, they have been found in some drinking water supplies (Grande, 2008).

EDC is a natural or synthetic chemical not produced in the body that mimics the function of a hormone and can disrupt normal physiological functions. It include hormones, plant products such as phytoestrogens, pesticides, plasticizers, phenols, or other industrial by-products and pollutants (Grande, 2008). These chemicals are found in many of the everyday products such as in some plastic bottles, metal food cans, detergents, flame retardants, food, toys, cosmetics and not forgetting pesticides (NIEHS, 2007; Amiridou and Voutsa, 2011).

2.2 TYPES OF EDCs

EDC exist in almost all everyday used products according to its kind and uses. Because hormone receptor systems are similar in humans and animals, effects observed in wildlife species raise concerns of potential human health effects.

The possible fates of EDCs once they enter the aquatic environment are mainly three. Firstly, the compound is ultimately mineralized to carbon dioxide and water. Secondly, the compound is lipophilic so it does not degrade readily and partially retained in the sedimentation sludge. Thirdly, the compound metabolizes to a more hydrophilic molecule, passes through the wastewater treatment plant and ends up in the receiving waters (which are surface waters, mainly rivers) (Klavarioti et al., 2009).

Although limited scientific information is available on the potential adverse human health effects, concern arises because EDC even while present in the environment at very low levels, have been shown to have adverse effects in wildlife

species, as well as in laboratory animals. Some scientific studies have shown reproductive abnormalities of amphibians and fish when exposed to low concentrations of EDC (Brouwer et al., 1999; NIEHS, 2007, Grande, 2008). It is believed that EDCs may be responsible for some reproductive problems in both women and men as well as for the increases in the frequency of certain types of cancer (Newbold and Liehr, 2000). EDCs have also been linked to developmental deficiencies and learning disabilities in children. Evaluating potential low dose effects of environmental estrogenic compounds has been identified as a major research priority.

In this section, the potential types of EDCs are described inclusive of its uses, exposure routes, health effects and characteristics.

2.2.1 Dicholorodiphenyl Trichloroethane (DDT)

A wide range of pesticides has been implicated as endocrine disruptors. Excess usage in agricultural field is the caused for the existence of most pesticide found in surface waters. It can also enter water source by wastewater discharges, spillage or as runoff from urban and suburban areas.

DDT or 1,1,1-trichloro-2,2'bis(*p*-chlorophenyl)ethane, was first introduced as an organochlorine insecticide to eliminate mosquito-borne malaria in the United States and Europe (Beard, 2006). It has the characteristic of very persistent in both environment and human body since its solubility in fats and most organic solvents are high but insoluble in water. The stability of this chemical caused the DDT being slowly discharge by most living bodies.

The exposures have been widespread and prolonged through food chain from animal species to human lives. In a report, high DDT contamination has been detected in Lake Maggiore, Northern Italy where zebra mussel populations were evaluated. It is observed that polluted mussels showed a delay in oocyte maturation (Binelli et al., 2004). In another report, the occurrence of organochlorine residue (including DDT) has been detected in a Chinese pesticide-exposed area, where they reported presence of higher DDT level in children's blood than in their mothers', also high level of DDT in

breast milk and umbilical cord, causing damage on male reproducibility and behavioral changes (Wang et al., 2008).

Quite recently in Africa, malaria killed 750,000 million people in 2009 and insecticides have still been used to exterminate malaria. Quests for using pyrethroids as an alternative method to replace the use of risky DDT in diminishing malaria were almost successful in some countries. However, since malaria mosquito has become resistant to pyrethroids, most of sub-Saharan Africa requested continuing usage of DDT on the proof that DDT was the most effective insecticide and relatively low cost (WHO, 2006). Due to the prolonged usage of insecticides, DDT concentration in breast milk of Manhisa district mothers were observed to be increasing.

This pattern may lead to decreases of child cognitive skills, alterations of thyroid hormones and asthma problem (Manaca et al., 2011). Furthermore, alarming adverse effects as reported in 2006 observed in young and adult male rat offspring exposed to mixture of pesticides, which included reduced prostate and epididymis weights, increased density of mammary glands, reduced sperm counts and decreased spatial learning (Jacobsen et al., 2006)

2.2.2 Polychlorinated Biphenyls (PCB)

Polychlorinated biphenyls, or PCBs, are a group of 209 different chemical structures known as congeners that consists of two connected benzene rings and 1 to 10 chlorine atoms. PCBs were discovered and manufactured commercially over 100 years ago. They have an amazing electrical insulating properties and flame resistance leading to their massive demand to be used as insulators and coolants in transformers and other electrical equipment. Moreover, because PCBs substitute combustible insulating fluids, they reduced fire risks in potential buildings. They also can be made smaller, therefore reducing the equipment cost.

Subsequent researches have proved that some congeners of PCB released to the environment degrade rather slowly and most likely can build up in the food chain (Ross, 2004; Donato et al., 2006). An important implication of PCB exposure is that the

alterations in early development can have extended effects on behavior and growth (Cromwell et al., 2007). Health risk incidents began in the late 1960s, and grow concerns on potential health effects among humans which rendered the restriction of PCBs production thereby decreasing their usage abruptly since. Despite their banned in many industrialized countries, this compound is still present in the environment due to its structural stability. Human and wildlife can be exposed to PCB through equipment leakage during manufacturing process causing PCB-containing heat transfer fluid ingested into foods.

A disastrous event took place in Yucheng, Taiwan where mass poisoning occurred due to PCB-contaminated cooking oil. The exposed women were found affected causing shorter menstrual cycles and have longer bleeding period duration. Also, among them who were exposed at age 5 to 9 years started menarche slightly earlier than normal referents (Yang et al., 2009)

A report made in 2009, found that an industrialized town with a 50 years old operational PCB factory has been water polluted by PCB discharge and accumulated in the sewers. After investigation on exposed rat, they found significant changes in hypothalamic brain neurons and pituitary cells that control growth and hunger and changes in joints and bone tissues. These alterations could cause obesity and feminizing effects. In addition, it is stated that PCB effects are often sex-specific where the males appearing more sensitive than females (Cocchi et al., 2009).

Donato et al. (2006) reported to have found high levels of PCBs in soil, food and some farmers due to living close to a factory producing PCBs. After investigation on all consumers, it is observed that high PCBs level in blood were detected in PCB-contaminated food consumers rather than organic consumers. The effects of PCBs exposure also include; delayed puberty for boys and testosterone reduction in male babies (Grandjean et al., 2012; Cao et al., 2008) and feminization/demasculinization of male genital ducts in male frogs (Qin et al., 2007).

2.2.3 Alkylphenols

Nonylphenol and octylphenol are the largest volume of alkylphenol (AP) products manufactured where they are used to make alkylphenol ethoxylates (APEOs) with 80 to 20% ratios respectively. APEOs are types of nonionic surfactant widely used as sanitizing agents, solubilizers, emulsifiers and dispersants since the 50's (David et al., 2009). APEOs are the most likely to be discharged into sewage waters or directly released in the environment. They did not break down completely in sewage treatment plants or in the environment which end up accumulating in waters and soil.

Moreover, nonylphenol ethoxylate (NPE) with nine to ten member carbon chains are easily eluted in water. Humans and wildlife are likely being exposed to alkylphenols through contaminated drinking water and polluted sewage (EPA, 2001). Back in the 90's, APEO have been considered as EDCs and have antiandrogenic activity where it is reported able to mimic 17β-oestradiol hormone that will induce breast tumor cell (Soto et al., 1991; Gaido et al., 1997). This has rise concerns and considering their endocrine disruption potential, the European Union (EU) and Environmental Protection Agency (EPA) restricted usage of alkylphenols as low as 0.1 µg/l. However, many Asian and South American countries still use APEOs in large amounts without water quality control.

A review made by David and coworkers (2009) discussed on the presence of APs in coastal and marine ecosystems. They stated that the exposed male trout showed an increasing estradiol level that led to the induction of yolk protein normally occurs only in mature females with developing eggs (David et al., 2009).

Effects of AP were also done by Meier et al (2011) where they observed male and female cods at low to high AP concentration. It is found that juvenile females are advanced into puberty and maturation, while gonad development was delayed in both maturing females and males. They concluded that AP-exposure could affect the timing of the onset of puberty in fish even at extremely low concentration. The presence of APs was also detected in human population through observing human adipose tissues. At present, there are no reports of adverse health effects in humans; however, many reports

of APs causing production of female-associated liver protein in male fish rise concerns and draw a baseline for further investigation of possible consequences for human health (Ferrara et al., 2011)

2.2.4 Butylated Hydroxyanisole (BHA)

Butylated hydroxyanisole or BHA is a synthetic phenolic derivative that is widely used as preservative and antioxidant in food, food packing, cosmetics and pharmaceuticals. It prevents oxidative deterioration of fatty acids. Past studies have been focused on the estrogenic effect of this food preservative to which human is easily exposed via diet and food industrial products. Although there are many advantages of antioxidants, high dose of synthetic antioxidants induced growth retardation and altered metabolism (Hoffman, 2002). BHA has been approved by WHO (1999) with regulatory limit of 100 to 200 ppm for edible fat and oils including animal fats and vegetable oils and an acceptable daily intake of 0 to 0.5 µg/kg body weight.

Jeong et al (2005) investigated the effects of BHA on reproductive function and development by the treatment of mature male and female rats. The observations showed that high dose of BHA induce weak dysfunction and under development of reproductive system of male and female rats. This result was also approved by Kang et al (2005) where they evaluate estrogenic and androgenic activity of BHA using immature rats.

2.2.5 Parabens

Parabens are alkyl esters of p-hydroxybenzoic acid, which include methylparaben, ethylparaben, propylparaben, butylparaben, isobutylparaben, isopropylparaben and benzylparaben. These compounds are widely used as preservatives and anti-microbial agents in food, cosmetic merchandise and pharmaceuticals products since the past 50 years (Shaw and Decantazaro, 2009). Parabens stand out as the chosen substance as an ideal preservative because they are effective over broad pH ranges, soluble in water for an easy preparation of target concentrations, have no traceable odor or taste and stable over wide heat ranges (Tavares et al., 2009).

Generally, usage of parabens is believed as safe additive, since they metabolized into a less toxic compound, *p*-hydroxybenzoic acid. Therefore, they are manufactured and consumed in large quantities daily. Concerns rise due to the low and may be incomplete paraben metabolism in human skin upon constant applying. Parabens have been detected in nearly 100% of urine samples tested, also in the plasma of pregnant women and breast milk concentrations (Ye et al., 2006).

Recent report on postnatal female rat model indicate that exposure to parabens can produce adverse effects on response of hormones and can disrupt the morphology of reproductive target tissues. It is also concluded that effects of parabens can also be causing thyrotoxic during this critical stage of female rats' development (Thuy et al., 2010). This finding is also confirmed in the study made by Meeuwen et al (2008).

2.2.6 Phthalate

Phthalates are types of synthetic organic substances derived from phthalic acid such as di-2-ethylexylphthalate (DEHP) and mono-2-ethylexylphthalate (MEHP). They are used as plasticizers in PVC plastics to increase their flexibility. Living population is extensively exposed to phthalates because they are components of our daily used products such as plastic wear, cosmetic, lubricants and so on. It has been reported that phthalate transfer from food approximately 160 µg/day (Garcia-Mayor et al., 2012).

Moreover, phthalate plasticizers are not chemically bound to PVC since it is not a part of the polymer. Because of this, they can leach out and evaporate into air and foods resulting in a direct contact exposure through inhalation and ingestion (Hendorf et al., 2007). The exposure was observed in livestock animals using ewe (a type of sheep) as a model, where it is found that percentage of animals with presence of phthalate increases with age, mainly during pregnancy due to mobilization and accumulation in the body (Herreros et al., 2010). In another investigation, it is reported that phthalates could be weak carcinogens because of its weak estrogenic properties. Due to this, exposure of phthalates could increase the risk of developing cancers. In addition, phthalates exposure had been shown to be related with increased risk of development of

allergies and asthma (Singh and Li, 2012) and prenatal exposure to phthalates has said to have the potential to impact early brain development (Miodovnik et al., 2011).

2.2.7 Bisphenol A (BPA)

Bisphenol A (BPA) is an intermediate chemical that manufactured in polymer industries such as epoxy, polycarbonate, polysulphone, polyester resins, and numerous plastic articles (Lyons, 2000; Zhang et al., 2006; Bing-zhi et al., 2009). BPA is also present in various consumer products, such as in the interior coatings of food cans, milk containers, and baby formula bottles, as well as in dental sealants.

BPA has being classified as one of EDC that can give adverse effect to the environment as well as all living things. Although the exposure of BPA in our daily used products is acceptably low, but the enormous production and consumption these days, have raised concern on the consequences of BPA toxicity towards human and wildlife health and safety in the environment. Due to the highly water-soluble characteristic, BPA can be easily eluted out from the BPA-based products and endangered us all, the consumers (Lyons, 2000; Ikegami et al., 2004). There is also a report on the possibility of BPA leaching out into food, infant formula or straight into body due to the depolymerization of BPA-based product (Grasselli et al., 2010). In fact, BPA toxicity in human has been detected by its presence in human serum and follicular fluid, fetal serum and even in amniotic fluid (Inoue et al., 2000; Ikezuki et al., 2002; Benachour and Aris, 2009). Morphological and functional modifications after BPA exposure also have been documented in the ovary (Hunt et al., 2009).

The BPA compound could cause biological effects and very hazardous even at low level. It has been shown to disrupt hormonal system activities, which induce abnormal differentiation and development of reproductive organs by mimicking or interfering with the action of endogenous gonadal steroid hormones (Lyons, 2000; Zhang et al., 2006). It is also proven to have estrogenic effects in animals and hormonal effects, which increase breast cancer risk in human. BPA is also reported to act as anti-androgen that causes feminizing side effects in men (Bolong et al., 2009), and has the potential to cause reproductive and developmental damages (Murray et al., 2010). Most

upsetting is that, infants up to 2 or 3 months of age might have higher free BPA levels in blood and urine since detoxifying enzymes are not fully developed at this age (Edginton and Ritter, 2009; Mielke and Gundert-Remy, 2009 by Volkel et al., 2010).

As a result, it is noted that throughout the present study, bisphenol A was selected as the target template due to its application in almost everything in our daily used products which jeopardizing the health of all living population especially an alarming direct exposure to infant causing build up toxic in the bodies of the next generation. The overall types of EDCs discussed are presented in Table 2.1 together with its uses and health effects.

The summarized of exposure routes and potential fate of EDCs to humans and wildlife into the environment was illustrated in a diagram as shown in Figure 2.1. The figure shows EDCs included products such as canned foods, skincare and make-ups, and pharmaceutical products being manufactured and directly consumed by humans. As for the discharged waste, causing contamination of sewage and waterways, and being absorbed by aquatic animals, and into the soil, which consequently will be used and consumed by humans as well.

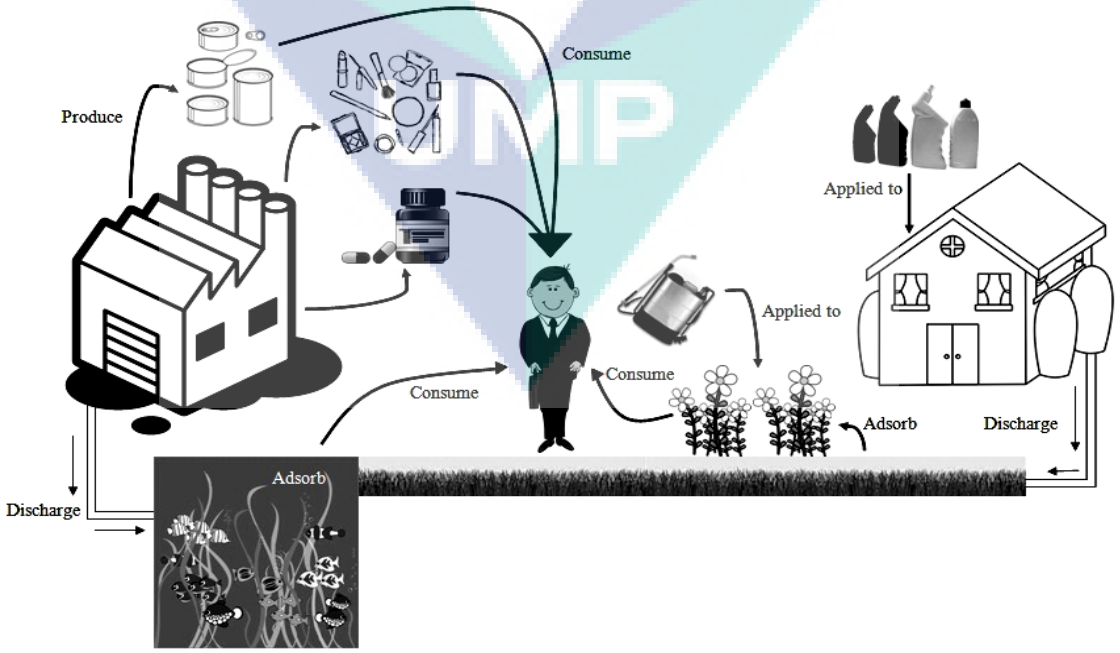

Figure 2.1: Exposure routes of EDC towards human from manufacturer and household

Table 2.1: Health effects and applications of endocrine disruptor compounds

Endocrine disrupting compounds	Applications	Health effects
Bisphenol A (BPA)	As intermediate chemical of epoxy, polyester resins, and plastic articles	• It caused feminizing side effects in men (Bolong et al., 2009). • Reproductive and developmental damages (Murray et al., 2010)
Dicholoro-diphenyl Trichloroethane (DDT)	Used as pesticides	• It damaged male reproducibility and behavioral changes (Wang et al., 2008). • Causing decreased child cognitive skills, altered thyroid hormones and asthma problem (Manaca et al., 2011).
Polychlorinated Biphenyls (PCB)	Used as insulators and coolants in electrical equipments	• It delayed puberty for boys and testosterone reduction in male babies (Grandjean et al., 2012; Cao et al., 2008). • Promote feminization/demasculinization of male genital ducts in male frogs (Qin et al., 2007).
Butylated Hydroxyanisole (BHA)	Used as a food antioxidant, preservatives	• Contribute to carcinogenicity or tumorigenicity (Helmenstine, 2010). • It was found toxic to aquatic organisms (Murray et al., 2010). • Estrogenic to breast cancer cells, rainbow trout estrogen receptor and stimulates human estrogen receptor (Jobling et al., 1995).
Alkylphenols	Used in detergents	• Mimicking estrogen and disturbing reproduction by increasing number of eggs (Bolong et al., 2009; Amiridou and Voutsa, 2010).
Phthalates	Used as plasticizers in plastic, PVC baby toys, flooring	• Exposure at high levels caused miscarriage and pregnancy complication (IEH, 1995).
Parabens	Used as preservatives, for anti-microbiological agent in cosmetics, toiletries and foods	• Weaken estrogenic activity, possibly contributing to rising breast cancer rates (Shaw and deCatanzaro, 2009).

2.3 TYPES OF REMOVAL TECHNIQUES

Water supplies use a variety of treatment processes to remove contaminants from drinking water. Individual processes may be arranged as series of processes applied in a sequence. In the following section various techniques used to remove EDC from water is described. The feasibility of each technique depends on the size of system and cost effectiveness. The most commonly used processes include flocculation, sedimentation, filtration, and disinfection for surface water. Some treatment techniques also include ion exchange and adsorption.

2.3.1 Coagulation/ Flocculation

Chemicals like iron salts, anionic or cationic polymers is added into the solution during coagulation process. Suspended particles will destabilize and coagulate becoming as floc. This floc is further removed via clarification and/or filtration. Conventional filtration includes pretreatment steps of chemical coagulation, rapid mixing, and flocculation, followed by floc removal via sedimentation or flotation. After clarification, the water is filtered using common filter media.

Coagulation technique was reviewed by Khiari (2007) in removing a number of EDC at bench, pilot and full-scale process. From the bench scale study, only hydrophobic compounds were able to coagulate using Aluminum Sulphate (alum) and Ferric Chloride. Results reported that hydrophobic compounds able to bind to particles and later removed during settling, while more water-soluble contaminants were not removed and only few EDCs and PPCPs could be removed by coagulation or softening alone. It is seem that coagulation is largely ineffective for EDCs removal (Khiari, 2007).

In another research done by Vieno et al., (2006), the same technique was used on selected pharmaceuticals such as dicloferac, ibuprofen, bezafibrate, carbamazepine and sulfamethoxazole. The jar test method was conducted in Milli Q water, lake water and commercial humic acid solution using Aluminium and Ferric Sulphate as coagulant aids/softening. Based on their study, only dicloferac reached a maximum removal by Ferric Sulphate while others pharmaceuticals required high amount of coagulant

aids/softening chemicals to enhance their removal. They also found that non-ionisable compounds, carbamazepine and sulfamethoxazole, were completely not affected by the processes studied and chemical used. They concluded that it is not possible to remove pharmaceuticals entirely from water by coagulation (Vieno et al., 2006).

From the above study, it is obviously showed that coagulation technique is not effective for EDCs removal because these chemicals are mostly water soluble and non-ionisable. EDC will not able to attract to the ion charges presented in the coagulants/flocculants and floc is not formed completely hence, they cannot be neutralized and will not be sticking together to settle. However, some EDC can still be removed by coagulant with the assists of high molecular weight polymers, called coagulant aids and alum, which help to bridge, bind, and strengthen the floc formation, add weight to floc, and increase the floc-settling rate. However, majority of coagulant aids are very expensive and pH sensitive with other different and limited properties. In addition, used alum can become waste, which lead to more pollution and require high-cost waste treatment or recycle process to reduce the waste piles.

2.3.2 Activated Carbon

Activated carbon is a material similar to charcoal in composition, but its surface has been altered to enhance its sorption properties. Activated carbon is made from a variety of materials including coal, wood, sawdust, bone, peat, and petroleum distillates. In drinking water treatment plants, activated carbon produced from wood and coal is most commonly used (Bodzek and Dudziak, 2006). The activation process is considered a two-step procedure in which amorphous material is burned off and pore size is increased. The base carbon material is dehydrated then carbonized through slow heating in the absence of air. It is then activated by oxidation at high temperatures (200 to 1000^{o}C), resulting in a highly porous, high surface area per unit mass material. Typically, Granular Activated Carbon (GAC), a type of activated carbon, has surface areas ranging from 500 to 1400 square meters/gram (Khiari, 2007).

Bodzek and Dudziak (2006) used activated carbon in their research to remove steroidal sex hormones. It is carried out on carbon columns filled with two types of

activated carbon, which were Powdered Activated Carbon (PAC) and GAC. This batch mode sorption was done by 4 hours of shaking. They found high sorption efficiency for both activated carbon on removing free estrogens, but trace amounts of 17β-estradiol were still exist in the effluent. Hence, it can be state that the removal process was incomplete.

In a study done by Khiari (2007) using GAC to remove several types of EDC chemicals known in water sources, only hydrophobic compounds such as steroid hormones achieved high removal compared to hydrophilic compounds. In general, most of the target compounds could be removed by GAC but water soluble EDC could be desorbed back through GAC relatively quick.

From these results, it can be said that activated carbon have limitations on its properties and only advantageous to hydrophobic compounds. Since the trace of these contaminants is largely dependent on particle-contaminant interactions, the competitive effects for surface sites (with other particulates) have lowered the extent of removal by activated carbon (Bolong et al., 2009). There are many types of activated carbons, which have to be well chosen to suit each toxic or contaminants. In addition, because of this too, the used of only one type of carbon will not be sufficient and for some cases, have to further with other treatment to completely remove EDCs altogether (Bodzek and Dudziak, 2006). Moreover, the spent activated carbons will become waste streams that contain toxic impurities. The handling and disposal of this waste streams can cause a huge economic burden on the waste generator (Berner, 1999). Besides, the regeneration of spent activated carbon is not economically feasible either.

2.3.3 Oxidation/Ozonation

Oxidation treatment is a destructive method widely used in drinking water treatment for disinfection, color removal, taste and odor control, decrease of disinfection byproducts formation, biodegradability increase and for the successful degradation of many organic contaminants. Oxidizers such as ozone, UV, chlorine, manganese and aluminium reacts with organic contaminants through both a direct reaction between the molecules or through indirect reactions with free radicals (including the hydroxyl

radical OH) produced by the decomposition of oxidizers (Gunten et al., 2005; Broseus et al., 2009; Forrez et al., 2009; Ikehata et al., 2008).

Chemical oxidation using ozone is proven an effective treatment process for a wide spectrum of organic micropollutants during bench, pilot and full-scale experiments in both wastewater and drinking water (Gunten et al., 2005; Esplugas et al., 2007). It is stated that molecular ozone reacts selectively with unsaturated bonds, aromatic systems and amino groups whereas the reaction with OH radicals is a faster and unselective process (Broseus et al., 2009). Ozone was also found to be highly effective in several drinking water treatment plants (DWTPs) from diverse locations, while chlorine and UV with same dose as ozone was less efficient (Snyder, 2008). UV/H_2O_2 and titanium dioxide photocatalysis are the light oxidation processes most used to destroy EDCs and PPCPs, which the removals obtained, were higher than 98% (Esplugas et al., 2007).

Gunten et al., (2005) conducted pilot experiments of pharmaceuticals oxidation during ozonation of wastewaster effluent. Experiments were carried out using a wastewater with a concentration representative with the selected pharmaceutical classes (macrolide and sulfonamide antibiotics, iodinated X-ray contrast media, estrogens and 3 acidic pharmaceuticals) were spiked to the wastewaster. Results showed that for fast reacting compounds such as antibiotics and estrogens achieved complete oxidation. Meanwhile, for other compounds only reached partial oxidation, even with the help of OH radical oxidants due to their lower reactivity with ozone. They claimed that, although suspended solids increase ozone demand, the influence is minor. 5 mg/L ozone doses were sufficient but higher doses were necessary for higher suspended solid concentrations (Gunten et al., 2005).

Khiari (2007) also reviewed oxidation method that used free chlorine and chloramines as oxidizers. This oxidation process is pH-dependent, with increased oxidation at lower pH. The results reviewed that the hormones with a phenol functional group were rapidly oxidized, while hormones with a ketone group were only partially oxidized when using free chlorine as oxidizers. The antibiotics sulfamethoxazole, trimethroprim, and erythromycin are among the compounds that showed high removal

by free chlorine but low removal by chloramines. This is because free chlorine is a stronger and faster oxidant than chloramines (Khiari, 2007).

Although oxidation is a promising removal mechanism, especially using ozone or chlorine, careful selection is needed as reaction of these chemicals was found to be reactive and produce byproducts, of which the effects are unknown (Bolong et al., 2009; Liu et al., 2010). Although it is also advantageous in terms of undependable on the water quality, but in many cases, the process is depending on pH of effluent. Furthermore, other physical separation processes produce wastes which have to be properly disposed of which is an exemption for oxidation process but still, it is likely to consume expensive cost to prepare it (Klavarioti et al., 2009).

2.3.4 Membrane Filtration

There are three main mechanisms in removing micropollutants by membranes, which include size/steric exclusion, adsorption and charge repulsion. The adsorption of the compounds on the membrane has been found to be an important factor affecting their retention and mechanism (Su-Hua et al., 2010). The retention of trace organics is often explained by the solution diffusion model. According to this model, solute transportation across the membrane is a two-step process: first, the solute is adsorbed or dissolved by the membrane; second, it migrates across the membrane by diffusion or convection (Nghiem et al., 2004; Nghiem et al., 2005).

Usually the adsorption is reported with the retention by nanofiltration (NF) or reverse osmosis (RO) since almost all of the compounds categorized as EDCs have molecular weights (MW) of >200 g/mol and thus it is reasonable to consider that NF and RO membranes would be effective in removing EDCs (Nghiem et al., 2005). However, microfiltration (MF) and ultrafiltration (UF) have much more available adsorption sites due to their higher porosities, so the adsorption trend may be better than NF and RO (Su-Hua et al., 2010).

Although RO and NF have shown a significant performance for EDCs removal, they need higher driving force for operation (Bing-zhi et al., 2010), which limit their

application in drinking water treatment. This is where application of various types of membranes such as flat sheet membrane, hollow fiber membrane or spiral wound membrane selections come in handy. There is also a study by Liu et al., (2010) which used a novel membrane type where a series of composite functional membranes containing immobilized activated carbon fiber powder (an adsorbent) and photo-catalyst on filter cloth to extract, separate and eventually oxidize BPA off-site efficiently.

Bing-zhi et al., (2010) carried out the experiment using MF hollow fiber membrane and investigated the factors influencing BPA removal, such as BPA initial concentration, pH, ionic strength and natural organic matter (NOM). Results showed that the BPA removal percentage were around 70 to 90%, with the effect of pH was the most significant factors affecting the removal. Other parameters were almost negligible and could be fixed by membrane backwashing when the membrane is saturated. Meanwhile, an adsorption by UF polysulfone membrane was conducted by Su-Hua et al., (2010), and same factors such as BPA initial concentration, pH, ionic strength, natural organic matter (NOM), and polymer materials (e.g: polysulfone) of the membrane were also investigated. Similar to above study, it appeared that the most significant factors affecting the membrane performance were pH of effluent and material of the membrane.

A study conducted by Nghiem et al., (2005) aimed to examine the removal mechanisms of three pharmaceuticals, which are sulfamethoxazole, carbamazepine, and ibuprofens by two thin-film composite NF membranes. Again, pH showed a major factor effecting the pharmaceuticals removal. They claimed that, pH can affect not only charge but also other physicochemical properties of the pharmaceuticals, particularly hydrophobicity and solubility. However, because the average pore radius of the NF membrane is substantially smaller than the radius of the three pharmaceuticals used in this study, no polarity effects can be observed with the tight NF membrane, and the retention is nearly complete.

From the above discussions, it shows that two most significant factors affecting EDC removal by membrane filtration regardless of the pore sizes are pH and membrane properties. Another thing to be considered when using membrane filtration is retentate

build-up or concentration polarization. The membrane will become saturated and had to undergo backwashing to recover back the membrane efficiency. Also, due to the adsorption–desorption balance, the membrane can be considered as a reservoir of EDCs and retained compounds can be released into permeate if the pollutant concentration in the raw water has an erratic behavior (Zhang et al., 2006; Bing-zhi et al., 2010). Some membrane filtration such as reverse osmosis was rather advantageous. However, it requires high investment and energy consumption, especially at a large community level (Liu et al., 2009).

2.3.5 Molecular Imprinted Polymer (MIP) Technique

Molecular imprinting technique has been developed quite intensively recently to provide a wide range of desired receptors. It is becoming newly preferred synthetic approach to mimic natural molecular recognition in artificial materials. In other words, it is a technique to create template-shaped cavities in polymer matrices with memory of the template molecules to be used in molecular recognition (Ikegami et al., 2004; Piletsky et al., 2001; Faizal et al., 2008; Zhang et al., 2009). This technique is based on the system used by enzymes for substrate recognition, which is called the "lock and key" model.

In the early 1970, Wulff and coworkers first synthesized organic material with recognition selectivity of target molecule (Wulff and Sarhan, 1972). In principle, molecularly imprinted materials (MIPs) are prepared by copolymerization of a template molecule and functional monomers in certain condition and subsequently are cross-linked to each other.

The functional monomers, which self-assembled around the template molecule by interaction between functional groups on both template and monomers, are polymerized to form an imprinted matrix as shown in Figure 2.2. Then the template molecule is removed from the matrix under certain conditions, leaving behind a cavity complementary in size and shape to the template. The obtained cavity can work as a selective binding site for that specific template molecule.

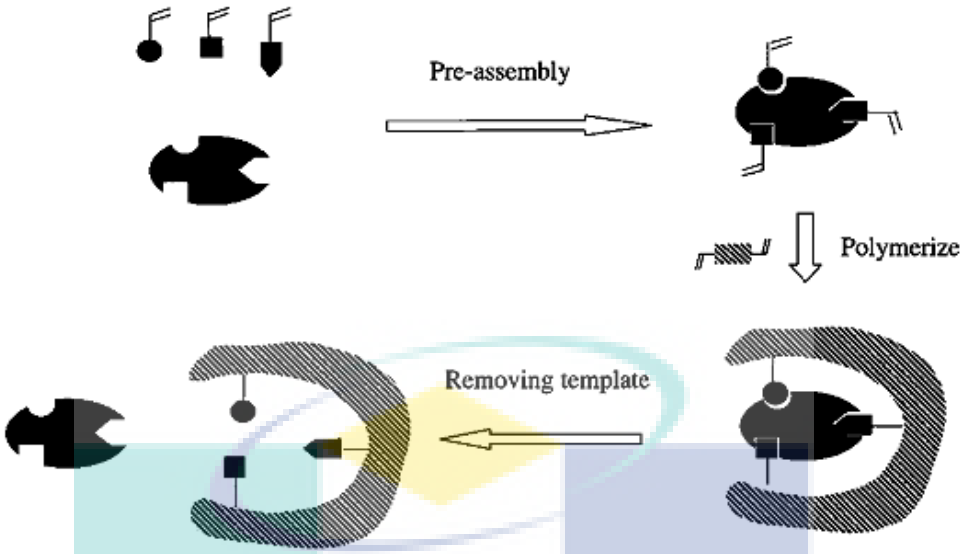

Figure 2.2: Schematic representation of MIP preparation (Ye and Mosbach, 2001)

Three significant features have made MIPs the aim of intense investigation as reviewed by Piletsky et al., (2001):

i. High affinity and recognition selectivity similar to those of natural receptors;
ii. Versatile and unique stability almost superior to that showed by natural biomolecules;
iii. The preparation is simple and easy to adapt for different field of applications.

Because of these reasons, MIP is selected as the removal technique in this study. The template used for the imprinting will be Bisphenol A. Elaboration on the MIP technique will be further discussed hereafter.

The advantages and disadvantages of removal techniques described earlier are summarized in Table 2.2.

Table 2.2: Summary of EDC removal techniques

Removal technologies	Benefit	Limitations
Coagulation / Flocculation	• Hydrophobic compounds were able to bind to particles and were subsequently removed during settling (Khiari, 2007)	• Few EDCs and pharmaceuticals and personal care products (PPCPs) could not be removed by coagulation or softening alone (Khiari, 2007 ; Vieno et al., 2006)
Activated Carbon	• Hydrophobic interactions in eliminating most organic compounds • Activated carbon was more efficient than coagulation (Bodzek and Dudziak, 2006)	• The competitive effects for surface sites and/or pore blocking (with other particulates) have lowered the extent of removal by activated carbon (Bolong et al., 2009)
Oxidation	• Oxidation is effective in degrading EDCs/PPCPs in low dissolved organic carbon (DOC) (Gunten et al., 2005)	• Higher doses were necessary for higher suspended solid concentrations (Gunten et al., 2005) • Careful selection is needed as reaction of these chemicals was found to be reactive and produce byproducts, of which the effects are unknown (Bolong et al., 2009)
Membrane Filtration	• Can separate much smaller size particles (sub-micron size), • Able to filter 99.9% of the insoluble or suspended solids and soluble compounds such as oils and large proteins (Goliath, 2008)	• The membrane can be considered as a reservoir of EDCs and retained compounds can be released into permeate due to the adsorption–desorption balance. This is because EDCs are highly soluble in water and hard to be separated (Zhang et al., 2006).
Molecular imprinted polymer (MIP)	• High affinity and recognition (Takeda and Kobayashi, 2005), • Unique stability (Faizal et al.,2008), • The preparation is simple and easy (Piletsky et al., 2001)	• It is a challenge in selecting solvents to produce high quality and rigid fine polymer particles (Faizal et al., 2008).

2.4 MIP PREPARATION TECHNIQUE

There are two basic approaches in molecular imprinting, according to the bonding nature between monomers and template molecule, either covalent or non-covalent imprinting. In covalent technique imprinting, the target molecule or template is attached to a polymerizable monomer by covalent bond via independent chemical formation and forming into a functionalized template. This type of binding formation relies on reversible covalent bonds.

Then, the template-monomer is copolymerized with a cross-linker in a solvent. This results in a fixed template arrangement within the polymer matrix. The target molecule is removed from the matrix to leave a specific recognition imprint cavities. This technique is claimed to produce highly homogenous site recognitions and non-specific binding can be greatly reduced. First report of MIP production using this approach was by Wulf (1995), utilizing boronate esters covalently bound to mannopyranoside as template molecule, which then copolymerized with cross-linker. The results showed strong and selective bound targeted molecule onto imprinted polymer (Wulf, 1995).

Khasawneh et al., (2001) also worked on covalent imprinting technique in order to tackle low chromatographic efficiency that arose from peak tailing. An improved peak shape in chromatographic analysis of target compound is showed by using 4-vinylphenylcarbamate moiety for nortriptyline template recognition. Figure 2.3 shows the mechanism of covalent imprinting of nortriptyline on Khasawneh's work.

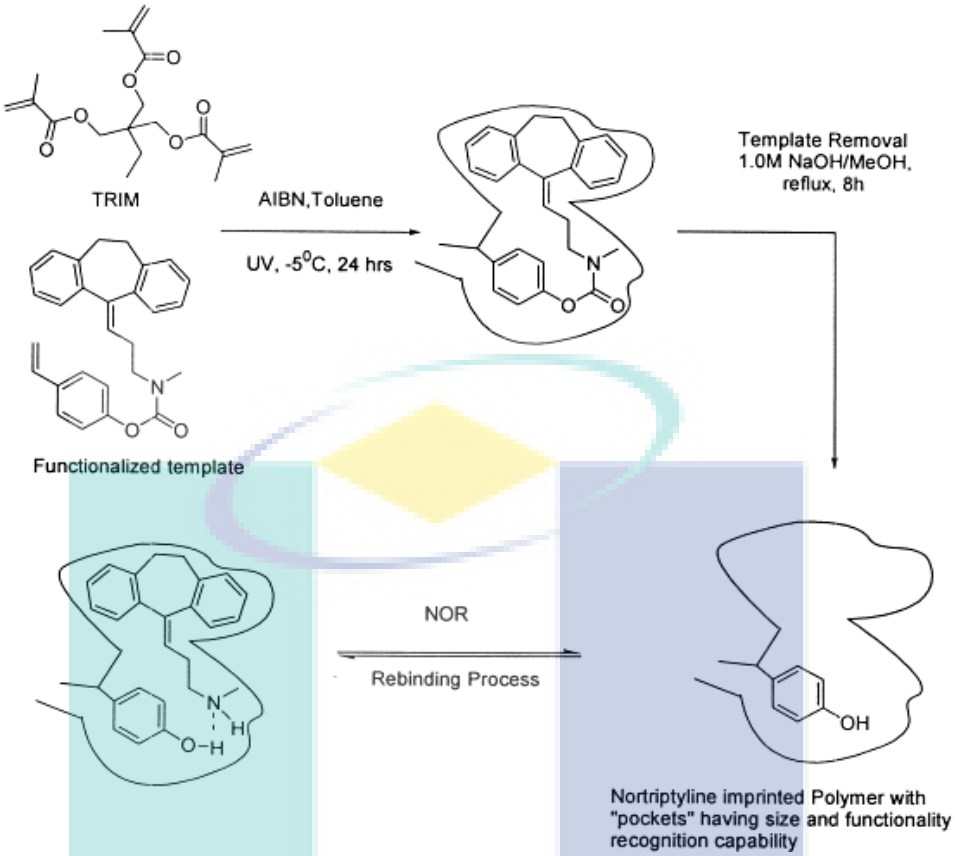

Figure 2.3: Covalent imprinting of nortriptyline using 4-vinylphenylcarbamate as functional monomer performed by Khasawneh et al. (2001)

Second approach on molecular imprinting is non-covalent imprinting. This approach is well-known technique in imprinting simply because of its straightforward procedures. It involves by adding and mixing monomer and template in one reaction vessel and allows them to form non-covalent bonding by itself. Various type non-covalent bonding could be formed between substrate and polymer such as electrostatic, hydrogen bonding, π-π bonding and hydrophobic effect of substrate and polymer. Due to its versatility, non-covalent approach is more favorable. In addition, many compounds, biological including, are capable to have non-covalent interactions with other molecules. This approach was first developed by Mosbach et al. (1993) by imprinting methacrylic acid with theophylline through electrostatic interaction and hydrogen bonding.

Furthermore, Gomez-pineda et al., (2011) used non-covalent approach where they imprinted flavonol as template on methacrylic acid monomer as shown in Figure 2.4. They investigated the intermolecular interactions occurring while imprinting and concluded that the morphology of imprint materials was solvent-dependent.

.

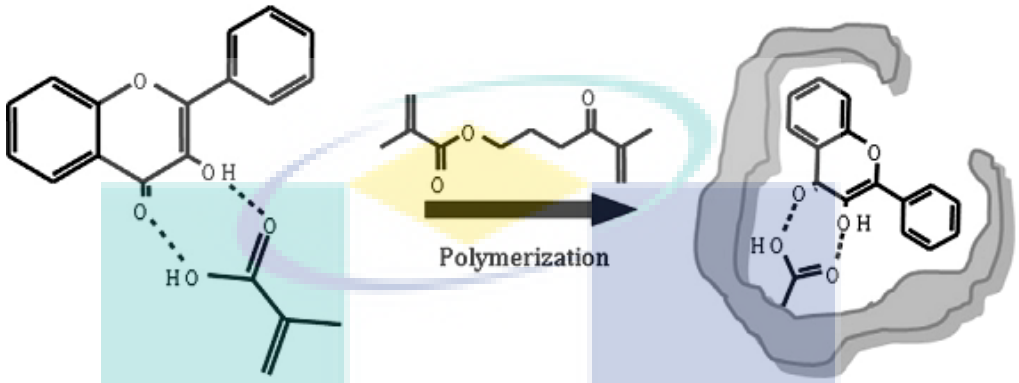

Figure 2.4: Non-covalent imprinting of flavonol using methacrylic acid as monomer demonstrated by Gomez-pineda et al. (2011)

Non-covalent offers simplicity and more flexibility with respect to the functionalities on a template targeted and does not require any chemistry of pre-synthesis as required in covalent adducts. However, it has some adverse effects where the non-covalent interactions are relatively weak and rather sensitive to environment condition (Malaisamy and Ulbricht, 2004) such as in polar solvents like water.

Even though, the covalent interactions need to inquire specific monomer to develop MIPs, it is believed that covalent imprinting is superior to non-covalent imprinting in terms of imprinting accuracy and homogeneous recognition sites as well as uniform affinity. Therefore, covalent bonding is selected in this research for the polymerization of molecular imprinting polymers.

2.5 PARTICLE SIZE OF MOLECULAR IMPRINTED POLYMER

The most common way to obtain MIP is by producing bulky polymers followed by grinding and sieving them to produce shaped particles with wide size distribution typically in the range of 0.5-5 mm (Bruggemann et al., 2000). Although this process is

well established and acceptable, it is time consuming and less than 50 % of usable MIPs yields (Yoshimatsu et al., 2007) are achieved. In addition, this laborious process could compromise the quality of imprinting sites in MIP. It is also said that bulk polymerization does not suit for the use of industrial filed because of its poor heat dispersal (Tan and Tong, 2007). Many studies have been conducted in order to be able to produce the appropriate size of particles to satisfy particular applications.

For example, in a solid phase extraction process, a regular shape and size of MIP is derived to ensure reliable cartridge packing and to possess good mass transfer between the phases in order to increase efficiency of adsorbent cartridge (Beltran et al., 2009). That said, past studies have shown a range of particle size where it most suited in chromatographic system such as high performance liquid chromatography (HPLC) or solid phase extraction (SPE), an appropriate particle size of microspheres in the range of 1 to 10 µm is desired (Valero-Navarro et al., 2011). A smaller particle size possibly nanosize to less than one µm with narrow size distribution is well suited for binding assays or biomimetic sensors (Wei et al., 2006).

2.5.1 Nanoparticles Imprinted Polymers

In the work of assay formats as applied in present study, both bulk and nano polymers are acceptably equivalent to have good binding characteristic. However, recently many researches opt for nano-size polymers in order to increase the amount of binding capacity and enhance separation properties of their system.

In contrast to bulk polymers, nano-size polymers is believed to possess higher surface area to volume ratios, and because of this, much higher access to imprinted sites could be achieved (Gao et al., 2007). In addition, its small size shortens diffusional length within the polymer and leading to fast equilibration with substrate (Tokonami et al., 2009). Other researchers also claimed that nanoparticles molecule exhibit unique characteristic in terms of thermally, magnetically and optically improvised (Anyaogu et al., 2008; Chinie et al., 2005). Other applications of MIP nanoparticles so far includes to be used as enzyme substitute (Amaya et al., 2007), drug delivery systems (Ciardelli et

al., 2004), antibody substitutes (Yoshimatsu et al., 2008), and also used as sensors (Reimhult et al., 2008).

There are several techniques to synthesis molecular imprinted nanoparticles depending on the applications used. Most researchers choose techniques that are simple and fast, but there are some who select their methods according to the restrict application that they used. Here are some examples of MIP nanoparticles synthesis.

A work done by Wei and coworkers (2006) involved in the synthesis of micro and nanospheres imprinted molecules to recognize 17β-estradiol selectively. They prepared the MIPs using procedure of one-step precipitation polymerization and compared with commonly obtained polymer from bulk polymerization. It is reported that the key to a successful precipitation is by accurate control of parameters affecting the size and morphology, which in their study, the temperature during polymerization and type and ratio of cross-linkers. In about 400nm size was obtained for radioligand binding assays application. The MIP nanospheres showed competitive binding and selectivity to17β-estradiol compared to bulk polymers (Wei et al., 2006).

Similarly, Yoshimatsu and colleagues developed binding assays separations using MIP nanoparticles with racemic propanolol recognition. They obtained MIP beads in the range of 130 nm to 2.4 μm by using a simple precipitation polymerization method with the variation of cross-linking monomer composition. As a result, the presented MIP beads have shown increase chiral selectivity by six to seven fold compared to conventional bulk polymers (Yoshimatsu et al., 2007).

Moreover, there is a study reported for the application of partial filling capillary electromatography (CEC) of S-propanolol where it has also used simple precipitation polymerization. MIP nanoparticles are achieved with only low template concentration used during copolymerization. They obtained high selectivity and separation properties of MIP with only some few micrograms of nanoparticles are used. Therefore, it is proven more cost-effective than monolithic MIPs (Spegel et al., 2003)

Another technique is suspension polymerization; by adding silver nanoparticles as dispersants to synthesis high molecular weight poly(methylmethacrylate) spheres (Yeum and Deng, 2005), by applying silicon oil as dispersion phase rather than water and liquid perfluorocarbon (Wang et al., 2006), and by nanoparticle on microsphere MIP method (Suedee et al., 2012; Jantarat et al., 2008). There is also, a technique of mini emulsion polymerization was reported by adding surfactant to produce nanoparticles MIP for capillary electromatography (Priego-Capote et al., 2008). Other than that, a multi step swelling polymerization to produce MIP for phenol and estradiol recognition is applied by Sanbe and Haginaka, (2002). These methods risk in contamination due to the usage of surfactants and dispersants during polymerization and most of the time suffer from the need of polar organic solvents, which decrease MIPs specific interactions (Wei and Mizaikoff, 2007).

Due to this, author selected precipitation polymerization throughout this study to obtain and control size of nanoparticle, simply because it is, ease operational in producing high yield MIP particles and efficiently proven binding performance. Table 2.3 summarized previous study producing MIP in wide range of particle sizes and Table 2.4 shows the reviewed made by Yan and Row (2006) about the advantages and limitation of different techniques to prepare MIP.

Table 2.3: Summary of molecular imprinting studies in the past decade using different approach producing MIP in wide range of particle sizes for various applications

MIP approach	Template	Polymerization	Application	Range of size	Researcher
Covalent	1-(methyl acrylate)-3-methylimidazolium bromide	Inverse emulsion-suspension polymerization	Magnetic adsorbents to remove acid dyes	20 to 100 µm	Luo et al., 2011
Covalent	Bisphenol A	High shear dispersion, Modified precipitation	Hybrid MIP membrane	0.3-0.7 µm	Son et al., 2011
Covalent	Bisphenol A	Two step modified precipitation	Hollow fiber HMIP membrane	0.1-1 µm	Son and Takaomi, 2011
Covalent	Indole-3-ethanol	Bulk polymerization	Hybrid MIP	<63 µm	Takeda et al., 2007
Covalent	Nortriptyline	Suspension polymerization	Chromatography	20-30 µm	Khasawneh et al., 2001
Covalent	Bisphenol A	Bulk polymerization	Chromatography	32-63 µm	Ikegami et al., 2004
Non-covalent	Flavonol	Free radical polymerization	Binding assay	100-200 nm	Gomez-Pineda et al., 2011
Non-covalent	Mixed of tetracycline antibiotics	Precipitation polymerization	Adsorbents in food industry	± 3 µm	Jing et al., 2010
Non-covalent	17β-estradiol	Precipitation polymerization	Binding assay, Packed columns	± 400 nm ± 3 µm	Wei et al., 2006
Non-covalent	2-(morpholin-4-yl)ethyl (2-methoxyphenyl)carba-mate	Bulk polymerization	Stationary phase in HPLC	40 µm	Denderz et al., 2012
Non-covalent	Quercetin	Precipitation polymerization	Solid extraction	300 nm	Lopez et al., 2012
Non-covalent	Diphenylamine	Precipitation polymerization	Sensor	200-800 nm	Granado et al., 2012

Continue,

MIP approach	Template	Polymerization	Application	Range of size	Researcher
Non-covalent	Caffeic acid	Precipitation polymerization	Extraction	1.5-5 µm	Valero-Navarro et al., 2011
Non-covalent	Carbamazepine drug	Precipitation polymerization	Solid phase extraction	micro	Beltran et al., 2009
Non-covalent	Bisphenol A	Surface imprinting-Sol-gel method	Binding assay	450 nm	Ren et al., 2012
Non-covalent	Bisphenol A	MIP fiber coating	Solid phase microextraction	< 1 µm pores	Tan et al., 2009
Non-covalent	Fungicide thiabendazole	Pre-polimerization in capillay	Capillary electro-matography	Monolith	Cacho et al., 2008
Non-covalent	Rhodamine	Phase inversion	SPE by MIP membrane	Macro-pores	Malaisamy and Ulbricht, 2004
Non-covalent	Glutamic acid	Electrospray deposition	Chiral separation by nanofiber membrane MIP	200-500 nm	Sueyosi et al., 2010
Non-covalent	Lovastatin acid	Surface functionalized imprinting	Binding by hollow fiber MIP membrane	< 2 µm pores	Wang et al., 2008
Non-covalent	Chloramphenicol succinate	Photo-polymerization	Sensor by molecular imprinted film	100 nm	Zhang et al., 2008
Non-covalent	Bisphenol A	Multi step swelling polymerization	Chromatography	micro	Sanbe and Haginaka, 2002
Non-covalent	Bisphenol A	Precipitation polymerization	Solid phase extraction	micro	Lin et al., 2008
Non-covalent	(*S*)-propanolol	Precipitation polymerization	Sensor by quartz crystal microbalance coated with MIP nano	130 nm	Reimhult et al., 2008
Non-covalent	(*S*)-propanolol	Miniemulsion polymerization	Capillary electro-matography	30-150 nm	Priego-Capote et al., 2008

Continue,

MIP approach	Template	Polymerization	Application	Range of size	Researcher
Non-covalent	Herbicide 2,4-dichlorophenoxyacetic acid	Precipitation polymerization	Enzyme immunoassay	micro	Surugiu et al., 2000
Non-covalent	Aspirin	Bulk polymerization	Biomimetic adsorbent	212 µm	Byun et al., 2010
Non-covalent	Catechol	Bulk polymerization	Solid phase extraction	≤ 106 µm	Tarley and Kubota, 2005
Non-covalent	α-tocopherol	Polymer membrane scaffolding	Binding assay	100-135 µm thickness	Faizal et al., 2009
Non-covalent	Bisphenol A	Cryo-polymerization	Solid phase extraction by MIP embedded cryogel	<10 µm	Baggiani et al., 2010
Non-covalent	Bisphenol A	Precipitation polymerization	Solid phase extraction	1-5 µm	Zhang et al., 2006
Non-covalent	Dibenzofuran	Phase inversion	Membrane adsorbents	1 µm pores	Kobayashi et al., 2002
Non-covalent	Theophylline	Phase inversion	Membrane adsorbents	Macro-voids	Kobayashi et al., 2002
Non-covalent	2,4-dichlorophenoxyacetic acid	Suspension polymerization	Adsorbents	10-100 µm	Wang et al., 2006
Non-covalent	Propanolol	Electrospinning	SPE by nano MIP in nanofiber membrane	nano	Yoshimatsu et al., 2008
Non-covalent	(S)-propanolol	Precipitation polymerization	Binding assay (nano), choromatography (micro)	130 nm-2.4 µm	Yoshimatsu et al., 2007

Table 2.4: Summary of MIP prepared by different methods as reviewed by Yan and Row (2006).

MIP Preparation Techniques	Benefits	Limitations
Bulk polymerization	• Polymerization is simple and versatile, • Do not require specific skills or complicated instrumentation	• Tedious work of grinding, sieving and column packing, • Irregular shape and size, • Low performance
Suspension polymerization	• Spherical particles, • Highly reproducible results, • Possible for large scale	• Rather complicated system, • Water is incompatible with most imprinting, • Specific surfactant required
Multi step swelling polymerization	• Uniform beads of controlled diameter, • Excellent particle for chromatography	• Complicated procedures and reaction conditions, • Need for aqueous emulsions
Precipitation polymerization	• Microspheres and nanobeads, • Uniform size and high yields	• Large amount of template, • High dilution factor
Surface polymerization	• Thin imprinted layers, • Monodisperse product	• Complicated system, • Time consuming
In-situ polymerization	• Time and cost effective, • In-situ preparation, • High porosity	• Extensive optimization required for each new template system

2.6 MULTIVARIATE STATISTICAL ANALYSIS

One of the limitations during preparation of MIP is that it does not have an automated procedure that can be utilized for various different analyte. Different parameters could be affecting the fabrication of MIP depending on the nature of the template or cross-linker monomers and the requirement of application itself. Besides that, there are many other factors could affect imprinted polymer characteristics and performance such as properties of template, functional monomers, cross-linkers, solvent, initiator and other chemical compound required in polymerization. The categorical factors, includes type of polymerization initiation, use of mechanical stirrer/shaker and time to prolong polymerization can also affects MIP process.

One-at-a-time screening and optimization has been used conventionally to prepare MIP. It is done by varying one factor at one time while others factors are kept constant at a certain literature value and assumed-to-be at the optimized level. The same approach is then repeated for all other factors studied. This method is time consuming and the real interactions for optimum level could be misleading due to different effects could occur for different substrates. It is rather problematic to follow this commonly used protocols when synthesize new templates in molecular imprinting (Nicholls et al., 2009). In order to overcome this problem limitation, a multivariate approach could be utilized. In multivariate analysis, all factors is varied at once to determine their interactions with each other factors as well as to understand the effects of factor at every level of parameters. Multivariate analysis is well established and have been used in the performance study of adsorbents (Safa and Bhatti, 2011), acid degradation (Barka et al., 2011), drug loading (Derakhshandeh et al., 2007) and many others.

Usually, chemometrics analysis is employed to describe the application of mathematical and statistical methods for the experimental design. This method is especially advantageous in predicting the optimum conditions and at the same time, number of experiments needed is reduced. After all data were obtained, the statistical information of the results can be analyzed. Chemometrics also provide various tools to be used in order to recognize patterns of the data and suggest predicted optimums as well as presenting error analysis (Davies et al., 2004).

2.6.1 Experimental Design

Generally, the basic concept of experimental designs is based on chemometric analyses. All studied factors are change simultaneously over a set of organized experiments. Then, the results are interpreted using mathematical models. There are different methods can been applied depend on the objective of the research. Some of it are, full and factorial designs (FFD) where it is used to screen the factors, and the response surface method (RSM) is used for surface modeling and optimization. Analysis of variance (ANOVA) is generally used to analyze the results from design of experiment. Another advantage of chemometrics is able handle great number of variables while also select the most important variables (Baggiani et al., 2010).

The technique of factorial design is an efficient method of indicating the relative significance of a number of variables and their interactions. It is also an excellent tool to obtain an appropriate mathematical model with minimum experiments for optimization of formulation design. Studies based on factorial designs allow all the factors to be varied simultaneously, thus enabling evaluation of the effects of each variable at each level and showing interrelationship among them.

It is required to define a specific purpose of the experiments and a quantitative target function of the system accurately before experiments are designed. Most important variables that affect the system function are selected and systemic experiments are then performed to the specified factorial design. The number of independent variables selected decides the number of experiments that are to be performed. The response/s (Y) is/are measured for each experiment and then either simple linear, interactive, or quadratic model is generated by carrying out multiple regression analysis and F-statistics to identify statistically significant terms. Responses obtained from the reduced equation, an equation containing only statistically significant terms, are used for drawing response surface plots to visualize the impact of changing variables. The optimum point may be identified from the plot and replicate trials may be run to verify the prediction of optimum response (Bhavsar et al., 2006; Gohel and Amin, 1998).

Koohpaei et al., (2008) have applied multivariate analysis for the screening of MIPs with ametryn as the template. Using software Minitab, Release 14, they studied six factors, which are the type and amounts of functional monomers and solvents, template amount, cross-linker, initiator and polymerization temperature. The method used to screen and optimized all the factors was two-level factorial design (2^6) and central composite design (CCD), respectively. Value of R^2 generated by ANOVA was 0.806, indicating a valid model. Based on their study, the most significant factors were polymerization temperature and type of solvent used during polymerization (Koohpaei et al., 2008).

Another example used of experimental design is by Mijangos et al., (2006) to optimize the performance of ephedrine based MIPs. Two parameters were studied, which are the amount of initiator and the polymerization time. A two-level full factorial design was employed using MODDE 6.0 software. With a valid model obtained, they found that to achieve a great performance in enantioseparation, imprinted polymers should be let copolymerized rather slowly in prolong time with low initiator concentration and low temperature (Mijangos et al., 2006).

Various other work utilizing experimental designs in molecular imprinting strategies are presented in Table 2.5. In this study, factorial design based on two-level factorial method is selected to screen and identify effects of factors in controlling BPA molecular imprinted nanoparticles. Four selected factors to study are polymerization temperature, rate of agitation, solvent to cross-linker ratio and percentage of initiator. Selection is based on feasibility and suitability with covalent precipitation polymerization. A 2^4 full factorial design using Design Expert 7.0.0 software was employed to evaluate the combined effect of the selected variables on the size (sub-µm) of the prepared BPA MIP. As more work is done using multivariate statistical analysis to understand the pillar of molecular imprinting and its limitations, as well as improvements in molecular modeling capabilities, the ability to predict the composition and performance of MIPs will unquestionably improve and will surely be used more often to facilitate MIP field.

Table 2.5: Summary of molecular imprinting using experimental designs applications

Substrate	Objectives	Software / Methods	Parameters	Authors
(-)-ephederine	Optimize polymer performance	MODDE 6.0/ Two-level full factorial design	1) Amount of initiator, 2) Polymerization time	Mijangos et al., 2006
Bisphenol A	Identify factors and optimize polymer structure and properties	MODDE 5.0/ Fractional factorial design	1) Amount of functional monomer, 2) Amount of cross-linker, 3) Amount of initiator, 4) Amount of template, 5) Polymerization solvent, 6) Initiation procedure	Navarro-Villoslada et al., 2004
Fluorescin isothiocyanate	Evaluate effects of variables on the polymer size	Response surface method	1) Polymer concentration, 2) Amount of added nanoparticles, 3) Speed of homogenization	Bhavsar et al., 2006
Sulfamethazine	Optimization of MIPs	Design Expert Software/ Three-level full factorial design	1) Amount of template, 2) Amount of monomer 3) Amount of cross-linker	Davies et al., 2004
Ametryn	Optimize factors influencing polymer efficiency	Minitab, Release 14/ Two-level full factorial design, Central composite design	1) Amount of functional monomer, 2) Amount of template, 3) Amount of cross-linker, 4) Amount of solvent, 5) Amount of initiator, 6) Polymerization temperature	Koohpaei et al., 2008

2.7 MOLECULAR IMPRINTED MEMBRANE

MIPs have the advantage of higher reusability, selectivity and lower consumption (Luo et al., 2011). This polymeric material is robust and is highly stable at elevated temperature, pressure and pH and inertness towards organic solvents (O'Mahony et al., 2006). Because of this, MIPs are always favorable than biological molecules such as antibodies, enzymes, and others.

The development of MIP throughout the decade has shown extensive work on producing uniform size distribution of polymers to suit wide range of applications. However, imprinted molecules in the nanosize particle have some limitations in terms of flow ability to bind and tediously laborious work with handling powder-like polymer materials, which require careful handling to minimize the loss of particle during the process.

Molecule scaffold polymers which have multi-interaction sites to wrap the three-dimensional template complementary has been considered as the best solution to introduce more sophisticated separation process (Tasselli et al., 2008; Zhang et al., 2007). Scaffold imprinted polymers for molecular imprinted membrane has opened new approach of applications in various field. Membrane technology has been widely applied in many industrial technologies such as, environment, food industries, energy, medical field, and many others. The possibility to build in specific recognition sites in the membrane promises a rigid transportation for specific substances. It is usually synthesized by phase inversion technique (Kobayashi et al., 2002).

BPA and its kind (EDCs) have molecular weight value of more than 200 $gmol^{-1}$. Referring to Figure 2.5 where it shows the filtration membrane limitation, it seems that separation of BPA or EDCs using basic ultrafiltration membrane alone wouldn't be much effective (Nghiem et al., 2005). Usually the adsorption is reported with the retention of nanofiltration or reverse osmosis. However, they need a higher driving force for operation, which restrict their application in drinking water treatment (Bing-zhi et al., 2010). So instead, researchers opt in an advanced yet straightforward technique, which is molecular

imprinted membrane (MIM) in separation or adsorption field (Zhao et al., 2008; Takeda et al., 2007).

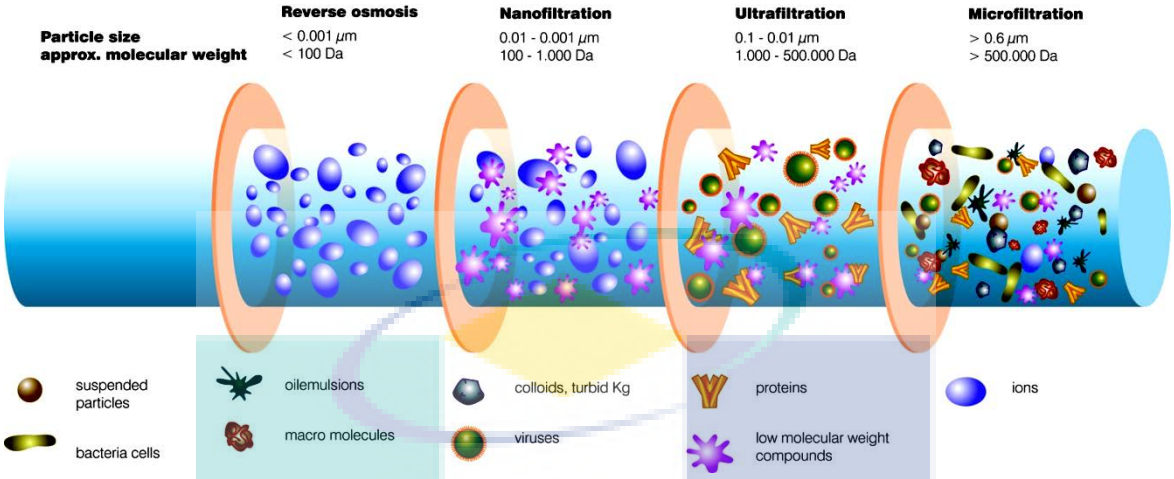

Figure 2.5: The use and limitation of membrane filtration system (Gérard and Maire, 2013). 1 Da = 1 $gmol^{-1}$

An imprinted membrane is able to distinguish selectively between target molecules and other molecules and it improved process separation (Tasselli et al., 2008). It can also bind the target molecule in continuous permeation operation (Takeda and Kobayashi, 2006). This technique attracted so many interests among researches and scientist for its unique properties. The MIP membrane had been prepared for the recognition of natural antioxidant compound or other various compounds such as flavonoid naringin (Tasselli et al., 2008), and tocopherol (Faizal et al., 2008), biomolecules (Silvestri et al., 2006), as well as hazardous environmental pollutants (Kobayashi et al., 2002; Takeda and Kobayashi, 2006; Zhang et al., 2007; Zhao et al., 2008).

Imprinted membranes are also advantageous in practical applications of medicine and technology, for example, as a selective binding and separation of medicinal chemicals (Suedee et al., 2004; Zhang et al., 2008), removal of turbidity (Yoshimi et al., 2010) and toxic compounds (Wang et al., 2008), and as sensors (Zhang et al., 2008). The major advantage of separation by using MIP membrane is that, the retained compound will not be released into the permeate when process requires high feed flow rate because the selected

compound has been selectively captured by the MIP hence, the process will not be affected.

Because of this advantage, author applied this MIP membrane by the technique hybridization of MIP (HMIP) with scaffold polymer. Another reason is that, handling powder-form MIP could be a little tedious since it could scatter in air easily. By utilizing this technique, it can also be observed how well the resultant nano-size MIP would be implanted into the membrane, and should the binding performance be enhanced. Figure 2.6 is the illustration of scaffold molecular imprinting procedure for imprinted membrane formation.

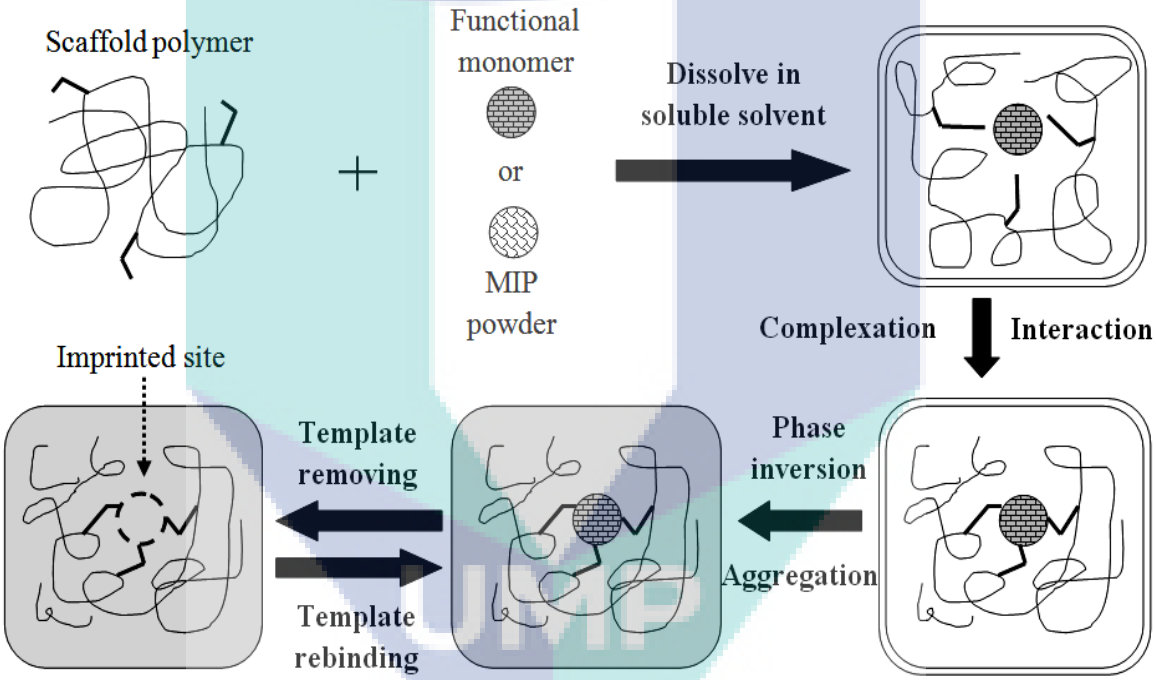

Figure 2.6: Illustration of scaffold molecular imprinting procedure for imprinted membrane formation

2.8 SUMMARY

The adverse effects of endocrine disruptor compounds (EDCs) rise concerns among consumers. Among all types of EDCs, one in particular, Bisphenol A (BPA), have been used extensively to produce plastic resins and can be found in waterways since it's the closest dump of waste discharging by numerous polymer factories and with the BPA being highly soluble in water, it could not be filtered completely by a simple filtration alone. Because of this, it could contaminate drinking water and endanger the consumers. Therefore, BPA is selected to be the template in this research to be able to recognize and trap BPA from water.

The technique to remove BPA in this study is the molecular imprinting technique (MIP). Due to its ability to entrap specific target molecule and having unique stability and properties, this MIP technique is more advantageous than others are, so far.

The size of MIP particles is considered to have effects on its binding performance. For that reason, this study aim to produce nanoparticles MIP. The ability to control nano-size MIP is assisted by the application of Full Factorial Design (FFD) using Design Expert 7.0.0 software, which is the novelty of this study. The four factors to be studied are polymerization temperature, rate of agitation, solvent to cross-linker ratio and percentage of initiator, selected based on its relevant and significant effect from others' past studies.

Further application of MIP will be consider as well by implant the resultant MIPs into a hybrid molecular imprinted membrane (HMIP). This application is useful as a support media for the MIP powder, which makes it easier to handle and preserve.

In the next chapter, detail elaboration on methodology of covalent imprinting, experimental design, phase inversion technique, and characterization test as well as performance analysis is shown.

CHAPTER 3

MATERIALS AND METHODOLOGY

This chapter discussed on the materials, methods and procedures applied in every experiment, which includes the preparation of materials, and the statistical and analytical method. Generally, the experiment can be divided into three (3) major parts, which are screening, characterization and performance study.

3.1 MATERIALS

Bisphenol A (BPA as the template, Bisphenol A dimethacrylate (BADM) as the functional monomer, 2,2'-Azobis(2-methylpropionitrile) (AIBN) as the initiator, Trimethylolpropane trimethacrylate (TRIM) as cross-linker, Polyethersulfone (PES) and Polysulfone (PSf) as polymer scaffold, dimethyl acetamide (DMAC) and N-methyl-pyrrolidone (NMP) for polymer solution were purchased from Sigma Aldrich.Co. Tetrahydrofuran (THF) as eluant, and Acetonitrile (ACN) as polar solvent were of HPLC grade were bought from Fisher Scientific. The main ingredients in the molecular imprinting for BPA are the functional monomer (BADM), and cross-linker (TRIM). Their chemical structures are given in Figure 3.1.

(a)

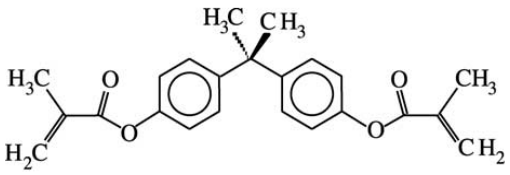

BADM

(b)

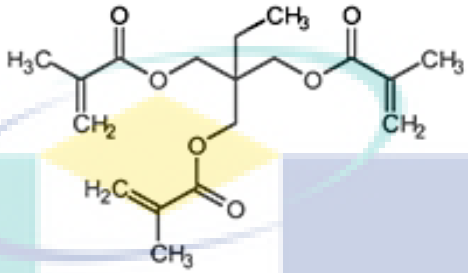

TRIM

Figure 3.1: Chemical structure of: (a) Bisphenol A dimethacrylate (BADM) (Takeda and Kobayashi, 2005) and (b) Trimethylolpropane trimethacrylate (TRIM) (Khasawneh et al., 2001)

3.2 PREPARATION OF MIP

Covalent precipitation polymerization approach was used to synthesis nano-size MIP spheres due to it simple and ease preparation procedure (Poma et al., 2010; Davies et al., 2004). Several sets of MIP were prepared using thermal initiation copolymerization by varying four selected factors, which are temperature, agitation, crosslinker to solvent ratios, and initiator percentage as described in Chapter 2 (see section 2.6.1). These factors were selected based on their importance and effect on the copolymerization as elaborated in Chapter 2 previously. Other factors such as monomer to cross-linker ratio and copolymerization time were fixed at constant value throughout the experiments. The detail on the factor variation will be explained later in the following section under experimental design part.

Figure 3.2 shows the steps involve in the preparation of MIP copolymer. Monomer of BADM was mixed with TRIM cross-linker at a ratio of 1 mol BADM:10 mol TRIM (Takeda and Kobayashi, 2005) in ACN solvent. This monomer solution was then introduced into 250 mL three-neck flask with the presence of AIBN as an initiator

under nitrogen atmosphere. The mixture was allowed to copolymerize for 12 hours. The resulting precipitate copolymer was centrifuged, filtered and gently crushed with pestle and mortar. Resultant copolymer particle was washed with ACN, followed by THF washing and finally filtered under vacuum. The polymer particle was stored in desiccator for further use.

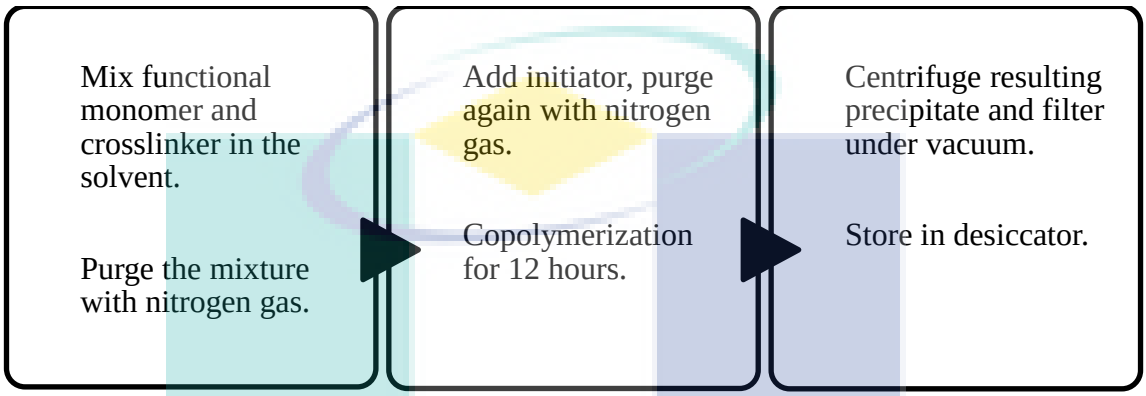

Figure 3.2: Flow of MIP preparation

Template removal was carried out via hydrolysis reaction in aqueous solution containing 1M Sodium Hydroxide (NaOH) at 50 ^{o}C with agitation until BPA concentration reached constant which the concentration reading were taken using UV-Visible Spectrophotometer (UV-Vis). The effect of the hydrolysis reaction was confirmed by the weight loss (*WL*) (Takeda and Kobayashi, 2005), evaluated using the following Eq. (3.1)

$$WL = \left[\left(\frac{W_{before} - W_{after}}{W_{before}}\right)\right] \times 100 \quad (3.1)$$

Here, W_{before} and W_{after}, represent the weights of the copolymer before and after the hydrolysis reaction, respectively.

The hydrolyzed polymers were washed with excess water until neutral pH. Non-imprinted polymer P(TRIM) were prepared following the same condition but without the functional monomer. The schematic diagram of BPA MIP synthesis was shown in Figure 3.3.

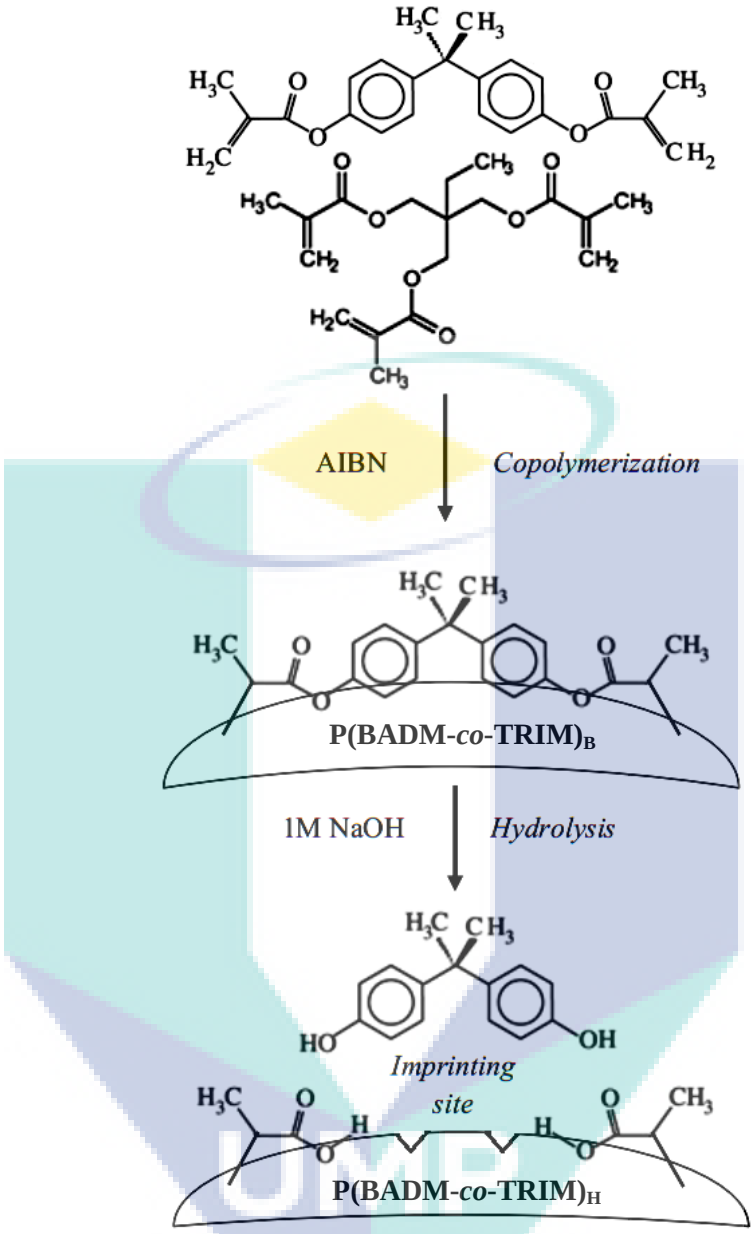

Figure 3.3: Schematic diagram of BPA imprinted copolymer synthesis. P(BADM-*co*-TRIM)$_B$ is BPA-MIP before hydrolysis and P(BADM-*co*-TRIM)$_H$ is BPA MIP after hydrolysis

3.3 CHARACTERIZATION OF MIP

To examine the copolymers characteristics, Fourier Transform Infra Red (FTIR) spectra and Scanning Electron Microscope (SEM) images were measured using FTIR Thermo Scientific Nicolet and SEM Carl Zeiss, respectively. Particle distribution was

analyzed using Mastersizer 2000 Particle Size Analyzer, Malvern. Transmission Electron Microscope (TEM) images were captured with TEM H7100 Hitachi. Image of MIP particles were also observed under Optical Microscope. The thermal properties of MIPs were investigated using Thermogravimetric Analyzer (TGA) Q500, TA Instruments. Surface area and pore size distribution was determined using Brunaer, Emmet and Taller method (BET) from Surface Area Analyzer (SURFER), Thermo Scientific. Flow chart of BPA-MIP characterization studies was presented in Figure 3.4.

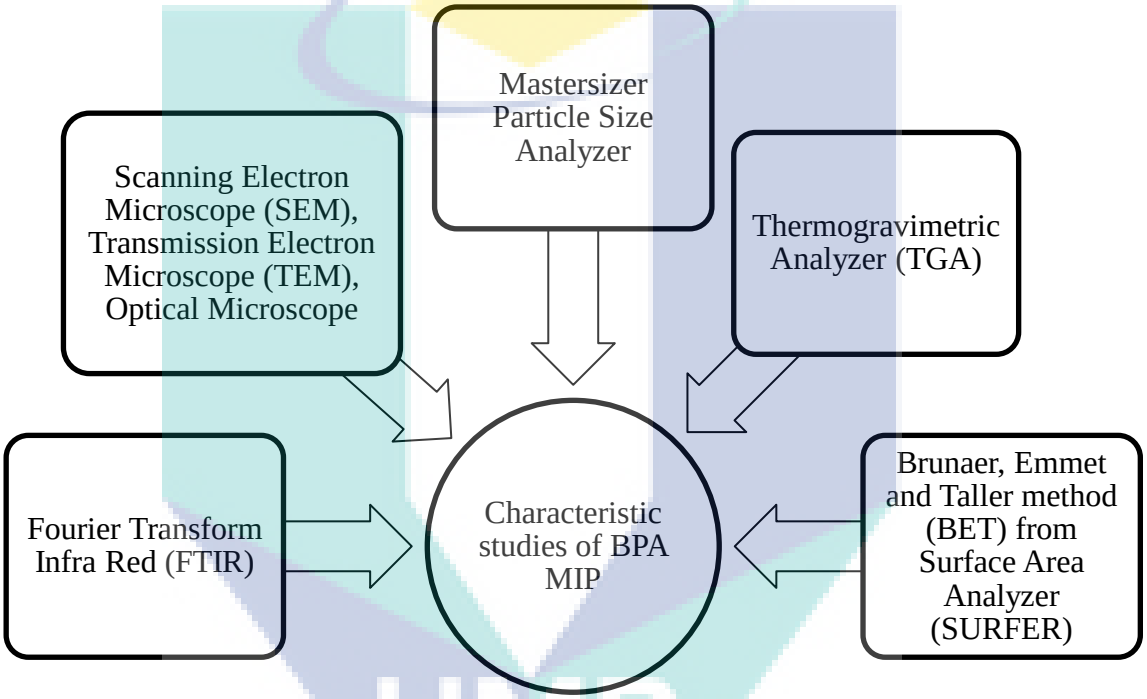

Figure 3.4: Flow chart of BPA-MIP characteristic studies

3.4 EXPERIMENTAL DESIGN

Design Expert Software (Stat-Ease Inc., Minneapolis, MN, USA, version 8.0.6) was used in the experimental design to screen the process parameters or factors involve during preparation of BPA-MIP particles. The full factorial design was applied which requires fewer measurements compare to the classical one-at-a-time experiment. Furthermore, this approach can detects and estimates any interaction between the factors, which the classical experiment cannot do. The order of experiments run was restrictedly randomized to eliminate the possible bias (in this case, the restricted factor was the polymerization temperature) (Koohpaei et al, 2008).

The standard approach to the analysis of the experimental design data is to evaluate a list of the main and two-way interaction effects supported by an ANOVA table, indicating which effects are significant (Zularisam et al, 2009). Four factors were selected that had potentially affected the binding efficiency. These factors can be grouped as compositional variable, which are amount of solvent for polymerization and amount of initiator, and operational variables, which are polymerization temperature and agitation rate. The range and levels of the factors investigated is shown in Table 3.1. The range was set based on findings in the literature.

Table 3.1: Factors with coded and actual levels used

Variable	Symbol	Real value of levels		
		-1	**0**	**+1**
Temperature (°C)	A	45	62.5	80
Agitation (rpm)	B	0	50	100
Solvent to crosslinker ratio (%)	C	50	65	80
Initiator percentage (%)	D	1	2	3

A two-level full factorial design of 2^4 was utilized following a linear regression model as in Eq. (3.2), indicating which effects are significant (Zularisam et al., 2009).

$$\hat{y}_i = b_0 + \sum_{i=1}^{n} b_i X_i \qquad (3.2)$$

In Eq.1, $\hat{y}_i$ represents the value of the response or depen-dent variable, b_0 is the interception coefficient, b_i the linear coefficients, n the number of variables studied, and X_i represents the coded independent variables.

A total of sixteen (16) sets of experiments and three (3) replicates at the center point were run to demonstrate the statistical significance of the temperature (*A*;^{o}C), agitation rate (*B*;rpm), amount of solvent (*C*;mol %), and amount of initiator (*D*;mol %) as shown in Table 3.2. The dependant variables selected are particle size, µm (Response 1) and binding capacity, µmol/g (Response 2). Only Response 1 will be discussed thoroughly in DOE software due to the main objective of this study, to control size of MIP particles.

Validation of the experimental design was performed by selecting the most desired condition with value of desirability in Ramp graph close to one (1). The percentage error was calculated with an acceptable range at below than 10%.

Table 3.2: The range and levels of the variables in the 2^4 full factorial design model

Run	Values of independent variables			
	A: Temperature [^{o}C]	**B: Agitation [rpm]**	**C: Solvent to crosslinker ratio [%]**	**D: Initiator percentage [%]**
MIP 1	80.00	100.00	50.00	1.00
MIP 2	80.00	0.00	80.00	1.00
MIP 3	45.00	100.00	80.00	1.00
MIP 4	80.00	0.00	80.00	3.00
MIP 5	80.00	100.00	80.00	3.00
MIP 6	80.00	0.00	50.00	1.00
MIP 7	45.00	0.00	50.00	3.00
MIP 8	45.00	100.00	50.00	3.00
MIP 9	45.00	0.00	80.00	1.00
MIP 10	80.00	100.00	50.00	3.00
MIP 11	62.50	50.00	65.00	2.00
MIP 12	45.00	100.00	80.00	3.00
MIP 13	45.00	100.00	50.00	1.00
MIP 14	45.00	0.00	80.00	3.00
MIP 15	45.00	0.00	50.00	1.00
MIP 16	80.00	0.00	50.00	3.00
MIP 17	80.00	100.00	80.00	1.00
MIP 18	62.50	50.00	65.00	2.00
MIP 19	62.50	50.00	65.00	2.00

3.5 BPA BINDING EXPERIMENTS

20 mg of MIP particle was added to 20 mL aqueous BPA solution with 200 µm concentration in glass flask. The mixture was shaken at 200 rpm at 30 ^{o}C for 24 hours. The final BPA concentration after binding was determined using the standard curve developed from UV-visible spectrophotometer by measuring the absorbance of solution at 275.5 nm. Figure 3.5 shows the standard curve developed for BPA concentration range of 20 µM to 500 µM. A control experiment was also conducted without the MIP particle in the BPA solution. The binding capacity, S [µmol/g] of BPA was calculated using Eq. (3.3) (Son et al., 2011)

$$[S] = \frac{(C_o - C_t)V}{W} \tag{3.3}$$

Where C_o and C_t represent the initial and final BPA concentration respectively, V is the volume of BPA solution and W is the weight of MIP.

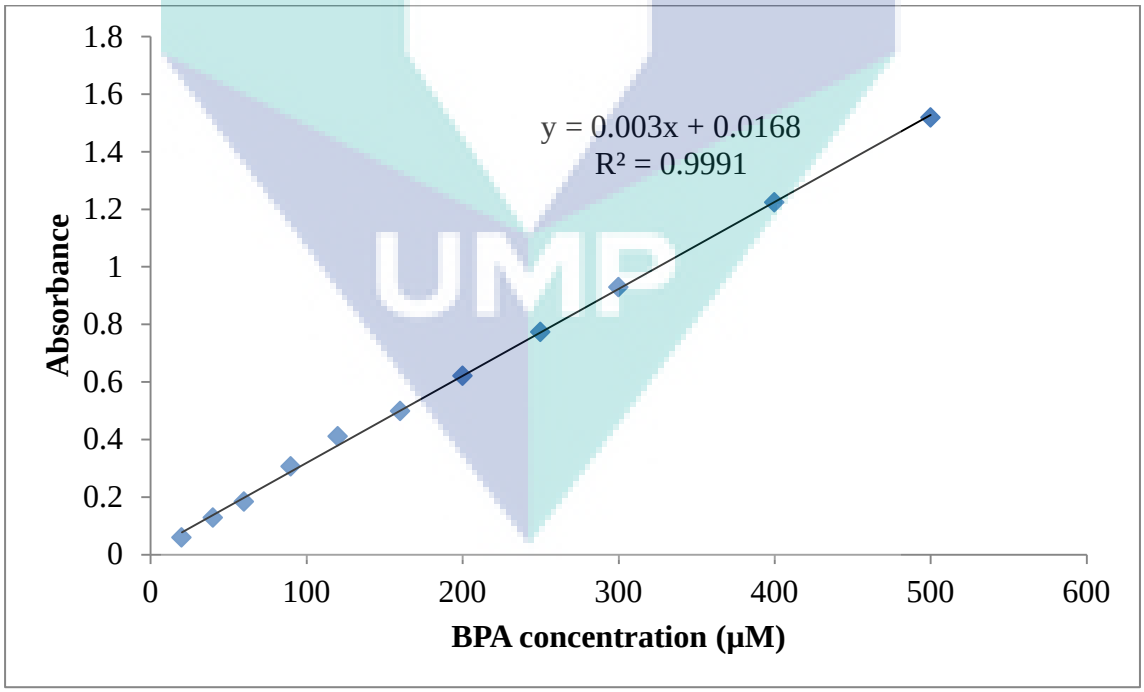

Figure 3.5: Absorbance-concentration standard curve of BPA at 275.5nm using UV-visible spectrophotometer

3.6 PREPARATION OF HYBRID MIP MEMBRANES

It is no doubt that the MIP particle had the ability to memorize it templates according to its shape and functionality. However, operate as in nano-size particle format; it can be easily dispersed into surrounding or difficult to recover back for reuse after binding. One possible alternative is by embedding the MIP particle in membrane matrix or known as hybrid molecular imprinting (HMIP) (Faizal et al, 2009). Phase inversion technique is used to prepare HMIP (Takeda and Kobayashi, 2006).

The preparation steps of HMIP membrane were shown in Figure 3.6. Two types of membrane polymers were used as scaffold media that is, polyethersulfone (PES) and polysulfone (PSf). Separately, PES and PSf was dissolved in their respective solution, DMAC and NMP, at 25 wt% concentration. BPA-MIP particles were mixed with membrane solution by stirring at 30 ^{o}C overnight. The BPA-MIP contents in the scaffold polymer solution were varied at 2 wt% and 5 wt%.

Conventional casting method was used to prepare flat sheet HMIP membrane. The homogenous MIP-scaffold polymer solution was spread uniformly on a glass plate and immersed in water at 25 ^{o}C to solidify the membrane. The resultant membrane was washed with excess water several times to remove the solvent. Blank membrane sheet was prepared following the same procedure without BPA-MIP particle inside it. The membranes were dried in 60 ^{o}C oven until the constant weight is achieved. SEM was used to characterize the structure of the HMIP membrane.

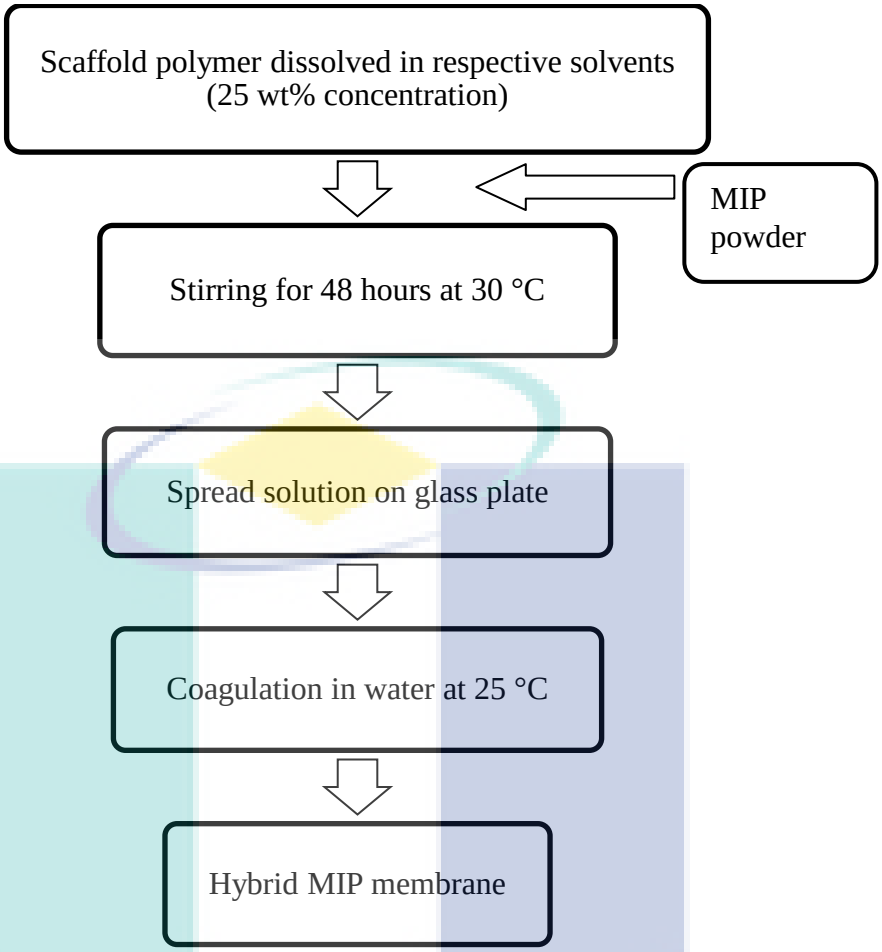

Figure 3.6: Flow of Hybrid polyethersulfone (PES) and polysulfone (PSf) membranes with P(BADM-*co*-TRIM)$_H$ MIP

3.7 BINDING EXPERIMENTS OF SUBSTRATE TO HMIP MEMBRANE

The membrane was cut in square with 2 cm x 2 cm dimension and bound to the 20 mL BPA solution of 200 µM for 48 hours. The same protocol and equation to determine BPA binding on MIP was followed for binding on HMIP (refer section 3.5).

3.8 SUMMARY

To summarize, method used to prepare molecular imprinted polymer (MIP) with Bisphenol A (BPA) recognition was precipitation polymerization with covalent approach. The control of BPA-MIP particle size was done with the screening of factors assisted by Full Factorial Design (FFD) consists of four investigated parameters which

were the temperature, agitation rate, solvent to crosslinker ratio, and amount of initiator. The analysis was discussed in detail through the next chapter. Characterization tests and performance study were carried out to determine the structure and properties of resultant BPA-MIP. The application of molecular imprinted membrane was also performed by hybridization of scaffold polymers with the BPA-MIP (HMIP) to enhance the binding performance and for the ease of handling powder formed MIP. The properties and morphologies of HMIP were observed in general to verify the successfulness of embedded MIP.

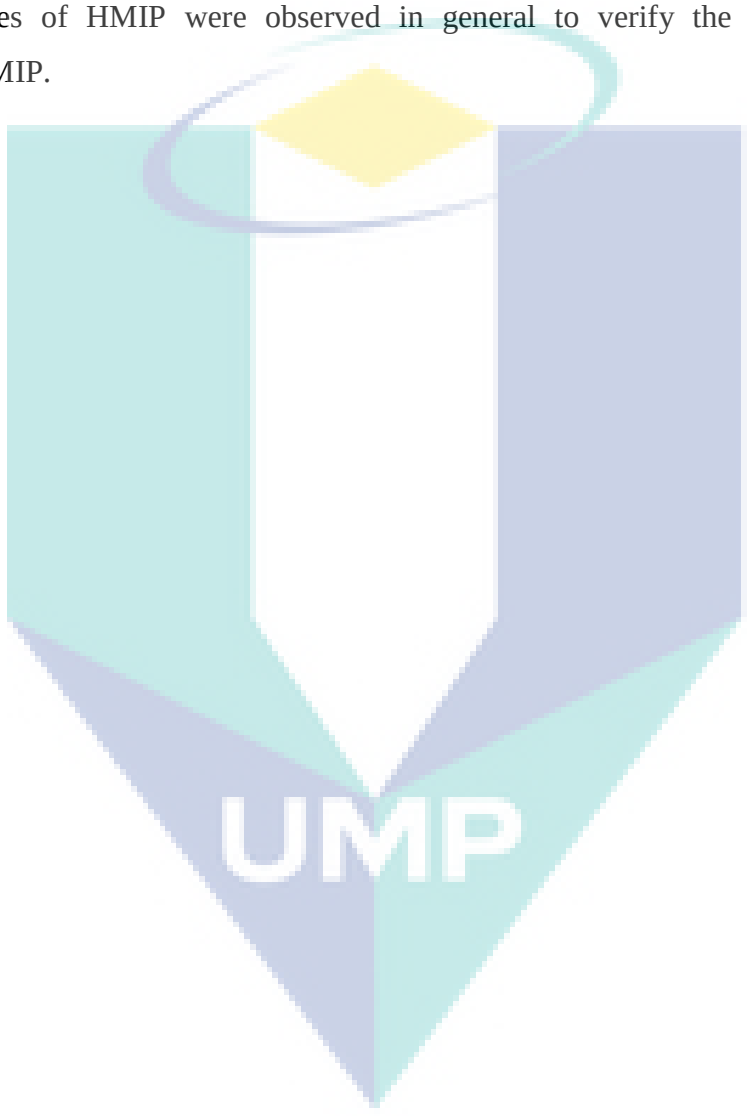

CHAPTER 4

RESULTS AND DISCUSSIONS

4.1 EXPERIMENTAL DESIGN – TWO LEVEL FACTORIAL

A systematic experimental data analysis using a complete 2^4 factorial design by Design Expert software was conducted to examine the effects of four factors and their interaction on the particle size of BPA-MIP. The factors studied are polymerization temperature (A), rate of agitation (B), solvent to crosslinker ratio (C) and percentage of initiator (D). Table 4.1 summarized the responses obtained in 16 sets of experiments run using a complete 2^4 factorial design at low and high levels of factor A, B, C and D. The effect of each factor or their interaction can be determined by monitoring the change of response at different level of the factor (Gottipati and Mishra, 2010).

As stated in Chapter 3, only the model for Response 1 (particle size) is discussed thoroughly in order to investigate the correlation of factors on controlling the size of particles. Pareto chart plot, normal probability plots, interaction effects plot, and surface contour plot were used to evaluate the influence of factors on the particle size of BPA-MIP particle. ANOVA and P-value significant levels were used to check the significance of the effect on particle size of BPA-MIP copolymers.

Table 4.1: List of experiment in 2^4 full factorial design model set randomly by the software.

Formatted: Indent: Left: 2.06 cm

Formatted Table

Run	Values of independent variables				Values of responses	
	A: Temperature (°C)	B: Agitation (rpm)	C: Solvent to crosslinker ratio (mol%)	D: Initiator percentage (mol%)	Mean Particle size (nm)	Binding capacity (µmol/g)
MIP 1	80.00	100.00	50.00	1.00	160	99.03
MIP 2	80.00	0.00	80.00	1.00	110	95.81
MIP 3	45.00	100.00	80.00	1.00	30	-
MIP 4	80.00	0.00	80.00	3.00	120	89.68
MIP 5	80.00	100.00	80.00	3.00	130	96.13
MIP 6	80.00	0.00	50.00	1.00	2000	92.90
MIP 7	45.00	0.00	50.00	3.00	120	90.65
MIP 8	45.00	100.00	50.00	3.00	30	-
MIP 9	45.00	0.00	80.00	1.00	100	82.26
MIP 10	80.00	100.00	50.00	3.00	2000	96.13
MIP 11	62.50	50.00	65.00	2.00	110	95.16
MIP 12	45.00	100.00	80.00	3.00	120	93.55
MIP 13	45.00	100.00	50.00	1.00	30	-
MIP 14	45.00	0.00	80.00	3.00	110	95.48
MIP 15	45.00	0.00	50.00	1.00	100	102.26
MIP 16	80.00	0.00	50.00	3.00	100	77.74
MIP 17	80.00	100.00	80.00	1.00	110	93.23
MIP 18	62.50	50.00	65.00	2.00	90	96.13
MIP 19	62.50	50.00	65.00	2.00	90	93.55

4.1.1 STUDENT'S T-TEST

Table 4.2 was generated from the experimental design in conjunction with the inserted data of particle size. It shows the percentage of contribution for individual factors and their interactions. In the first column, the symbol M represent selected model and E represent error. They were manually assigned based on their percentage of contribution. Any contributions below than 0.05% were excluded from the model except for main factors B and D. All individual factors will be elaborated accordingly. Since the method chosen in this study is the two-level factorial design, only two-way interactions are discussed herein.

Table 4.2: List of contribution effects on main factors and their interactions generated by the experimental design

Formatted: Indent: Left: 1.9 cm

Term	Stdized Effects	Sum of Squares	% Contribution
Intercept			
A-Temperature	511.25	1.046E+006	16.09
B-Agitation	-18.75	1406.25	0.022
C-Solvent ratio	-463.75	8.603E+005	13.24
D-% initiator	11.25	506.25	7.792E-003
AB	36.25	5256.25	0.081
AC	-483.75	9.361E+005	14.41
AD	-18.75	1406.25	0.022
BC	6.25	156.25	2.405E-003
BD	476.25	9.073E+005	13.96
CD	21.25	1806.25	0.028
ABC	-18.75	1406.25	0.022
ABD	461.25	8.510E+005	13.10
ACD	1.25	6.25	9.620E-005
BCD	-453.75	8.236E+005	12.68
ABCD	-478.75	9.168E+005	14.11
Curvature	-25943.33	1.443E+005	2.22
Lack Of Fit		0.000	0.000
Pure Error		266.67	4.105E-003
Lenth's ME	56.68		
Lenth's SME	103.93		

Student's t-test was employed to determine the significance of the regression coefficients of model. Horizontal line in Pareto chart shown in Figure 4.1 indicates the minimum statistically significant effect magnitude for a 95% confidence level, while the vertical bar lines showed the t-value for each effect. Based on Pareto chart, the t-value was equal to 4.3 for 95% of confidence level. The temperature (A) and solvent to crosslinker ratio (C) factor have a significant effect on BPA-MIP particle size. Besides that, the interaction among factors also had a pronounced effect on particle size such as interaction of AC, BD, ABD, BCD and ABCD. Any factor that showed the t-value above the 4.3 was statistically significant at 95% confidence (Bingol et al., 2010). Factors that show lower value than 4.3 can be ignored unless they are the main factor (such as C and D). The contribution and role of all main factors should be studied~~y~~ and analyzed in the model. A model with an adjusted square correlation coefficient (R^2 adj) of 94.8 % based on ANOVA analysis (will be discussed later in next section) has been derived as in Eq.~~uation~~ (4.1)~~;~~

$$Particle\ size = 297.89 + 255.63A - 9.38B - 231.88C + 5.63D + 18.13AB - 241.88AC + 238.12BD + 230.62ABD - 226.88BCD - 239.37ABCD \quad (4.1)$$

where A is for temperature, B is agitation, C is solvent to crosslinker ratio, D is percentage of initiator and AB, AC, BD, ABD, BCD and $ABCD$ are the interactions involved in the process.

~~Particle size = 297.89 + 255.63 × A - 9.38 × B - 231.88 × C + 5.63 × D + 18.13 × A × B - 241.88 × A × C + 238.12 × B × D + 230.62 × A × B × D - 226.88 × B × C × D - 239.37 × A × B × C × D (4.1)~~

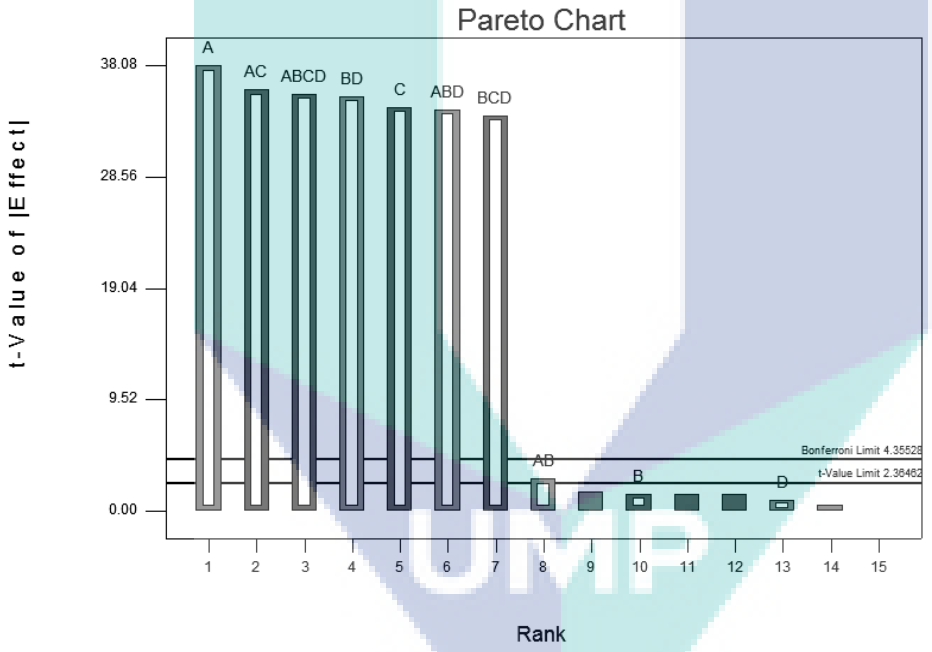

Figure 4.1: Pareto chart representing t-value for the model on particle size of BPA-MIP

Another way to identify the effects of factors or their interactions to the response is by using normal probability plot as shown in Figure 4.2. In the figure, points that fall closely to the fitted line at the middle of the plot show the insignificant effect on the response. Whereas, points that located further away from this line are likely

Formatted: Font: (Intl) Times New Roman
Formatted: Font: (Intl) Times New Roman
Formatted: Font: (Intl) Times New Roman
Formatted: Font: (Intl) Times New Roman
Formatted: Indent: Left: 0 cm, First line: 0 cm
Formatted: Font: (Intl) Times New Roman
Formatted: Font: (Intl) Times New Roman
Formatted: Font: (Intl) Times New Roman
Formatted: Font: (Intl) Times New Roman
Formatted: Font: (Intl) Times New Roman
Formatted: Font: (Intl) Times New Roman
Formatted: Font: Italic
Formatted: Font: Italic
Formatted: Font: Italic
Formatted: Font: Italic
Formatted: Font: Italic
Formatted: Font: Italic
Formatted: Font: Italic
Formatted: Font: Italic
Formatted: Font: Italic
Formatted: Font: Italic
Formatted: Indent: Left: 2.22 cm

representing the significant factor that affects the response (Brasil et al., 2006; Palanikumar and Dawim, 2009). It is clearly showed in Figure 4.2 that two main factor (A and C) and combination of factor AC, BD, BCD, ABD, and ABCD gave a greater effect on the particle size of BPA-MIP. Points that located on the left region of the line had a negative effect of contribution and points on the right had a positive effect. The negative and positive sign indicates whether the effects will decrease or increase the particle size respectively. Temperature factor (A) located furthest from the middle line had the largest effect on the response at the right region of the plot. Meanwhile at the left region, interaction of temperature and solvent to crosslinker ratio (AC) gives the largest effect on the response. Based on the standardized effect value of x-axis (the exact value can be obtained from Table 4.1), the effects of factors decreased as A>AC>ABCD>BD>C>ABD>BCD>AB similar with Pareto chart analysis previously.

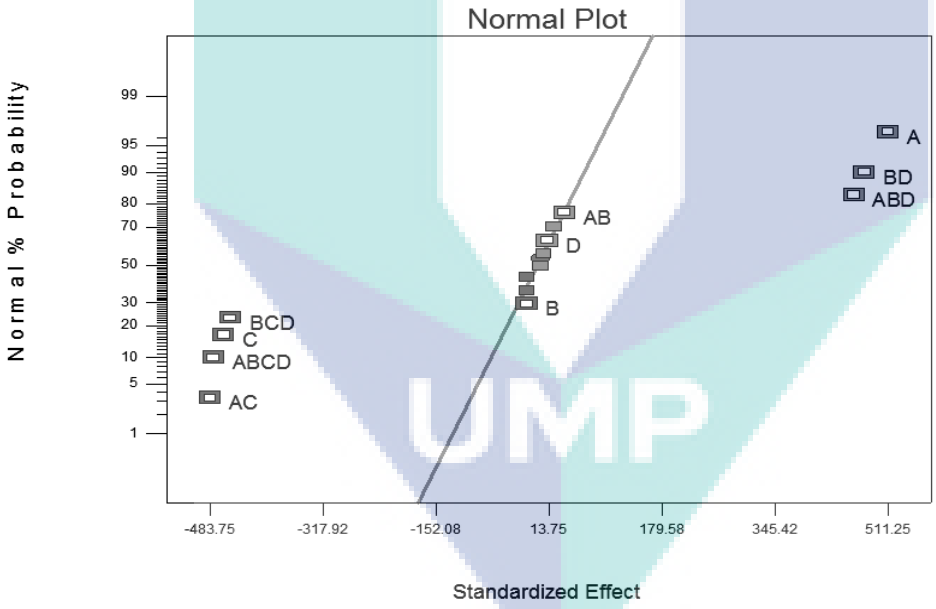

Figure 4.2: Normal probability plot of standardized effects on BPA-MIP particle size

4.1.2 ANALYSIS OF VARIENCE (ANOVA)

A statistical testing using Fisher's statistical test of ANOVA is shown in Table 4.3. In the table, sum of squares (SS) value is reflected to the importance of the factors

in the process. As the value of the SS increases, the significance of the corresponding factor also increases (Gottipati and Mishra, 2010).

Table 4.3: ANOVA for 2^4 full factorial design; response: particle size (nm)

Source	Effect	Coefficient	Sum of squares	F-value	Prob>F
Model		297.89	6.348E+006	880.23	< 0.0001[a]
A	16.0923	255.63	1.046E+006	1449.81	< 0.0001
B	0.0216449	-9.38	1406.25	1.95	0.2053
C	13.241	-231.88	8.603E+005	1192.93	< 0.0001
D	0.00779216	5.62	506.25	0.70	0.4298
AB	0.0809038	18.12	5256.25	7.29	0.0306
AC	14.4077	-241.88	9.361E+005	1298.04	< 0.0001
BD	13.9644	238.13	9.073E+005	1258.10	< 0.0001
ABD	13.0986	230.63	8.510E+005	1180.10	< 0.0001
BCD	12.6761	-226.88	8.236E+005	1142.03	< 0.0001
ABCD	14.1114	-239.38	9.168E+005	1271.35	< 0.0001
Curvature	2.22037	-238.96	1.443E+005	200.04	< 0.0001[a]
Residual			5047.92		
Lack of Fit			4781.25	7.17	0.1269[b]
Pure Error			266.67		
Cor Total			6.497E+006		
R^2	0.9770				
Adjusted R^2	0.9483				
Predicted R^2	0.9383				

Values of "Prob>F" less than 0.0500 indicate model terms are significant.
[a] Significant.
[b] Not Significant

The degree of significance can be ranked based on the F-ratio value. High F-value, normally correspond to small p-value, indicates the significant of the model and individual coefficient (Zularisam et al., 2009). Based on F-value in Table 4.3~~2~~, the main factor of A and C, and the interaction of factor ~~AB,~~ AC, BD, ABD, BCD and ABCD were significant on the effect of the BPA-MIP particle size. Two other main factors B and D and interaction AB exhibit less effect on the particle size as their confidence level

were less than 95% (P>0.05), but are still included in the model to be able to construct a significant model.

Value for R^2 presented from ANOVA analysis is 0.9770. Adjusted R^2 and predicted R^2 values are 0.9483 and 0.9383, respectively. A high value of R^2 is most desirable where it indicates there is very little variation around the average predictions of the model. If the model is significant, lack of fit insignificant, adjusted and predicted R^2 values are within 0.2 of each other, and the residuals are well fitted; then the model provides good predictions for average outcomes (Stat-Ease, 2011).

Among all two-ways interaction factor, AC interaction had the highest coefficient value. This was as expected since both individual main factor A and C showed highest significant effect on the particle size. The interaction of BD and AB are also significant.

Moreover, the coefficient value in ANOVA Ttable 4.32 can be used to explain the role and effect of main factors; A, B, C and D. These values represent the results of regression analysis and could provide a better explanation of the process. Coefficient values can be positive and negative depending on the directions of the effect. Positive value indicates that particle size is increased with the increase of factor. In contrast, particle size is decreased with the increase of factor for the negative coefficient value. The value of coefficient itself correspond to the degree of response change with the changed of factor. In addition, the coefficient value can also be related to the statistical significance of a factor to the process (Bingol et al. 2010).

Based on the coefficient value, the ascending order of main factor is as followed: A (255.63), C (-231.88), B (-9.38) and D (5.62). The particle size is increased with temperature (factor A) and decreased with ratio of solvent to crosslinker (factor C). However A had a greater effect on size of particles compared to C, based on the value of coefficient. Both factor B, agitation and D, initiator percentage had less effect on the particle size of BPA-MIP.

The distribution of residual values, defined as the difference between the predicted and the observed value were examined. Figure 4.3 showed the normal probability plot of residual values for the BPA-MIP particle size. It showed that the set of observed values closely followed the theoretical distribution. The experimental points were satisfactorily aligned, indicating a normal distribution which selected model sufficiently described the observed data.

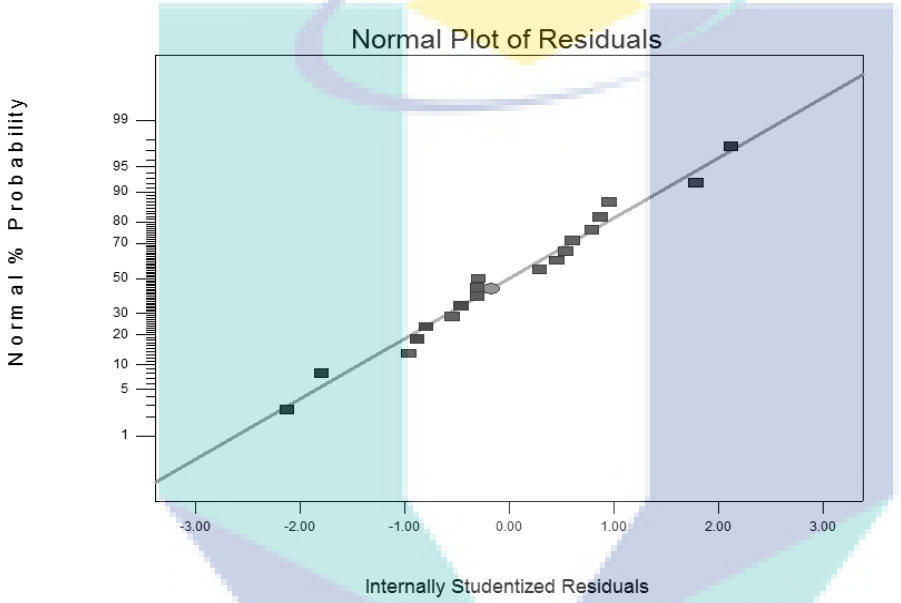

Figure 4.3: Normal probability of studentized residuals on BPA-MIP particle size

4.1.3 EFFECTS OF INTERACTION FACTORS

Figure 4.4 shows the effect of two factors interaction on the BPA-MIP particle size. The plots give a two nonparallel lines which indicate that the effect of one factor depends on the level of the other factor (Stat-Ease, 2011). In right side plot, downward slopes show that the increment of factor will decrease the particle size, and vice versa. Besides that, line with longer extension showed that the interaction factor had higher significance and contribution. Based on the plot, the interaction of AC gave the highest significant value followed by BD and AB.

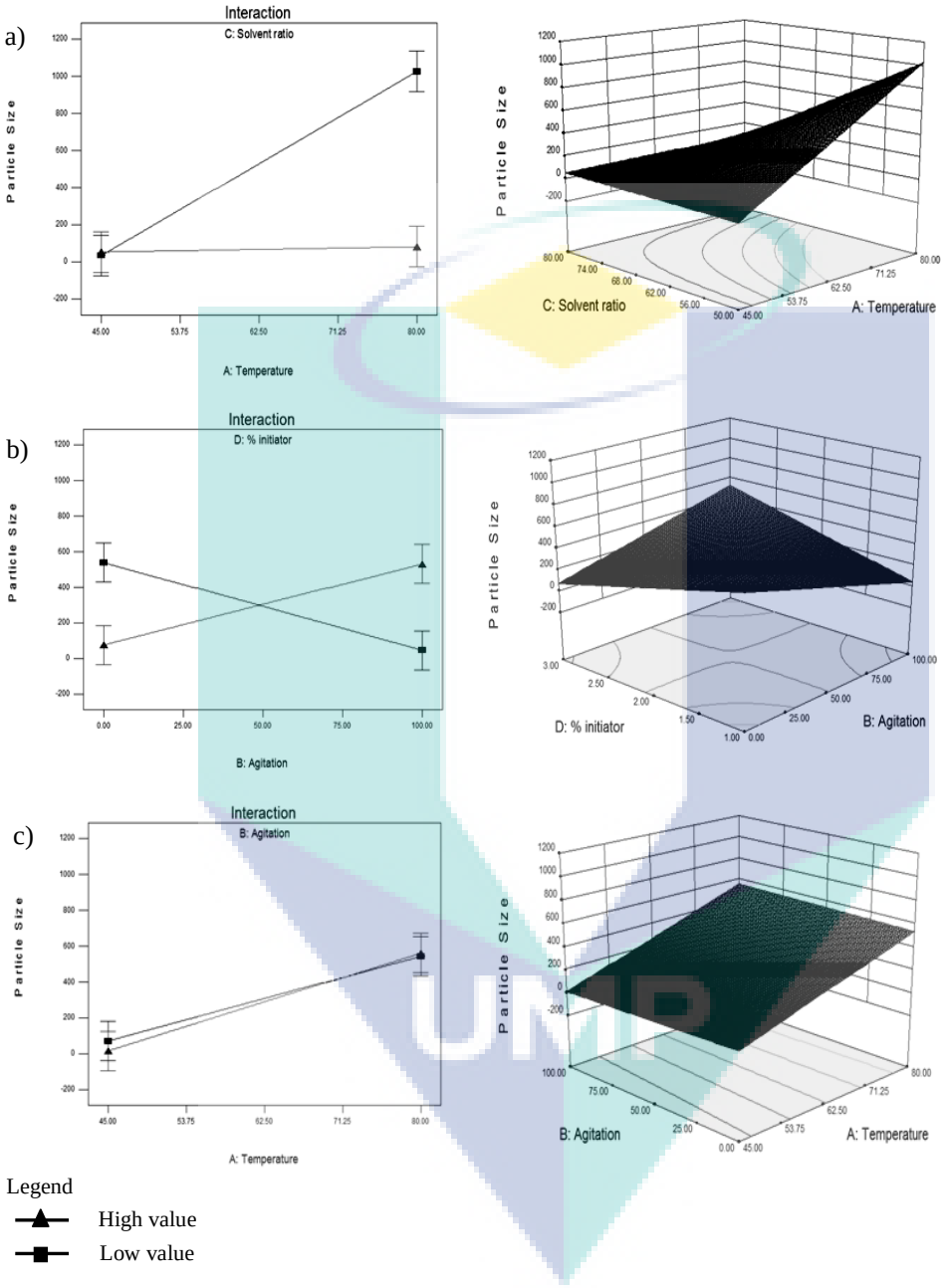

Figure 4.4: Plot of interaction effect for BPA-MIP particle size (nm): (a) effect between temperature and solvent to crosslinker ratio (AC), (b) effect between agitation and initiator percentage (BD), (c) effect between temperature and agitation (AB)

Figure 4.4 (a) illustrate two lines represent high and low solvent to crosslinker ratio (C) at different temperature (A). At low solvent to crosslinker ratio, the particle size increased with temperature. However, at high solvent to crosslinker ratio, the particle size did not affect too much by temperature, maintaining a value around 100 nm.

The role of temperature in BPA-MIP synthesis is as the drivinge force for copolymerization to occur. Normally, low temperature is enough to initiate the process and at the same time stabilize the complex reaction. High temperature often gives unsatisfactory influence in copolymerization in terms of the size of copolymers and rigidity of its structure (Mijangos et al., 2006; Lu et al., 2004)

Meanwhile, the use of solvent is to allow a swelling medium for polymers in order to create its morphology and pore (Koohpaei et al., 2008). Solvent used usually had the porogenic ability that is released in vapors during the reaction. This ability could alter the copolymers 3-dimensional functional groups structure configuration.

At low amount of solvent, the function of solvent as surrounding medium for the copolymerization was affected by the rising of temperature. It showed rapid increasing size of particles. Meanwhile, a stable reaction and maintained particle size is observed using high amount of solvent even when temperature increases. However, the abundance of surround medium diluting the monomers reaction that the copolymerization was distracted slowly occuring and almost didn't occurunchanged even at high temperature.

This behavior can be observed when varying factor A while keeping factor B and D constant at no agitation and 1% initiator during BPA-MIP synthesis. Particle size of BPA-MIP is maintained at approximately 100 to 110 nm when using high solvent to crosslinker ratio throughout increasing polymerization temperature. On the other hand, bigger size particle is obtained at high temperature when using low solvent to crosslinker ratio. Table 4.4 shows four MIPs at different values of factor A and C.

Table 4.4: The interaction effect of AC on BPA-MIP particle size. Factor B is kept at no agitation and factor D at 1 % initiator

A (°C)	C (%)	B (rpm)	D (%)	Particle size (nm)	MIP Run
45	50	0	1	100	MIP 15
45	80	0	1	100	MIP 9
80	50	0	1	2000	MIP 6
80	80	0	1	110	MIP 2

Meanwhile, Figure 4.4 (b) shows at high amount of initiator, the particle size of BPA-MIP increase as the agitation increasing. However, the opposite direction is observed for the low amount of initiator.

Agitation provides efficient dispersion of monomers in the solution mixture to help control the diameter of MIP produced. The speeding mixture would cause decreasing of the complex polymer length chain and because of that, the number of polymer particles would be increasing due to the nuclei aggregation (Faizal et al., 2009). This behavior resulted in smaller particle size with evenly distributed uniformity.

On the other hand, the role of initiator is to initiate the formation of a high amount of free radicals that would generate large number of growing nuclei and globules which then would produce smaller size of particles. These small size globules would then generate a large number of small pores into the MIP spheres and possessed a large surface area all at one (Mijangos et al., 2006).

The opposite direction of slopes in Figure 4.4 (b), indicate that; 1) at high use of initiator, heat would produced due to growing free radicals, and adding heat to the reaction could force the copolymerization to react rapidly and could disrupt the complex formation mechanism. Speed of agitation used could not help to stabilize the polymer chain and maintaining the particle size of BPA-MIP copolymers from increasing rapidly; 2) at low initiator, although the free radicals was limited, they were sufficiently enough to generate nuclei without any excess heat, and agitation could help in

separating polymer chain evenly into smaller particle size. The more speed introduced, the smaller the size of particle obtained.

These two lines intersected in the middle of the plot. This means that a moderate usage of both agitation and initiator appeared to be the most appropriate in maintaining the desired size of copolymers, which for this study, in the range of 100 to 150 nm.

Table 4.5 presents four MIP particle sizes at different values of factor B and D. When agitation is increasing, the particle size also increases from 100 nm to 2 µm approximately, using high amount of initiator. But oppositely, size of particles decrease from 2 µm to around 160 nm using low initiator amount.

Table 4.5: The interaction effect of BD on BPA-MIP particle size. Factor A is kept at 80 ^{o}C temperature and factor C at 50 % solvent to crosslinker ratio

B (rpm)	D (%)	A (^{o}C)	C (%)	Particle size (nm)	MIP Run
0	1	80	50	2000	MIP 6
100	1	80	50	160	MIP 1
0	3	80	50	100	MIP 16
100	3	80	50	2000	MIP 10

Figure 4.4 (c) shows the least contribution value of interaction factors, which was factor A, temperature and B, agitation. There was no obvious difference between both lines. The particle size of BPA-MIPs is increased with temperature for both cases of high and low agitation speed.

As mentioned earlier, temperature is functioned as a driving force for copolymerization. Normally, low temperature is enough to stabilize the monomer reaction. Meanwhile, high temperature could disrupt the reaction mechanism of copolymers. However, agitation helps in controlling the polymer diameter, where the speed causing the decrease in polymer chain length and producing high yield of small size copolymers.

Table 4.6 shows the data obtained according to AC interaction pattern. At both low and high agitation, size of BPA-MIP increase when temperature increases. The use of agitation to control the polymer size as well as stabilize the reaction mechanism seems ineffective because at high agitation, the resultant size of particles keep increasing with temperature. This interaction confirmed that the effect of temperature is superior than agitation speed.

Table 4.6: The interaction effect of AB on BPA-MIP particle size. Factor C is kept at 50 % solvent to crosslinker ratio and factor D at 1 % initiator

A (^{o}C)	B (rpm)	C (%)	D (%)	Particle size (nm)	MIP Run
45	0	50	1	100	MIP 15
80	0	50	1	2000	MIP 6
45	100	50	1	30	MIP 13
80	100	50	1	160	MIP 1

4.2 CHARACTERIZATION OF BPA-MIP COPOLYMER

All resultant copolymers undergone characterization analysis to determine and verify the polymer structure, rigidity, stability and strength properties. The copolymers were tested using FTIR, SEM, TEM, Optical Microscope, UV-Vis, Mastersizer, TGA and SURFER.

4.2.1 FOURIER TRANSFORM INFRA RED (FTIR)

The chemical functional group of BPA-MIP copolymer and it derivatives was analyzed using FTIR equipment. Figure 4.5 shows the IR spectra of BPA, BADM and P(BADM-*co*-TRIM)$_{B}$ for MIP before hydrolysis and P(BADM-*co*-TRIM)$_{H}$ for MIP after hydrolysis, while Table 4.7 summarize the peaks appeared in the IR spectra.

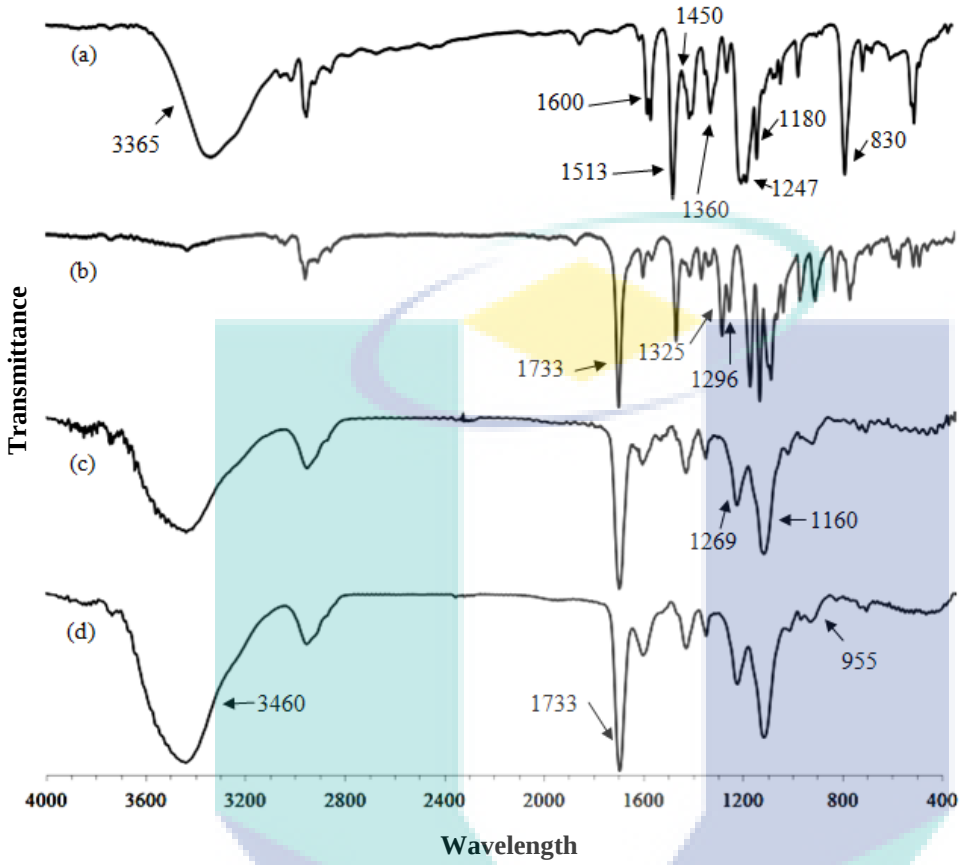

Figure 4.5: FTIR spectra of (a) Bisphenol A, (b) BADM, (c) P(BADM-*co*-TRIM)$_B$, (d) P(BADM-*co*-TRIM)$_H$

Table 4.7: Summary of peaks from Figure 4.5

Figure	Wavelength (cm^{-1})	Peaks
(a) BPA	3365	O-H stretch: Hydrogen bonded phenol group
	1600, 1513	C=C bend: Aromatic bonding
	1450, 1360	$-CH_3$ bond: Symmetric and asymmetric alkane
	1247, 1180	C-O stretch: Phenol skeleton
	830	C-H peak: Aromatic bonding
(b) BADM	1733	C=O stretch: Strong ester functional group
	1325, 1296	C-O peak: Ester functional group
(c) P(BADM-*co*-TRIM)$_B$	1733	C=O peak: ester bond
	1269, 1160	C-O stretch: shifting symmetric and asymmetric ester stretch
(d) P(BADM-*co*-TRIM)$_H$	3460	-COOH group increasing after hydrolysis

Formatted Table

Formatted Table

In Figure 4.5 (a), the major peaks of BPA IR spectra were observed at wavelength 3365 cm^{-1} for O-H stretch indicating the presence of hydrogen bonded phenol group, and also strong peaks at 1247 $cm^{-1}$and 1180 cm^{-1} assigned as the C-O stretch for the phenol skeleton. An aromatic bonding C-H group was appeared at 830 cm^{-1} while C=C bond was clear at 1600cm^{-1} and 1513 cm^{-1}. The IR bands at 1450 cm^{-1} and 1360 cm^{-1} was assigned as the symmetric and asymmetric $-CH_3$ bonding.

For the functional monomer, BADM, as in Figure 4.5 (b), it is clear that the hydroxyl stretch (3365 cm^{-1}) in BPA disappeared which verified the coupling between bisphenol A and methyl methacrylate, producing the BADM functional monomer. In line with the disappearances of that peak, a new significant peak appeared at 1733 cm^{-1} indicating strong C=O ester group in the monomer. Also, high signal intensity at 1325 and 1296 cm^{-1} matched with the presence of C-O ester functional group.

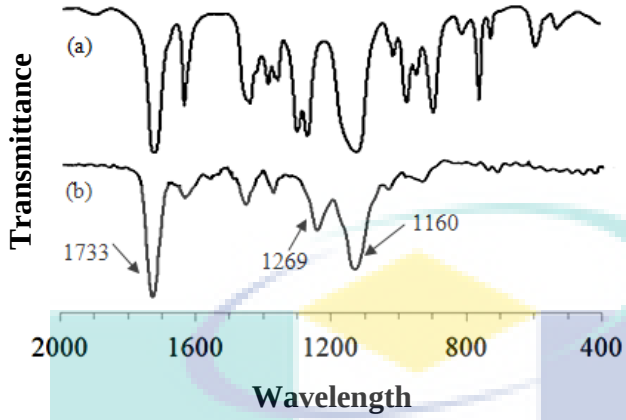

Figure 4.6: FTIR spectra of (a) TRIM, (b) P(BADM-*co*-TRIM)$_B$

P(BADM-co-TRIM)$_B$ shows strong ester bond C=O at 1733 cm^{-1} and a shift of symmetric and asymmetric C-O stretch at bands 1269 cm^{-1} and 1160 cm^{-1} indicating TRIM segments in the copolymers as shown in Figure 4.6. Therefore, the appearance of C-O group demonstrated the BPA-MIP had been successfully prepared. It is observed that peak near 955 cm^{-1} in BADM was decreasing in P(BADM-*co*-TRIM) before and after hydrolysis due to the out-of-plane alkene C-H bending vibration. There is also a significant broad peak at 3460 cm^{-1} after hydrolysis signifying the formation of –COOH group in the copolymers.

4.2.2 MORPHOLOGY OF BPA-MIP

The morphology of the BPA-MIP copolymers was observed under TEM and optical microscope as shown in Figure 4.7 with size of particle ranging from 30 nm to 150 nm. In the figure, due to limitation of equipment at the time of study, particle size below 100 nm is presented in TEM image and particle size in the range 100 to 150 nm is showed in optical microscopic image. Only images of BPA-MIP on the effect of factor A (temperature) is presented since temperature is the most significant factor between all four as determined earlier. Although it has been elaborated thoroughly in subchapter 4.1.3, this subchapter shows graphic illustration of the resultant BPA-MIP particle size.

(a)

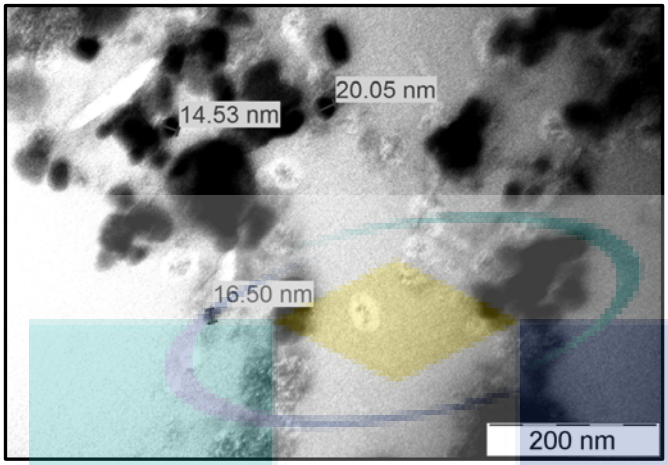

(b)

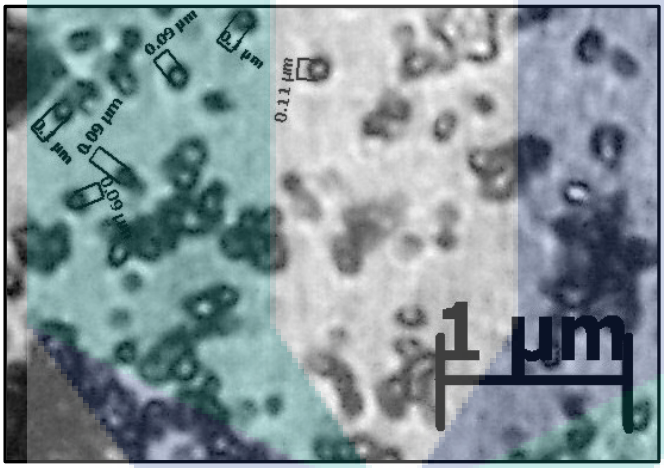

Figure 4.7: Morphology of BPA-MIP: (a) MIP 3 (45 ^{o}C) under TEM, and (b) MIP 17 (80 ^{o}C) under Optical Microscope

Figure 4.7 shows the TEM image of MIP 3 (a) and optical micrographs of MIP 17 (b). MIP 3 and MIP 17 were synthesized at different temperature of 45 ^{o}C and 80^{o}C respectively, while other factors are kept constant at 100 rpm agitation, 80% solvent to crosslinker ratio and 1% initiator. As discussed earlier, the use of low temperature is enough in providing heat to initiate copolymerization and at the same time stabilize reaction between monomers. On the other hand, high temperature could disrupt the complexity of the polymer formation and would produce undesirably bigger particle size (Mijangos et al., 2006; Lu et al., 2004).

From Figure 4.7 (a), MIP 3 with particle size at approximately 30 nm was obtained using 45 ^{o}C temperature. Although small nano-size particle was most desirable in serving the main objective, MIP 3 was difficult to recover for further analysis due to very low polymer yield. However, in Figure 4.7 (b), MIP 17 with particle size at approximately 110 nm was obtained using 80 ^{o}C temperature. Even though MIP 17 was slightly bigger nano-size than MIP 3, the polymer powder produced was easily recovered to be kept for further analysis. Besides, the particle size obtained is within the desirable range of nano-size, from 100 to 150 nm. It can be said that, a moderate value of temperature should be control to ensure the fabrication of desirable nano-size particle BPA-MIP.

4.2.3 PARTICLE SIZE DISTRIBUTION

Particle size distribution of MIP copolymer before and after hydrolysis was analyzed using Mastersizer. Figure 4.8 shows the particle size distribution of two selected MIPs, MIP 5 and MIP 12 prepared at different temperature. The particle size distribution of a rigid polymer showed considerably equal before and after hydrolysis proving that it possesses high solvent resistance.

From Figure 4.8, particle size distribution after hydrolysis was reduced by approximately 20 nm only for both MIP 5 and MIP 12. It is clearly observed that the uniformity and monodispersity of the spheres were well maintained after hydrolysis, and no obvious particle size deviation has been detected. It showed that these MIPs were stable and solvent resistant. According to Piletsky et al. (2001), MIPs have unique stability superior similar that demonstrated by natural biomolecules.

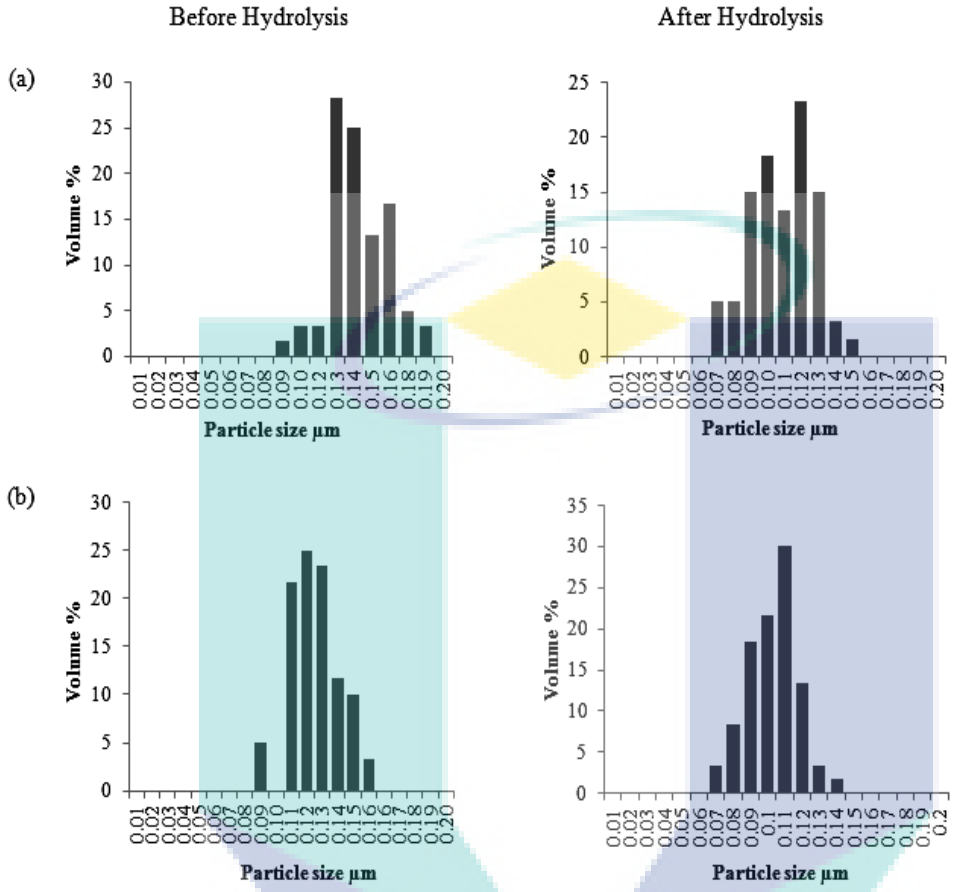

Figure 4.8: Particle size distribution of MIP copolymer prepared at different temperature (a) MIP 5 (80 ^{o}C), (b) MIP 12 (45 ^{o}C). Other factors are kept constant at 100 rpm agitation speed, 80% solvent to crosslinker ratio and 3% initiator.

4.2.4 DEGREE OF HYDROLYSIS – TEMPLATE REMOVAL

In order to produce BPA-MIP particle, the MIP copolymers were hydrolyzed in 1M NaOH at 200 rpm, 50 ^{o}C to remove the BPA molecule from copolymer. This will leave behind cages or cavities that had a specific affinity to the BPA molecule. The progress of template removal was monitored by UV-Visible spectroscopy until the BPA concentrations in the hydrolysis solution become constant. The percentage of BPA template removed calculated by monitoring weight loss after hydrolysis using Eq. (3.1) is in the range of 2 to 14%, which is comparable to the range achieved by Son et al. (2011) which was around 8 to 10% removal.

Figure 4.9 illustrated the comparison of ~~BPA removal~~weight loss between MIP synthesized at different temperature value. Two MIPs produced at 80 ^{o}C namely, MIP 12 and MIP 14 showed high percentage ~~removal of BPA~~ from 10 to 14 %, while another two MIPs at 45 ^{o}C namely, MIP 5 and MIP 4 showed low ~~BPA removal~~ percentage from 2 to 5 % approximately.

As discussed previously, temperature has the highest effect on particle size of BPA-MIPs. The use of high temperature generate bigger particle sizes and may disrupt the complex formation of MIPs in terms of its chemical structure stability and polymer rigidity. Although in the earlier subchapter (4.2.3), the effect of temperature did not produced apparent differences in terms of particle size distribution, the ~~percentage of~~ template removal ~~during hydrolysis~~ was affected by temperature during MIP synthesis.

Particle sizes for both MIP 12 and MIP 5 produced at 100 rpm had almost same size, about 120 nm and 130 nm respectively. MIP 12 was produced at 45 ^{o}C and MIP 5 at 80 ^{o}C. The percentage of ~~template removal~~weight loss during hydrolysis between these two MIP differed about 10~~2~~%. High temperature used during synthesis can affect the tightness of polymer structure. High tightness leads to difficulty in breaking the hydrogen bonds and releasing the template molecule to form the imprinted cavity in the copolymers (Koohpaei et al., 2008). In addition, high temperature could interrupt the robustness of chemical bondings during copolymerization. This could caused defect in the MIP structure and as a result, obtaining low degree of hydrolysis. It is important to

control the heat in the range of 45 - 80 °C during the synthesis of BPA-MIP copolymerization process.

Similar effect of temperature can be observed between MIP 14 and MIP 4, produced without agitation. MIP 14 was produced at 45 ^{o}C and MIP 4 at 80 ^{o}C. Obviously MIP 14, produced at lower temperature, show higher degree of hydrolysis compared to MIP 4.

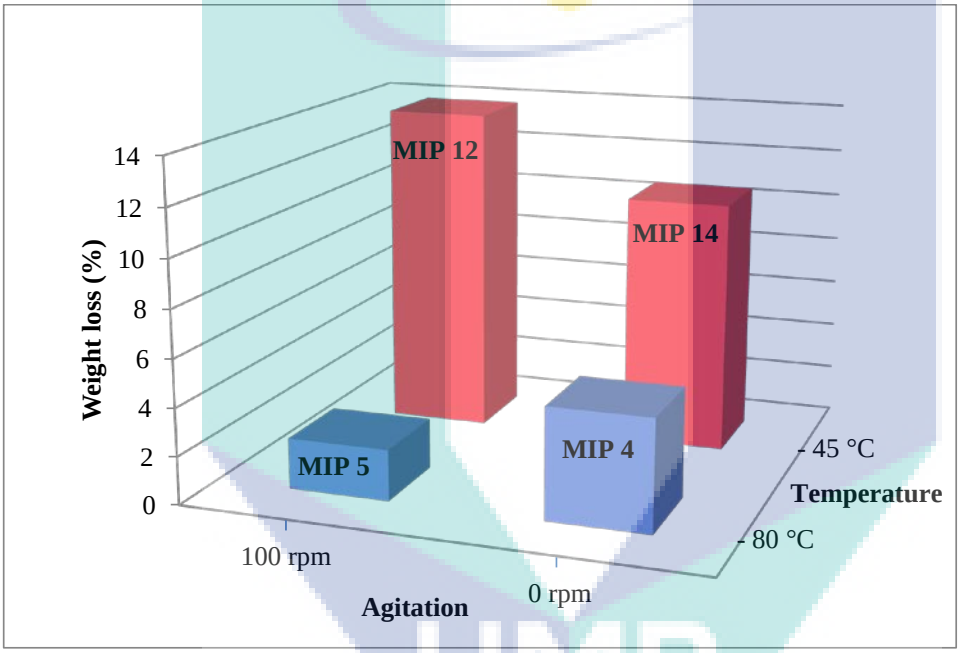

Figure 4.9: Percentage of ~~BPA template removal~~weight loss for effect of temperature at different agitation rate. Other parameters are constant at 80 % solvent to crosslinker ratio and 3 % initiator.

Formatted: Centered, Indent: Left: 0 cm, Tab stops: Not at 2.22 cm

Formatted: Indent: Left: 2.06 cm, Tab stops: Not at 2.22 cm

4.2.5 THERMAL GRAVIMETRIC ANALYSIS (TGA)

The thermal stability of two selected MIPs prepared at different temperature (MIP 12 and MIP 5) and a control non-imprinted polymer (NIP) were analyzed using

TGA at a heating rate of 5 ^{o}C/min. Figure 4.10 showed the pattern of weight loss of MIP and NIP undergone TGA analysis. Both MIPs and NIP gave almost similar degradation pattern. A small amount of 10% initial weight loss around 50 to 100 ^{o}C is due to the some moisture trapped within the particles. A drastic change of weight occurred at temperature range 280 to 430 ^{o}C mainly due to the break of the functional group exist in MIP and NIP. MIP is more stable to NIP based on the degradation temperature at approximately 300 ^{o}C for MIPs and 280 ^{o}C for NIP.

In addition, the total mass loss of MIP was approximately 75 to 80% compare to the NIP with the total mass loss of almost 85%. According to the weight loss obtained from TGA analysis, the amount of template that successfully imprinted in MIP particle was estimated at 5 to 10% of the total mass for BPA-MIP. Moreover, the results proved that presence of the template in the polymerization mixture affects the formation of the imprinting cavities resulting in higher mechanical strength and thermal resistance of the MIP in comparison with the NIP. Similar results were also reported by Wang et al. (2011) and Baghel et al. (2007).

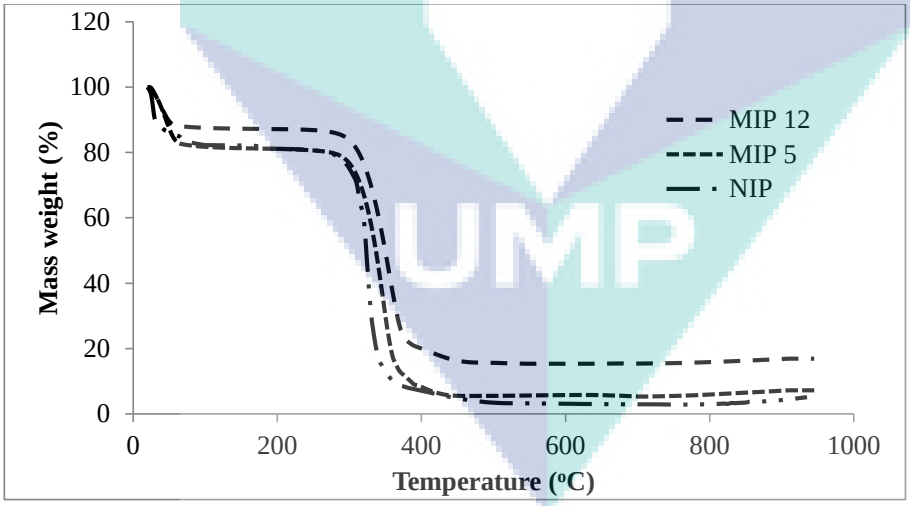

Figure 4.10: TGA plots of MIPs at different temperature; MIP 12 (45 ^{o}C), MIP 5 (80 ^{o}C); and NIP. Other factors are kept constant at 100 rpm agitation, 80% solvent to crosslinker ratio and 3% initiator.

4.2.6 SURFACE AREA ANALYSIS

Nitrogen adsorption/desorption analysis was used to measure the pore properties of MIP and NIP. Brunnauer-Emmet-Teller (BET) multi-point adsorption isotherm was applied to determine specific surface area and Barret-Jayner-Halenda (BJH) method applied for the estimation of pore diameter of the particle. Table 4.8 summarized the pore properties of MIP 12 and NIP. MIP 12 was selected for this comparison due to its characterization tests that stands out than other MIPs. The specific surface area of MIP 12 is around 202.75 m^2g^{-1} which is quite comparable to the published value from the literature in the range of 100 to 400 m^2g^{-1} (Casto-Lopez et al., 2012; Gomez-Pineda et al., 2011). The total pore volume and average pore diameter of MIP 12 were 0.41 cm^3g^{-1} and 1.56 nm, which exceed 13.2 and 0.4 times more than NIP, respectively.

Table 4.8: Value of BET and BJH analysis for MIP 12 and NIP

	MIP 12	NIP
BET surface area (m^2g^{-1})	202.75	132.40
BJH pore volume (cm^3g^{-1})	0.41	0.03
Average pore diameter (nm)	1.56	2.49

Formatted Table

The histogram of pore size distribution of MIP 12 and NIP was shown in Figure 4.11. Result reveals that the pore dimensions predominantly cluster in the range of 1.33 to 1.78 nm. The results also prove that the pore size was well distributed since the predominant range was above 50%. Therefore, it can be concluded that after imprinting process, the BPA-MIP was featured with greater specific surface area, pore volume, and pore size. Moreover, these findings were more desirable when compared with past research by Wei et al. (2006), where the surface area obtained from synthesized 17β-estradiol nano-spheres was rather low, around 10 m^2g^{-1}, and pore radius was over 20 nm. It can be summarized that the BPA-MIP in nano-size particle synthesized in this study contain homogenous pore radius leading to a higher surface area which was believed would enhance the binding ability of the MIP.

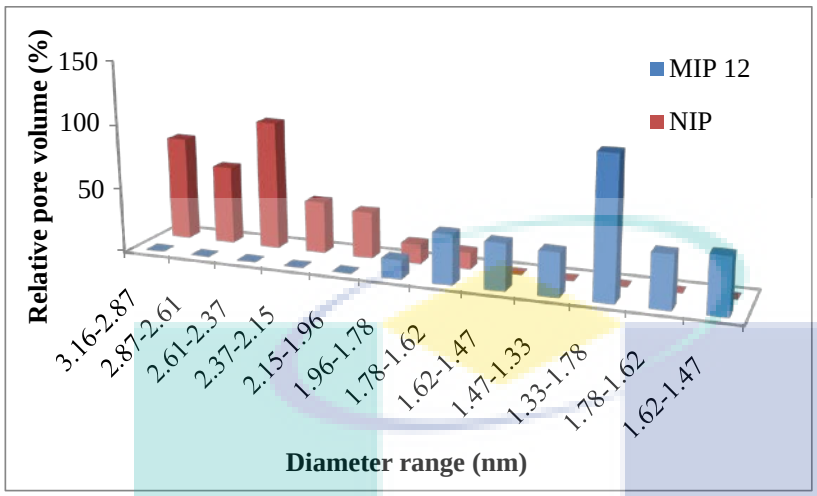

Figure 4.11: Histogram plot of pore volume distribution of MIP 12 and NIP

4.3 BINDING PERFORMANCE OF BPA-MIP

Figure 4.12 shows the BPA binding capacity for BPA-MIP particle prepared throughout this study. The highest BPA binding capacity was showed by MIP 15 with the value of 102.26 µmol g^{-1}. Majority of MIP had BPA binding capacity in the range of 83 to 99 µmol g^{-1}. However, there are three MIPs which are MIP 3, MIP 8 and MIP 13 that can not be retrieved after copolymerization due to its very low yield and extremely small nano-size. Due to this, the binding performance experiment could not be performed to these MIPs.

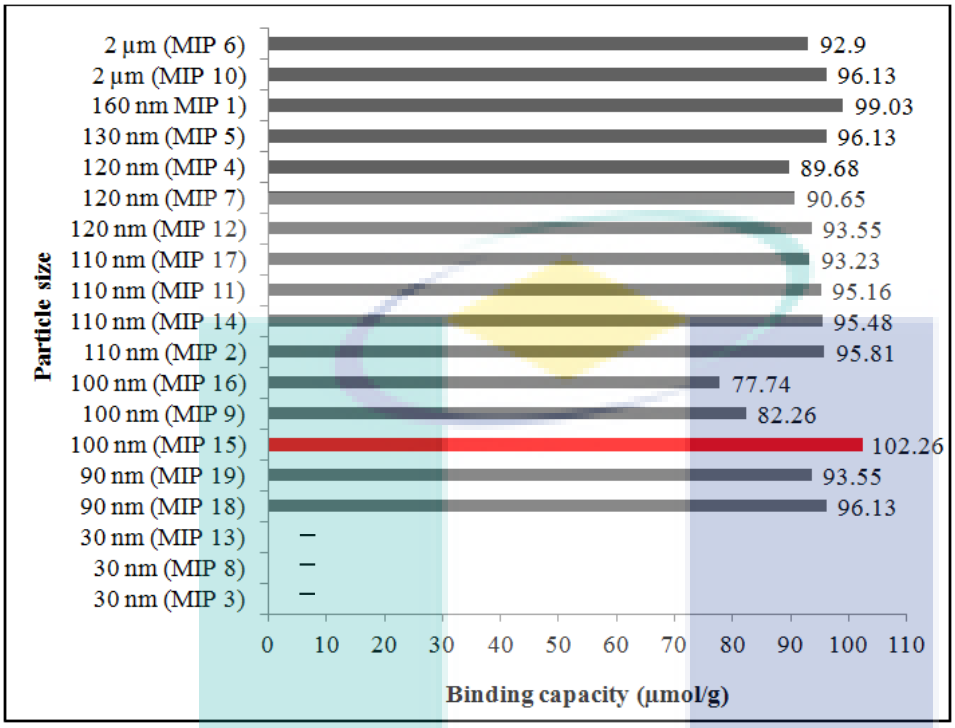

Figure 4.12: Binding capacity of BPA MIPs prepared at different conditions arranged according to their particle size from low to high

It is clearly presented that particle size from 90 nm to 2 µm, despite the huge size gap, had almost the same binding amount. The claim that smaller particle size of MIP would enhance a better binding performance was not applicable for this study. Regardless, all the binding amounts obtained were sufficiently high compared to other studies as shown in Table 4.9.

UMP

Table 4.9: Comparison on MIP binding amount results of current study and past research

Formatted: Indent: Left: 2.22 cm

Formatted Table

Author	Template	Size of particles	Binding capacity, µmol/g
This research	Bisphenol A (BPA)	90 nm - 2 µm	77.74 - 102.26
Ren et al. (2012)	Bisphenol A (BPA)	450nm	30.26
Takeda and Kobayashi (2005)	Bisphenol A (BPA)	Micropolymers	16.0
Son and Takaomi (2011)	Bisphenol A (BPA)	200 - 400 nm	78.0
Navarro-Villoslada et al. (20043)	Bisphenol A (BPA)	50-100 µm	0.09-1.6
Wang et al. (2006)	2,4-dichlorophenoxyacetic acid (2,4-D)	20 µm	24.93
Byun et al. (2010)	Aspirin	212 µm	53.0

Most of the MIPs synthesized in this study had particle sizes in the range from 100 to 150 nm. MIP particles below than 30 nm were resulted from insufficient reaction mechanism and MIP particles more than 2 µm resulted from rapid copolymerization which may lead to agglomeration of particles. Therefore, the range of particle size of BPA-MIPs nanoparticles produced in this study was reasonable and valid. Within the range of particle size achieved in this study, it can be said that the binding capacity of BPA-MIPs is not dependent on its particle sizes.

From here, the selected MIP having an optimum value is MIP 15 for obtaining the highest binding capacity, 102.26 $\mu molg^{-1}$ and particle size of 100 nm. It was synthesized at 45 ^{o}C, no agitation, 50 % of solvent to crosslinker ratio and 1% of initiator. Further work is to embed them in membrane scaffold for ease of use without tearing the membrane structure and could also increase membrane's separation efficiency.

UMP

4.4 VALIDATION TEST

To validate the model achieve in this study, BPA-MIP particle was prepared according to the prediction value generated by experimental design as shown in Figure 4.13. This value was obtained by first selecting the desired value of parameters (A, B, C, D) in the design, and then the value of particle size and binding capacity were predicted. Based on the suggested factor value, it is predicted to produce BPA-MIP particle with particle size of 150 nm and binding capacity of 97 µmolg^{-1}. After the actual value was obtained, they were compared with the predicted to calculate error of the prediction.

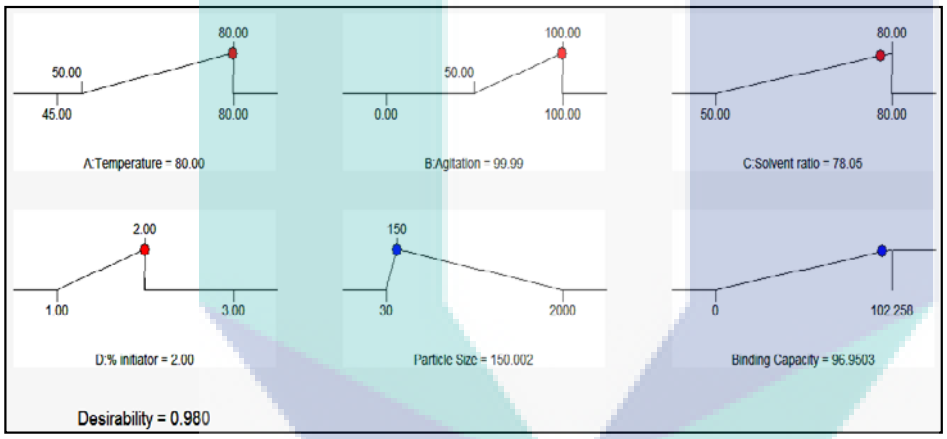

Figure 4.13: Ramp of prediction value generated by experimental design

The comparison between predicted and actual value of BPA-MIP prepared for validation test is summarized in Table 4.10. The predicted value had less than 10 % error which indicates that the model developed in this study is acceptable and valid. It also indicates that there is a correspondence between the mathematical model and the experiment (Barka et al., 2011).

Formatted: Indent: First line: 1.27 cm, No bullets or numbering

UMP

Table 4.10: Comparison of actual value and predicted value according to ramp selection with their percentage error

	Actual	Predicted	% error
Particle size	160 nm	150 nm	6.2
Binding capacity	93.23 µmol/g	96.95 µmol/g	3.9

Formatted: Justified, Indent: First line: 1.27 cm

Formatted: Indent: Left: 2.7 cm

Formatted Table

4.5 HYBRID BPA-MIP MEMBRANE

BPA and most of the EDCs have a molecular weight value in the range of 150 to 550 g mol^{-1}~~of more than 200 g mol^{-1}~~. Normal ultra/nanofiltration membrane (refer Section 2.7) is rather ineffective for separation of EDCs (Nghiem et al., 2005). In the current study, hybridization of molecular imprinting polymer (HMIP) where MIP is embedded into scaffold membrane was applied. This hybrid membrane combined the principle of adsorption and filtration.

Formatted: Superscript

MIP 15 was mixed with PES or PSf polymer solution at 2 wt% and 5 wt% based on polymer solution weight. Blank membrane without BPA-MIP was also prepared to compare the BPA uptake efficiency. SEM images are shown in Figure 4.14 and Figure 4.15 and ~~R~~results of binding capacity for each HMIP are presented in Figure 4.146~~ and their SEM images are shown in Figure 4.15 and Figure 4.16~~.

Observing SEM images in Figure 4.14 and Figure 4.15, it is clear that the MIP was in nano-size, trapped well-suited into the membrane matrix without tearing the membrane structure. Because of this, the total surface area of the membrane is much higher now since the matrix was added with high surface area BPA-MIP, therefore resulting in the increasing of BPA binding capacity.

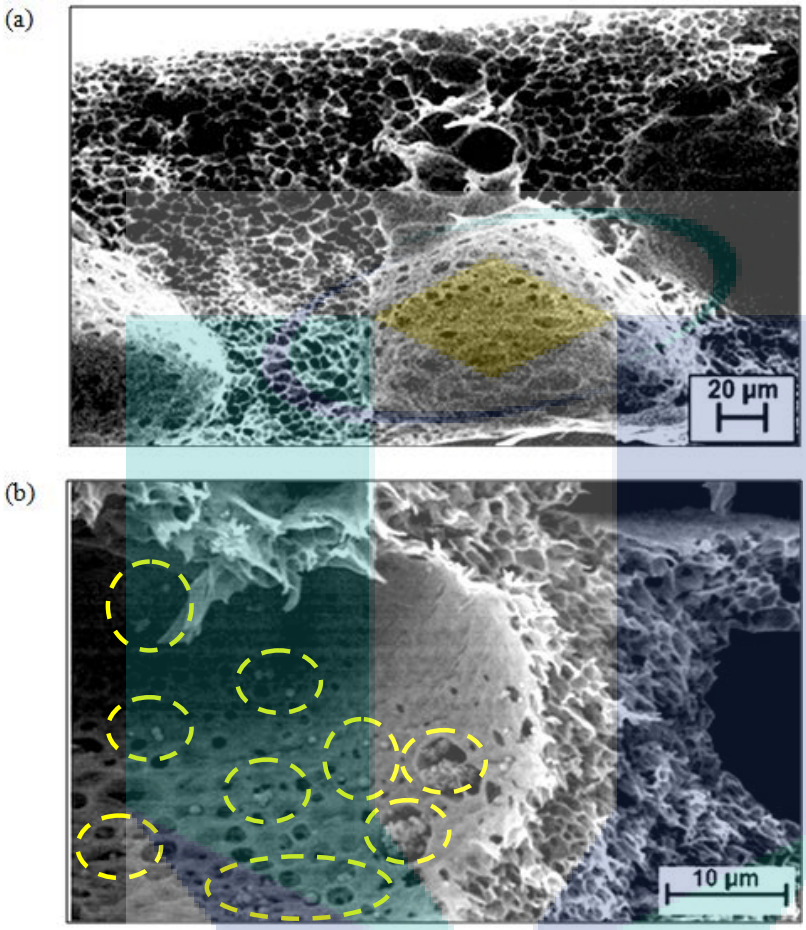

Figure 4.14: SEM cross section images of (a) PES-blank, (b) PES-HMIP membranes

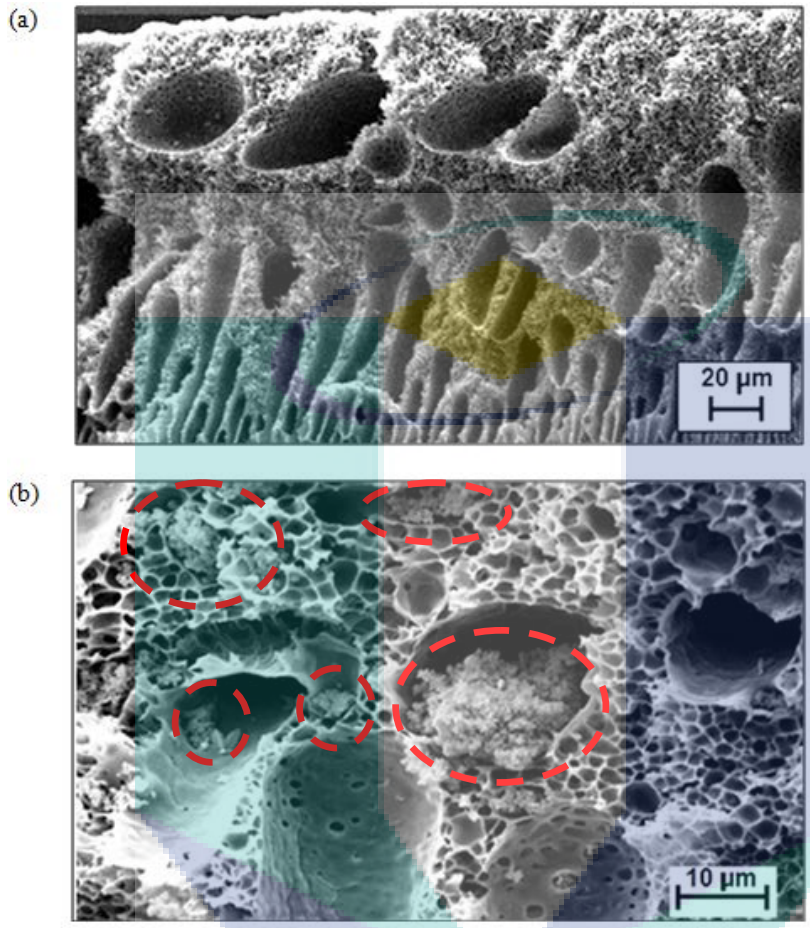

Figure 4.15: SEM cross section images of (a) PSf-blank, (b) PSf-HMIP membranes

Formatted: Justified, Indent: First line: 1.27 cm

Figure 4.16 showed that BPA was adsorbed onto the scaffold matrix of PES and PSf with the binding amount of 41.9 and 66.8 µmol g^{-1}, respectively. It is also revealed that the amount of BPA bound gradually increased with increasing amounts of loaded MIP 15 nanoparticles. When loading amount was 5 wt% in the scaffold membrane, the BPA binding amount were 166.1 and 102.3 µmol g^{-1} for PES and PSf-HMIP membrane, respectively.

Formatted: Justified, Indent: First line: 1.27 cm

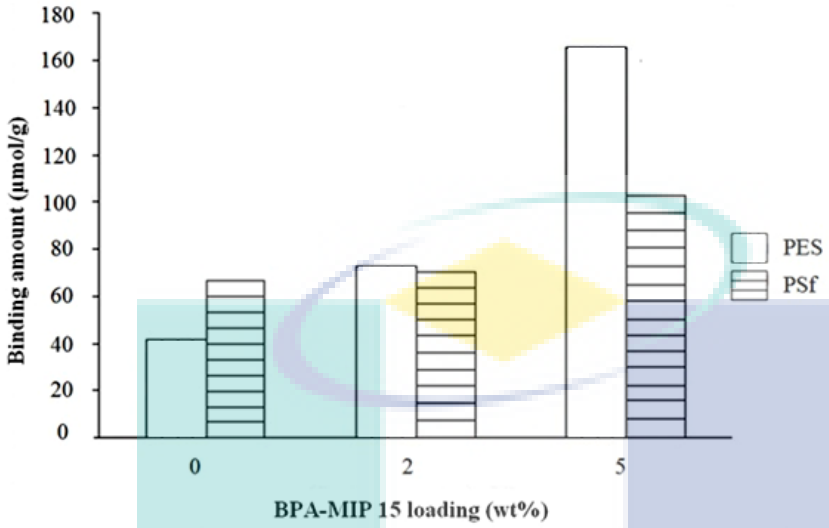

Figure 4.146: Binding amount of BPA for HMIP PES and PSf membrane at MIP 15 loading of 2 wt% and 5 wt%

~~Figure 4.14 showed that BPA was adsorbed onto the scaffold matrix of PES and PSf with the binding amount of 41.9 and 66.8 µmol g^{-1}, respectively. It is also revealed that the amount of BPA bound gradually increased with increasing amounts of loaded MIP 15 nanoparticles. When loading amount was 5 wt% in the scaffold membrane, the BPA binding amount were 166.1 and 102.3 µmol g^{-1} for PES and PSf HMIP membrane, respectively.~~

Similar result was obtained by Tasseli and co-workers in 2008 where they studied the effect of different monomers for the synthesis of flavonoid naringin MIP membrane via phase inversion technique. All prepared membranes exhibited good specific recognition properties. Blank membranes, prepared for comparison, only showed non-specific binding and the retained naringin was much lower than that of the corresponding imprinted membranes.

From graph in Figure 4.146, it can be observed that PES membrane had higher binding amount than PSf, after MIP particles were added in the solution mixture. This is maybe due to the sponge-like pore in PES (Barth et al., 2000) could trap more BPA

MIP particles than finger-pore like in PSf. ~~It can also may be due to PES having lower hydrophobicity than PSf (Ali et al., 2010) resulting in higher water flux.~~

Table 4.11 presents more comparisons between other past studies and current research. From the table, the binding capacity of BPA for PES HMIP membrane from this study is higher than PSf-MIP scaffold by Takeda et al. (2007) and Kobayashi et al. (2002). This is because of the different pore structures in the membrane. In comparison between PES membrane for this study and Son et al. (2011), the binding capacity of BPA is slightly lower. This is due to the effects of shear rate during membrane casting. As reported by Ismail and Hassan (2006), the shear rates and polymer concentrations affected membrane performance by providing to a certain extent, an oriented membrane skin structure which in turn exhibited an improvement in membrane separation ability.

Table 4.11: Comparison on HMIP binding amount results of current study and past research

Author	Template	Types of membrane	Binding capacity, µmol/g
This research	Bisphenol A (BPA)	Polyethersulfone (PES)	166.1
		Polysulfone (PSf)	102.3
Son et al. (2011)	Bisphenol A (BPA)	Polyethersulfone (PES)	173.0
Takeda et al. (2007)	Indole-4-ethanol (IE)	Polysulfone (PSf)	46.0
Kobayashi et al. (2002)	Dibenzofuran (DBF)	Polysulfone (PSf)	39.3

Ali et al. (2010) in his work on the formation of an asymmetry nanofiltration membrane to remove ammonia-nitrogen, used PES as the membrane material due to its high thermoplastic performance, hydrophilicity and good thermal stability. By changing the shear rate upon casting of membrane, the pore radius, thickness and charge density varied, which these affect the membrane performance. This shear rate factor could be applied in future studies as one of the parameters to enhance the HMIP membrane.

Noticed the low toleration for quality of HMIP membrane in this study was due to lack of investigation in terms of its mechanical strength. Here, the attempt on membrane hybridization only limit on the observation of their morphological and the possibility of increasing binding efficiency. Further investigation on the HMIP membrane is needed in order to optimize their performance and up-scaling purposes.

~~Other membrane comparisons and related works on membrane characteristics and performance are presented in Table 4.12. From the table, it is proven that PES is a good scaffold media for HMIP membrane. These studies can also be used as future references for further investigations on BPA-HMIP membrane.~~

Formatted: Justified, Indent: First line: 1.27 cm, Tab stops: 13.14 cm, Left

Formatted: Justified, Tab stops: 13.14 cm, Left

Formatted: Indent: Left: 2.22 cm

Formatted: Left, Tab stops: 1.69 cm, Centered + 3.38 cm, Right

Formatted Table

Observing SEM images in Figure 4.15 and Figure 4.16, it is clear that the MIP was in nano size, trapped well suited into the membrane matrix without tearing the membrane structure. Because of this, the total surface area of the membrane is much higher now since the matrix was added with high surface area BPA-MIP, therefore resulting in the increasing of BPA binding capacity.

Table 4.12: Membrane comparisons and other related works on membrane characteristics and performances

Author	Membrane application	Types of membrane	Remarks
Mukerjee et al., (2008)	Isolation of trypsin from goat pancreas	Polysulfone (PSf) and Polyethersulfone (PES) 30 kDA molecular weight cut off (commercial)	• Total protein recovery:; PES membrane 70% , PSf membrane 46% • Yield of trypsin:; PES membrane 74%, PSf membrane 70% • Washing and& elution : PES had higher vVolumetrix flux & pPermeated protein
Patsioura et al., (2011)	Optimization for the recovery of β-glucan from oat mill waste.	Polysulfone (PSf), Polyethersulfone (PES) and regenerated cellulose (RC) 100 kDa molecular weight cut off (commercial)	• RC had the highest retention coefficients • PES had the higher flux and permeability valuves • Both RC & PES limited for polar β-glucan lead to low flux recovery • PSf had satisfactory results on all effects.
Rahimpour and Madaeni, (2006)	Comparison of membranes for milk concentration	Polysulfone (PSf) and Polyethersulfone (PES)	• PES membrane had better water flux • PSf membrane showed high resistance in opposite to protein fouling
Barth et al., (2000)	Effects of thermodynamic conditions during membrane formation on their performance	Polysulfone (PSf) and Polyethersulfone (PES) PES 49 kDa, PSf 39 kDa molecular weight cut off (commercial)	• PES had more polarity and higher affinity to water • PES had higher water flux and greater flexibility • PES more suitable for liquid separation • PSf more suitable for gas separation and high pressure separation.

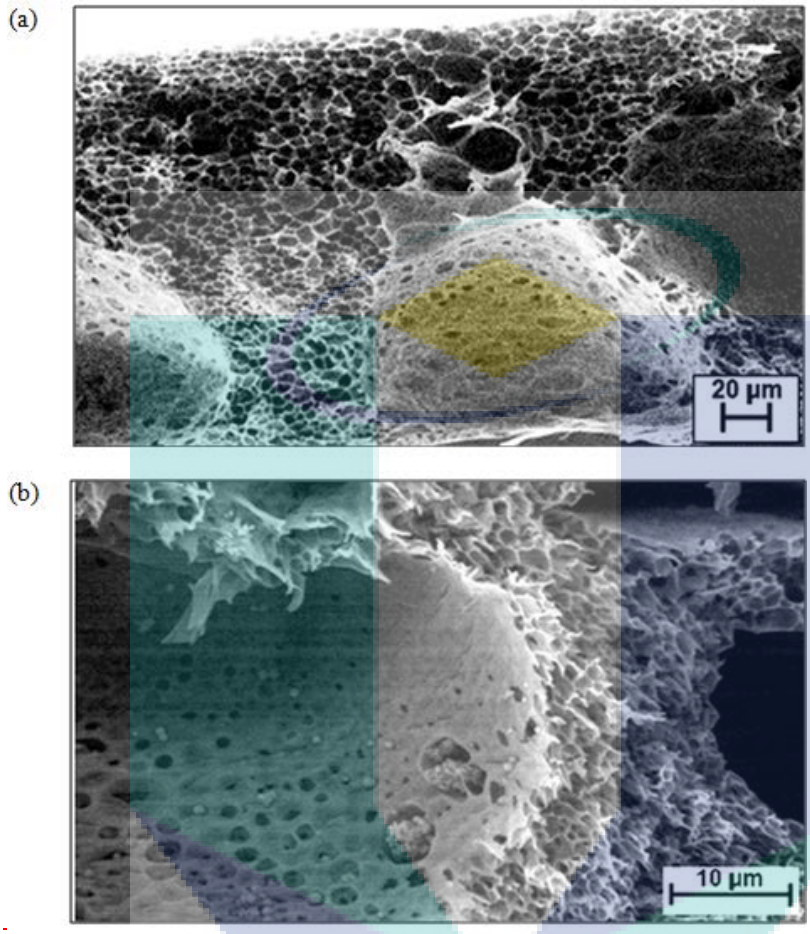

Figure 4.15: SEM cross section images of (a) PES blank, (b) PES HMIP membranes

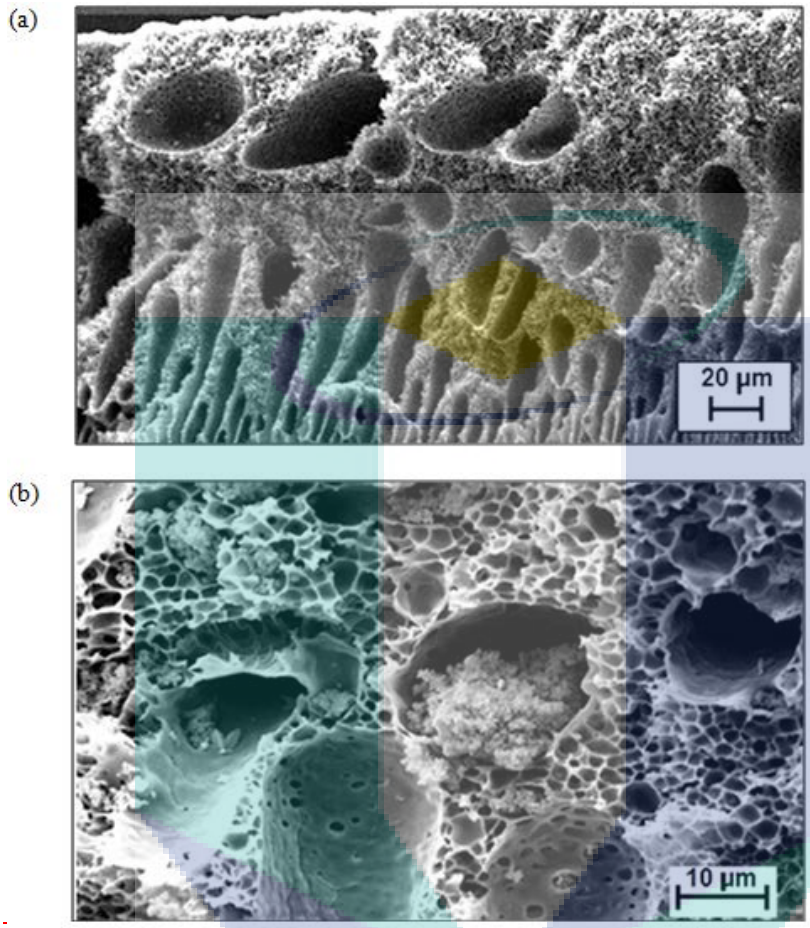

Figure 4.16: SEM cross section images of (a) PSf blank, (b) PSf HMIP membranes

From this analysis, it can be confirmed that BPA-MIP nanoparticles are successfully implanted into membrane which also had high binding amount. These results can be used for other studies in the future to better enhance the properties of membrane and its separation efficiency.

4.6 SUMMARY

The size of particles can be controlled using Design of Experiment software by determining the suitable range of factors to be studied. Particle sizes successfully obtained from this study were in the range of 90 nm to 2 µm. The factors involved in

this study were polymerization temperature, agitation rate, solvent to crosslinker ratio and percentage of initiator. It is found that polymerization temperature was the most significant factor that affects the synthesis of BPA-MIP, similar with other past researches. Two-way interaction of polymerization temperature and solvent to crosslinker ratio was also found highly significant in affecting BPA-MIP. An acceptable value for R^2 presented from ANOVA analysis is 0.9770. Adjusted R^2 and predicted R^2 values are 0.9483 and 0.9383, respectively. The characterization studies also support a good rigidity and stable thermal properties of BPA-MIP particles.

It is also discovered that most of the resultant BPA-MIP copolymers had significantly high BPA binding capacity ranging from 77.74 to 102.26 µmol/g. However, the aim that smaller MIP particle size would have higher binding capacity was not applicable for this study. It was found that, particle size of 2 µm obtained a satisfactory similar binding capacity ~~comparable~~ with the ones with 90 nm. Nevertheless, most of the BPA-MIP produced falls in the range of 100 to 150 nm particle size. The optimum condition of BPA-MIP synthesis factors selected from this study was MIP 15 due to its highest binding capacity, 102.26 µmol/g and desirable particle size of 100 nm. It was synthesized at 45 ^{o}C, no agitation, 50 % of solvent to crosslinker ratio and 1% of initiator.

An investigation was made on the hybridization of scaffold media with BPA-MIP using polyethersulfone (PES) and polysulfone (PSf) where their binding performance was examined. The result showed that PES HMIP membrane obtained higher BPA binding amount than PSf HMIP. It was probably due to their different physical properties and characteristics reckoning that PES membrane is the more suitable scaffold media for BPA-HMIP. More analysis and characterization of this scaffold media as well as comparisons with other types is necessary, should there be any further work on the study of BPA-HMIP membrane in the future.

CHAPTER 5

CONCLUSIONS AND RECOMMENDATIONS

5.1 CONCLUSIONS

Generally, both objectives in this study, which are to control molecular imprinted polymer (MIP) particle size using design of experimental (DOE) software and to synthesize MIP nanoparticle with recognition of Bisphenol A (BPA), were achieved. The BPA-MIP particle size can be controlled using DOE by screening the effect of factors involved. Besides, the software could also assist the author to find the optimum range of factors value involved to synthesize MIPs nanoparticles with high binding performance of BPA.

5.1.1 Control of MIP particle size using DOE Software

This study had demonstrated the application of 2-level full factorial experimental design in order to control particle size of BPA-MIP molecular imprinted particles in the range of 30 nm to 2 µm. The effect of polymerization temperature, agitation rate, solvent to crosslinker ratio and amount of initiator were investigated on the size of BPA-MIP particles. Sixteen sets of BPA-MIP particle with three center point replications were produced according to factor combination set by Design Expert Software. Almost all obtained particle sizes were in the range of 90 to 160 nm, but the smallest size obtained were MIP 3, MIP 8 and MIP 13, which is 30nm, and the largest size is obtained by MIP 6 and MIP 10 with the size of 2 µm.

The effect of temperature has the highest contribution in the control of BPA-MIP particle size. Effect of other parameters following temperature is amount of solvent, agitation rate and the least is amount of initiator. Two-way interaction of polymerization temperature and solvent to crosslinker ratio was also found highly significant in affecting BPA-MIP. An acceptable value for R^2 presented from ANOVA analysis is 0.9770. Adjusted R^2 and predicted R^2 values are 0.9483 and 0.9383, respectively. A model has been derived as in Equation 4.1:

$$Particle\ size = 297.89 + 255.63A - 9.38B - 231.88C + 5.63D + 18.13AB - 241.88AC + 238.12BD + 230.62ABD - 226.88BCD - 239.37ABCD \quad (4.1)$$

where A is for temperature, B is agitation, C is solvent to crosslinker ratio, D is percentage of initiator and *AB*, *AC*, *BD*, *ABD*, *BCD* and *ABCD* are the interactions involved in the process.

The role of temperature in BPA-MIP synthesis is as the drive force for copolymerization to occur. Lower temperature was enough to initiate the process and at the same time stabilizing the complex reaction. High temperature often disrupted the reaction and gave unsatisfactory result, where bigger particle sizes were obtained (Mijangos et al., 2006; Lu et al., 2004).

5.1.2 Nanoparticles BPA-MIP with Bisphenol A Recognition

Highest BPA binding of 102.26 µmol/g was obtained by MIP 15 with size 100 nm, which synthesized at 45 °C, no agitation, 50 % of solvent to crosslinker ratio and 1 % of initiator. Meanwhile, the lowest BPA binding of 77.74 µmol/g was achieved from MIP 16 with the same size, which produced at 80 °C, no agitation, 50 % of solvent to crosslinker ratio and 3 % of initiator.

From this, it can be concluded that the smaller the size of imprinted polymer, does not necessarily improved its binding ability. Although no significant improvement of binding were showed by reducing the particle size achieved within this study, small

particle size is necessary especially when producing hybrid BPA-MIP membrane, where it enhance the encapsulation of BPA-MIP particles within the membrane matrix.

5.1.3 Hybrid BPA-MIP nanoparticles membrane and its performance

BPA-MIP particles were successfully embedded in polyetehrsulfone (PES) and polysulfone (PSf) polymer matrix in the preparation of the hybrid MIP membrane (HMIP). The extension of this study, to embed the resultant BPA-MIP into a scaffold polymer was also a success where a robust structure of membrane cross-section was observed through SEM images. This is because obtained nanoparticle size MIP is small and can fit ideally inside the pores of scaffold polymers without tearing the membrane structure. Both hybrid MIP membranes showed increasing binding amount of BPA, but PES had the higher BPA binding than PSf with almost 40 % difference. This is due to the sponge-like pore in PES (Barth et al., 2000) trapped more BPA-MIP particles than finger-like pore in PSf. It could also may be due to PES having lower hydrophobicity than PSf (Ali et al., 2010) lead to a higher water flux.

In overall, experimental design approach used in this study could overcome tedious procedure involves in controlling the size of BPA-MIP within the nano size. Nano size BPA-MIP is required to produce high performance hybrid MIP membrane that can be easily handle and operate. Although this study is concern on producing BPA-MIP particle, but it can be further extend to any other templates for different applications.

5.2 RECOMMENDATIONS AND FUTURE DEVELOPMENTS

In this study, only four main factors were screened in the experimental design to observe their effects on particles size and BPA binding performance. Other factors can be further investigated such as type of solvent, polymerization initiations, type of crosslinkers, amount of functional monomers and others.

The binding experiment done in this study is only limited on the pure BPA solution. To prove the selectivity of BPA-MIP particle, binding experiment using

various derivatives of BPA molecules can be carried out. Furthermore, not only pure BPA solution is used, but also real sample or different sources of BPA contaminant should be tested such as from industrial wastewater, drain water and even tap water.

Only limited study is done on hybrid MIP membrane during this study. There are still a lot of opportunity to be explored related to hybrid MIP membrane such as using different scaffold polymer and composition, study the effect of particle size on the membrane performance or producing hybrid membrane with different format like hollow fiber and spiral membrane.

Study on the mass transfer and thermodynamic modeling between the monomers, cross-linker and scaffold polymer is also important in the development of MIP particles. The information from that study is expected to give a better understanding on the mechanism and correlations involved in the preparing high performance MIP particles.

REFERENCES

Ali, N., Halim, N.S.A., Jusoh, A., and Endut, A., 2010. The formation and characterisation of an asymmetric nanofiltration membrane for ammonia–nitrogen removal: Effect of shear rate, *Bioresource Technology*, 101 : 1459–1465

Amaya, T., Saio, D., and Hirao, T. 2007. Template synthesis of polyaniline/Pd nanoparticle and its catalytic application. *Tetrahedron letters*, 48(15): 2729-2732.

Amiridou, D., and Voutsa, D. 2011. Alkylphenols and phthalates in bottled waters. *Journal of hazardous materials*, 185(1): 281-286.

Anna Patsioura, Charis M. Galanakis, Vassilis Gekas. 2011. Ultrafiltration optimization for the recovery of β-glucan from oat mill waste, *Journal of Membrane Science*, 373: 53–63.

Anyaogu, K.C., Fedorov, A.V., and Neckers, D.C. 2008. Synthesis, characterization, and antifouling potential of functionalized copper nanoparticles. *Langmuir*, 24(8): 4340-4346.

Baggiani, C., Baravalle, P., Giovannoli, C., Anfossi, L., and Giraudi, G. 2010. Molecularly imprinted polymer/cryogel composites for solid-phase extraction of bisphenol A from river water and wine. *Analytical and bioanalytical chemistry*,397(2): 815-822.

Baghel, A., M. Boopathi, Singh, B., Pandey, P., Mahato, T.H., P.K. Gutch, K. Sekhar. 2007. Synthesis and characterization of metal ion imprinted nano-porous polymer for the selective recognition of copper, *Biosensors and Bioelectronics* 22 : 3326–3334

Barka, N., M. Abdennouri, A. Boussaoud, A. Galadi, M. Baâlala, M. Bensitel, A. Sahibed-Dine, K. Nohair, and M. Sadiq. 2011. Full factorial experimental design applied to oxalic acid photocatalytic degradation in TiO_2 aqueous suspension. *Arabian Journal of Chemistry*.

Barth, C., Gonçalves, M.C., Pires, A.T.N., Roeder, J., Wolf, B.A. 2000. Asymmetric polysulfone and polyethersulfone membranes: effects of thermodynamic conditions during formation on their performance, *Journal of Membrane Science* 169 : 287–299

Beard, J. 2006. DDT and human health. *Science of the Total Environment*. 355(1): 78-89.

Beltran, A., Marcé, R.M., Cormack, P.A.G., and Borrull, F. 2009. Synthesis by precipitation polymerisation of molecularly imprinted polymer microspheres for the selective extraction of carbamazepine and oxcarbazepine from human urine. *Journal of Chromatography A*, 1216(12): 2248-2253.

Benachour, N., amd Aris, A. 2009. Toxic effects of low doses of Bisphenol-A on human placental cells. *Toxicology and applied pharmacology*, 241(3): 322-328.

Berner Scott.1999. *Recycling Activated Carbon*. Joint Service Polution Prevention Opportunity Handbook.

Bhavsar, M.D., Tiwari, S.B., and Amiji, M.M. 2006. Formulation optimization for the nanoparticles-in-microsphere hybrid oral delivery system using factorial design. *Journal of controlled release*, 110(2): 422-430.

Binelli, A., Riva, C., and Provini, A. 2007. Biomarkers in Zebra mussel for monitoring and quality assessment of Lake Maggiore (Italy). *Biomarkers*. 12(4): 349-368.

Bing-zhi, D., Hua-qiang, C., Lin, W., Sheng-ji, X., and Nai-yun, G. 2010. The removal of bisphenol A by hollow fiber microfiltration membrane. *Desalination*,250(2): 693-697.

Bingol, D., Tekin, N., Alkan, M. 2010. Brilliant Yellow dye adsorption onto sepiolite using a full factorial design, *Applied Clay Science* 50 : 315–321

Bolong, N., Ismail, A. F., Salim, M. R., and Matsuura, T. 2009. A review of the effects of emerging contaminants in wastewater and options for their removal. *Desalination*, 239(1): 229-246.

Bodzek, M., and Dudziak, M. 2006. Elimination of steroidal sex hormones by conventional water treatment and membrane processes. *Desalination*, 198(1): 24-32.

Bowen, Richard L., Mark A. Smith, Peggy L.R Harris, Zvezdana K., Ralph N. Martins, Rudolph J. Castellani, George P., and Craig S.A. 2002. Elevated luteinizing hormone expression colocalizes with neurons vulnerable to Alzheimer's disease pathology. *Journal of neuroscience research* 70(3): 514-518.

Brasil, J. L, Ricardo R. Ev, Caroline D. Milcharek, Lucas C. Martins, Flavio A. Pavan, Araci A. dos Santos Jr., Silvio L.P. Dias, Jairton Dupont, Caciano P. Zapata Noreña, Eder C. Lima. 2006. Statistical design of experiments as a tool for optimizing the batch conditions to Cr(VI) biosorption on Araucaria angustifolia wastes, *Journal of Hazardous Materials* 133(1–3): 143-153.

Brouwer, Abraham, Matthew P. Longnecker, Linda S. Birnbaum, Jim Cogliano, Paul Kostyniak, Jack Moore, Suzan Schantz, and Gerhard Winneke. 1999. Characterization of potential endocrine-related health effects at low-dose levels of exposure to PCBs. *Environmental Health Perspectives* 107(4): 639.

Broséus, R., Vincent, S., Aboulfadl, K., Daneshvar, A., Sauvé, S., Barbeau, B., and Prévost, M. 2009. Ozone oxidation of pharmaceuticals, endocrine disruptors and pesticides during drinking water treatment. *Water research*, 43(18): 4707.

Brüggemann, O., Haupt, K., Ye, L., Yilmaz, E., and Mosbach, K. 2000. New configurations and applications of molecularly imprinted polymers. *Journal of Chromatography A*, 889(1): 15-24.

Byun, H. S., Youn, Y. N., Yun, Y. H., and Yoon, S. D. 2010. Selective separation of aspirin using molecularly imprinted polymers. *Separation and Purification Technology*, 74(1): 144-153.

Cao, Yuguang, Gerhard Winneke, Michael Wilhelm, J rgen Wittsiepe, Friederike Lemm, Peter Fürst, Ulrich Ranft et al. 2008. Environmental exposure to dioxins and polychlorinated biphenyls reduce levels of gonadal hormones in newborns: results from the Duisburg cohort study. *International journal of hygiene and environmental health* 211(1-2): 30-39.

Cacho, C., Schweitz, L., Turiel, E., and Pérez-Conde, C. 2008. Molecularly imprinted capillary electrochromatography for selective determination of thiabendazole in citrus samples. *Journal of Chromatography A*, 1179(2): 216-223.

Castro López, M.d.M, M.C. Cela Pérez, María Sonia Dopico García , José Manuel López Vilarino, María Victoria González Rodríguez, Luis F. Barral Losada. 2012. Preparation, evaluation and characterization of quercetin-molecularly imprinted polymer for preconcentration and clean-up of catechins, *Analytica Chimica Acta* 721 : 68– 78.

Chinie, A. M., Stefan, A., and Georgescu, S. 2005. Synthesis by a citrate sol-gel method and characterization of Eu^{3+}-doped yttrium aluminum garnet nanocrystals. *Romanian Reports in Physics*, 57(3): 433.

Ciardelli, G., Cioni, B., Cristallini, C., Barbani, N., Silvestri, D., and Giusti, P. 2004. Acrylic polymeric nanospheres for the release and recognition of molecules of clinical interest. *Biosensors and Bioelectronics*, 20(6): 1083-1090.

Cocchi, Daniela, Giovanni Tulipano, Alessandra Colciago, Valeria Sibilia, Francesca Pagani, Daniela Viganò, Tiziana Rubino et al. 2009. Chronic treatment with polychlorinated biphenyls (PCB) during pregnancy and lactation in the rat: Part 1: Effects on somatic growth, growth hormone-axis activity and bone mass in the offspring. *Toxicology and applied pharmacology* 237(2): 127-136.

Cromwell, Howard C., Asia Johnson, Logan McKnight, Maegan Horinek, Christina Asbrock, Shannon Burt, Banafsheh Jolous-Jamshidi, and Lee A. Meserve. 2007. Effects of polychlorinated biphenyls on maternal odor conditioning in rat pups. *Physiology and behavior* 91(5): 658-666.

David, A., Fenet, H., and Gomez, E. 2009. Alkylphenols in marine environments: Distribution monitoring strategies and detection considerations. *Marine pollution bulletin*. 58(7): 953-960.

Davies, M. P., De Biasi, V., and Perrett, D. 2004. Approaches to the rational design of molecularly imprinted polymers. *Analytica chimica acta*, 504(1): 7-14.

Denderz, N., Lehotay, J., Čižmárik, J., Cibulková, Z., and Šimon, P. 2012. Thermodynamic study of molecularly imprinted polymer used as the stationary phase in high performance liquid chromatography. *Journal of Chromatography A*.

Derakhshandeh, K., Erfan, M., and Dadashzadeh, S. 2007. Encapsulation of 9-nitrocamptothecin, a novel anticancer drug, in biodegradable nanoparticles: factorial design, characterization and release kinetics. *European Journal of Pharmaceutics and Biopharmaceutics*, 66(1): 34-41.

Donato, F., Magoni, M., Bergonzi, R., Scarcella, C., Indelicato, A., Carasi, S., and Apostoli, P. 2006. Exposure to polychlorinated biphenyls in residents near a chemical factory in Italy: the food chain as main source of contamination.*Chemosphere*, 64(9): 1562-1572.

Edginton, A. N., and Ritter, L. 2009. Predicting plasma concentrations of bisphenol A in children younger than 2 years of age after typical feeding schedules, using a physiologically based toxicokinetic model. *Environmental health perspectives*, 117(4): 645.

Faizal, C. K. M., Hoshina, Y., and Kobayashi, T. 2008. Scaffold membranes for selective adsorption of α-tocopherol by phase inversion covalently imprinting technique. *Journal of Membrane Science*. 322(2): 503-511.

Faizal, C. K. M., Kikuchi, Y., and Kobayashi, T. 2009. Molecular imprinting targeted for α-tocopherol by calix [4] resorcarenes derivative in membrane scaffold prepared by phase inversion. *Journal of Membrane Science*, 334(1): 110-116.

Ferrara, F., Ademollo, N., Orrù, M. A., Silvestroni, L., and Funari, E. 2011. Alkylphenols in adipose tissues of Italian population. *Chemosphere*, 82(7): 1044-1049.

Forrez, I., Carballa, M., Noppe, H., De Brabander, H., Boon, N., and Verstraete, W. 2009. Influence of manganese and ammonium oxidation on the removal of 17 a-ethinylestradiol (EE2). *Water Research*, 43: 77-86.

Gaido, K. W., Leonard, L. S., Lovell, S., Gould, J. C., Babaï, D., Portier, C. J., and McDonnell, D. P. 1997. Evaluation of chemicals with endocrine modulating activity in a yeast-based steroid hormone receptor gene transcription assay. *Toxicology and applied pharmacology*, 143(1): 205-212.

Gao, D., Zhang, Z., Wu, M., Xie, C., Guan, G., and Wang, D. 2007. A surface functional monomer-directing strategy for highly dense imprinting of TNT at surface of silica nanoparticles. *Journal of the American Chemical Society*,129(25): 7859-7866.

García-Mayor, R. V., Larrañaga Vidal, A., Docet Caamaño, M. F., Lafuente Giménez, A., and Ascaso, J. F. 2011. Disruptores endocrinos y obesidad: obesógenos. *Endocrinología y nutrición (papel)*, 195: 02.

Georgellis, A., and Rydström, J. 1989. Cell-specific metabolic activation of 7, 12-dimethylbenz anthracene in rat testis. *Chemico-biological interactions*, 72(1): 65-78.

Gérard, M. S., Maire, M. A. 2013. The specialist for membrane filtration – Glossary (online). www.alting.fr/en_US/glossaire.

Gohel, M. C., and Amin, A. F. 1998. Formulation optimization of controlled release diclofenac sodium microspheres using factorial design. *Journal of Controlled Release*, 51(2): 115-122.

Gómez-Pineda, L. E., Pina-Luis, G. E., Cuán, Á., García-Calzón, J. A., and Díaz-García, M. E. 2011. Physico-chemical characterization of flavonol molecularly imprinted polymers. *Reactive and Functional Polymers*, 71(4): 402-408.

Gottipati, R., Mishra, S. 2010. Process optimization of adsorption of Cr(VI) on activated carbons prepared from plant precursors by a two-level full factorial design. *Chemical Engineering Journal* 160:99–107

Granado, V.L.V., Rudnitskaya, A., Oliveira, J.A.B.P., and Gomes, M.T.S.R. 2012. Design of molecularly imprinted polymers for diphenylamine sensing.*Talanta*.

Grande Joseph. 2008. Emerging contaminants- Pharmaceuticals and Endocrine Disrupting Compounds. *Madison Water Utility*.

Grandjean, Philippe, Ciea Grønlund, Ina M. Kjær, Tina Kold Jensen, Nikolina Sørensen, Anna-Maria Andersson, Anders Juul, Niels E. Skakkebæk, Esben Budtz-Jørgensen, and Pal Weihe. 2012. Reproductive hormone profile and pubertal development in 14-year-old boys prenatally exposed to polychlorinated biphenyls. *Reproductive Toxicology*.

Grasselli, F., Baratta, L., Baioni, L., Bussolati, S., Ramoni, R., Grolli, S., and Basini, G. 2010. Bisphenol A disrupts granulosa cell function. *Domestic animal endocrinology*, 39(1): 34-39.

Gundersen, J.L. 2001. Separation of isomers of nonylphenol and select nonylphenol polyethoxylates by high-performance liquid chromatography on a graphitic carbon column. *Journal of Chromatography A*, 914(1): 161-166.

Gunnet, J. W., Lookingland, K. J., Lindley, S. E., and Moore, K. E. 1987. Effect of electrical stimulation of the arcuate nucleus on neurochemical estimates of tuberoinfundibular and tuberohypophysical dopaminergic neuronal activities. *Brain research*, 424(2): 371-378.

Gunten Urs von and Huber M.M, Gobel Anke, Adriano Joss, Hermann Nadine, Loffler Dirk, McArdell S. Christa, Ried Achim, Siegrist Hansruedi and Ternes A. Thomas. 2005. Oxidation of Pharmaceuticals during ozonation of Municipal Wastewater Effluents: A Pilot Study. *IOA 17th World Ozone Congress, Strasbourg*: 1-7

Hendorft U, Mersch-Sundermann V. Angerer. J. 2007. Phthalates:toxicology and exposure. *International Journal Hygiene Enviromental Health* 210: 623-634

Herreros, M. A., Gonzalez-Bulnes, A., Iñigo-Nuñez, S., Letelier, C., Contreras-Solis, I., Ros-Rodriguez, J. M., and Encinas, T. 2010. Pregnancy-associated changes in plasma concentration of the endocrine disruptor di (2-ethylhexyl) phthalate in a sheep model. *Theriogenology*, 73(2): 141-146.

Helmenstine. L. A., and Widjastuti, T. 2010. Volatile compounds formation in frozen carcass that dipped in butylated hydroxy toluene and sodium trypoly phosphate during eight week storage. *International Symposium Modern Animal Husbandry-Food Safety and Socio-Economic Development, Iaşi, Romania* (53): 85-88

Hoffmann, C., Zollfrank, C., and Ziegler, G. 2008. Enzyme-catalysed synthesis of calcium phosphates. *Journal of Materials Science: Materials in Medicine* 19(2): 907-915.

Huber, Marc M., Anke GÖbel, Adriano Joss, Nadine Hermann, Dirk LÖffler, Christa S. McArdell, Achim Ried, Hansruedi Siegrist, Thomas A. Ternes, and Urs von Gunten. 2005. Oxidation of pharmaceuticals during ozonation of municipal wastewater effluents: a pilot study. *Environmental science and technology* 39(11): 4290-4299.

Hunt, P. A., Susiarjo, M., Rubio, C., and Hassold, T. J. 2009. The bisphenol A experience: a primer for the analysis of environmental effects on mammalian reproduction. *Biology of reproduction*, 81(5): 807-813.

IEH. 1995. Environmental estrogens: consequences to human health and wildlife. Leicester, UK *Institute for Environment and Health* :107.

Ikegami, T., Mukawa, T., Nariai, H., and Takeuchi, T. 2004. Bisphenol A-recognition polymers prepared by covalent molecular imprinting. *Analytica chimica acta*. 504(1): 131-135.

Ikehata, K., El-Din, M. G., and Snyder, S. A. 2008. Ozonation and advanced oxidation treatment of emerging organic pollutants in water and wastewater.*Ozone: Science and Engineering*, 30(1): 21-26.

Ikezuki, Y., Tsutsumi, O., Takai, Y., Kamei, Y., and Taketani, Y. 2002. Determination of bisphenol A concentrations in human biological fluids reveals significant early prenatal exposure. *Human Reproduction*, 17(11): 2839-2841.

Ismail, A.F., Hassan, A.R., 2006. Formation and characterization of asymmetric nanofiltration membrane: Effect of shear rate and polymer concentration, *Journal of Membrane Science* 270 : 57–72

Jacobsen, Pernille Rosenskjold, Marta Axelstad, Julie Boberg, Louise Krag Isling, Sofie Christiansen, Karen Riiber Mandrup, Line Olrik Berthelsen, Anne Marie Vinggaard, and

Ulla Hass. 2012. Persistent developmental toxicity in rat offspring after low dose exposure to a mixture of endocrine disrupting pesticides. *Reproductive Toxicology*.

Jeong, S.H., Kim, B.Y., Kang, H.G., Ku, H.O., and Cho, J.H. 2005. Effects of butylated hydroxyanisole on the development and functions of reproductive system in rats. *Toxicology*, 208(1): 49-62.

Jing, T., Wang, Y., Dai, Q., Xia, H., Niu, J., Hao, Q. Hao, S. Mei and Zhou, Y. 2010. Preparation of mixed-templates molecularly imprinted polymers and investigation of the recognition ability for tetracycline antibiotics. *Biosensors and Bioelectronics*, 25(10): 2218-2224.

Jobling, S., Reynolds, T., White, R., Parker, M. G., and Sumpter, J. P. 1995. A variety of environmentally persistent chemicals, including some phthalate plasticizers, are weakly estrogenic. *Environmental health perspectives*, 103(6): 582.

Kang, H. G., Jeong, S. H., Cho, J. H., Kim, D. G., Park, J. M., and Cho, M. H. 2005. Evaluation of estrogenic and androgenic activity of butylated hydroxyanisole in immature female and castrated rats. *Toxicology*, 213(1): 147-156.

Khasawneh, M. A., Vallano, P. T., and Remcho, V. T. 2001. Affinity screening by packed capillary high performance liquid chromatography using molecular imprinted sorbents: II. Covalent imprinted polymers. *Journal of Chromatography A*, 922(1): 87-97.

Khiari Djanette. 2007. Endocrine disruptors,pharmaceuticals, and personal care products in drinking water: An overview of AwwaRF Research to date. *Awwa Research Foundation(Drinking Water Research):* 1-6

Klavarioti, M., Mantzavinos, D., and Kassinos, D. 2009. Removal of residual pharmaceuticals from aqueous systems by advanced oxidation processes. *Environment International*, 35(2): 402-417.

Kobayashi T., Reddy S. P., Ohta M., Abe M. and Fujii N. 2002. Molecularly imprinted Polysulfone membranes having acceptor sites for donor Dibenzofuran as novel membrane adsorbents: Charge transfer interaction as recognition origin. *Chemical Mater*(14): 2499-2505

Kobayashi T., Fukaya T., Abe M. and Fujii N. 2002. Phase inversion molecular imprinting by using template copolymers for high substrate recognition. *Langmuir* (18): 2866-2872

Koohpaei, A., Shahtaheri, S. J. A. D., Ganjali, M., and Forushani, A. R. 2008. Molecular imprinted solid phase extraction for determination of atrazine in environmental samples. *Iranian Journal of Environmental Health Science and Engineering*, 5(4).

Lin, Y., Shi, Y., Jiang, M., Jin, Y., Peng, Y., Lu, B., and Dai, K. 2008. Removal of phenolic estrogen pollutants from different sources of water using molecularly imprinted polymeric microspheres. *Environmental Pollution*, 153(2): 483-491.

Liu, Y., Sato, T., O'Rourke, B., and Marban, E. 1998. Mitochondrial ATP-dependent potassium channels: novel effectors of cardioprotection. *Circulation*,97(24): 2463-2469.

Liu, Jia Daniel, Hung-Jue Sue, Zachary J. Thompson, Frank S. Bates, Marv Dettloff, George Jacob, Nikhil Verghese, and Ha Pham. 2009. Strain rate effect on toughening of nano-sized PEP–PEO block copolymer modified epoxy. *Acta Materialia* 57(9): 2691-2701.

Liu, Jia Daniel, Hung-Jue Sue, Zachary J. Thompson, Frank S. Bates, Marv Dettloff, George Jacob, Nikhil Verghese, and Ha Pham. 2009. Effect of crosslink density on fracture behavior of model epoxies containing block copolymer nanoparticles. *Polymer* 50(19): 4683-4689.

Liu, Y., Yue, Z., and Gao, J. 2010. Synthesis, characterization, and thermally activated polymerization behavior of bisphenol-S/aniline based benzoxazine. *Polymer*, 51(16): 3722-3729.

Liu, M., Yu, S., Qi, M., Pan, Q., and Gao, C. 2010. Impact of manufacture technique on seawater desalination performance of thin-film composite polyamide-urethane reverse osmosis membranes and their spiral wound elements. *Journal of Membrane Science*, 348(1): 268-276.

López, C. M. D. M., Pérez, C., Dopico García, M. S., López Vilariño, J. M., González Rodríguez, M. V., and Barral Losada, L. F. 2012. Preparation, evaluation and characterization of quercetin-molecularly imprinted polymer for preconcentration and clean-up of catechins. *Analytica chimica acta*.

Lu, Y., Chenxi Li, Xudong Wang, Pingchuan Sun, Xianghua Xing. 2004. Influence of polymerization temperature on the molecular recognition of imprinted polymers. *Journal of Chromatography B* 804(1): 53-59.

Luo, X., Zhan, Y., Huang, Y., Yang, L., Tu, X., and Luo, S. 2011. Removal of water-soluble acid dyes from water environment using a novel magnetic molecularly imprinted polymer. *Journal of hazardous materials*, 187(1): 274-282.

Lyons, G. (2000). Bisphenol A: a known endocrine disruptor. *A WWF European Toxics Programme Report*, 37.

Malaisamy, R., and Ulbricht, M. 2004. Evaluation of molecularly imprinted polymer blend filtration membranes under solid phase extraction conditions. *Separation and purification technology*, 39(3): 211-219.

Manaca, Maria N., Joan O. Grimalt, Jordi Sunyer, Inacio Mandomando, Raquel Gonzalez, Jahit Sacarlal, Carlota Dobaño, Pedro L. Alonso, and Clara Menendez. 2011. Concentration of DDT compounds in breast milk from African women (Manhiça, Mozambique) at the

early stages of domestic indoor spraying with this insecticide. *Chemosphere* 85(3): 307-314.

Mijangos, I., Navarro-Villoslada, F., Antonio Guerreiro, Elena Piletska, Iva Chianella, Kal Karim, Anthony Turner, and Sergey Piletsky. 2006. Influence of initiator and different polymerisation conditions on performance of molecularly imprinted polymers. *Biosensors and Bioelectronics* 22(3): 381-387.

Miodovnik, Amir, Stephanie M. Engel, Chenbo Zhu, Xiaoyun Ye, Latha V. Soorya, Manori J. Silva, Antonia M. Calafat, and Mary S. Wolff. 2011. Endocrine disruptors and childhood social impairment. *Neurotoxicology* 32(2): 261-267.

Mielke, H., and Gundert-Remy,U. 2009. Bisphenol A levels in blood depend on age and exposure. *Toxicology letters*, 190(1): 32-40.

Mosbach, K. 1994. Molecular imprinting. *Trends in biochemical sciences*,19(1): 9-14.

Mukherjee S., Roy D., Bhattacharya P. 2008. Comparative performance study of polyethersulfone and polysulfone membranes for trypsin isolation from goat pancreas using affinity ultrafiltration. *Separation and Purification Technology*, 60: 345–351.

Murray, K. E., Thomas, S. M., and Bodour, A. A. 2010. Prioritizing research for trace pollutants and emerging contaminants in the freshwater environment. *Environmental pollution*, 158(12): 3462-3471.

Navarro-Villoslada, F., Vicente, B. S., and Moreno-Bondi, M. C. 2004. Application of multivariate analysis to the screening of molecularly imprinted polymers for bisphenol A. *Analytica chimica acta*, 504(1): 149-162.

Nghiem, L. D., Manis, A., Soldenhoff, K., and Schäfer, A. I. 2004. Estrogenic hormone removal from wastewater using NF/RO membranes. *Journal of Membrane Science*, 242(1): 37-45.

Nghiem, L. D., Schäfer, A. I., and Elimelech, M. 2005. Pharmaceutical retention mechanisms by nanofiltration membranes. *Environmental science and technology*, 39(19): 7698-7705.

Nicholls, I. A., Andersson, H. S., Charlton, C., Henschel, H., Karlsson, B. C., Karlsson, J. G., and Wikman, S. 2009. Theoretical and computational strategies for rational molecularly imprinted polymer design. *Biosensors and Bioelectronics*, 25(3): 543-552.

NIESH and NTP. Raleigh; NC: 2001. 2007. Final Report of the Endocrine Disruptors Low Dose Peer Review Panel. http://ntp.niehs.nih.gov/index.cfm?objectid=06F5CE98-E82F-8182-7FA81C02D3690D47ml. (June 8, 2007)

Newbold, R. R., and Liehr, J. G. 2000. Induction of uterine adenocarcinoma in CD-1 mice by catechol estrogens. *Cancer research*, 60(2): 235-237.

O'Mahony, J., Molinelli, A., Nolan, K., Smyth, M. R., and Mizaikoff, B. 2006. Anatomy of a successful imprint: Analysing the recognition mechanisms of a molecularly imprinted polymer for quercetin. *Biosensors and Bioelectronics*,21(7): 1383-1392.

Palanikumar, K., Dawim, J.P., 2009. Assessment of some factors influencing tool wear on the machining of glassfibre-reinforced plastics by coated cemented carbide tools. *J. Mater. Process . Technol*. 209, 511– 519.

Piletsky, S. A., Panasyuk, T. L., Piletskaya, E. V., Nicholls, I. A., and Ulbricht, M. 1999. Receptor and transport properties of imprinted polymer membranes–a review. *Journal of membrane science*. 157(2): 263-278

Piletsky, S. A., Alcock, S., and Turner, A. P. 2001. Molecular imprinting: at the edge of the third millennium. *TRENDS in Biotechnology*. 19(1): 9-12.

Poma, A., Turner, A. P., and Piletsky, S. A. 2010. Advances in the manufacture of MIP nanoparticles. *Trends in biotechnology*, 28(12): 629-637.

Priego-Capote, F., Ye, L., Shakil, S., Shamsi, S. A., and Nilsson, S. 2008. Monoclonal behavior of molecularly imprinted polymer nanoparticles in capillary electrochromatography. *Analytical chemistry*, 80(8): 2881-2887.

Qin, Z.F., Qin, X.F., Yang, L., Li, H.T., Zhao, X.R., and Xu, X.B. 2007. Feminizing/demasculinizing effects of polychlorinated biphenyls on the secondary sexual development of Xenopus laevis. *Aquatic Toxicology*,84(3): 321-327.

Reimhult, K., Yoshimatsu, K., Risveden, K., Chen, S., Ye, L., and Krozer, A. 2008. Characterization of QCM sensor surfaces coated with molecularly imprinted nanoparticles. *Biosensors and Bioelectronics*, 23(12): 1908-1914.

Ren, Y., Ma, W., Ma, J., Wen, Q., Wang, J., and Zhao, F. 2011. Synthesis and properties of bisphenol A molecular imprinted particle for selective recognition of BPA from water. *Journal of colloid and interface science* 367 :355-361

Ross Gilbert. (2004). The public health implications of polychlorinated biphenyls (PCBs) in the environment. *Ecotoxicology and Environmental Safety*. 59: 275-291.

Safa, Y., and Bhatti, H. N. 2011. Adsorptive removal of direct textile dyes by low cost agricultural waste: Application of factorial design analysis. *Chemical Engineering Journal*, 167(1): 35-41.

Sanbe, H., and Haginaka, J. 2003. Uniformly sized molecularly imprinted polymers for bisphenol A and β-estradiol: retention and molecular recognition properties in hydro-organic mobile phases. *Journal of pharmaceutical and biomedical analysis*, 30(6): 1835-1844.

Shaw, J., and deCatanzaro, D. 2009. Estrogenicity of parabens revisited: Impact of parabens on early pregnancy and an uterotrophic assay in mice. *Reproductive toxicology*, 28(1): 26-31.

Singh, S.; Li, SSL. 2012. Bisphenol A and phthalates exhibit similar toxicogenomics and health effects. *Gene* 494: 85-91

Silvestri, D., Barbani, N., Cristallini, C., Giusti, P., and Ciardelli, G. 2006. Molecularly imprinted membranes for an improved recognition of biomolecules in aqueous medium. *Journal of membrane science*, 282(1): 284-295.

Snyder, S. A. 2008. Occurrence, treatment, and toxicological relevance of EDCs and pharmaceuticals in water. *Ozone: Science and Engineering*, 30(1): 65-69.

Son, L. T., Katagawa, K., and Kobayashi, T. 2011. Using molecularly imprinted polymeric spheres for hybrid membranes with selective adsorption of bisphenol A derivatives. *Journal of Membrane Science*, 375(1): 295-303.

Son, L. T., and Takaomi, K. 2011. Hollow-fiber membrane absorbents embedded molecularly imprinted polymeric spheres for bisphenol A target. *Journal of Membrane Science*, 384(1): 117-125.

Soto, A. M., Justicia, H., Wray, J. W., and Sonnenschein, C. 1991. p-Nonyl-phenol: an estrogenic xenobiotic released from" modified" polystyrene. *Environmental health perspectives*. 92: 167.

Spégel, P., Schweitz, L., and Nilsson, S. 2003. Selectivity toward multiple predetermined targets in nanoparticle capillary electrochromatography. *Analytical chemistry*, 75(23): 6608-6613.

Stat-ease, Inc. 2011. Minneapolis, MN, USA, Design Expert Version 8.0.6.

Suedee, R., Jantarat, C., Lindner, W., Viernstein, H., Songkro, S., and Srichana, T. 2010. Development of a pH-responsive drug delivery system for enantioselective-controlled delivery of racemic drugs. *Journal of Controlled Release*, 142(1): 122-131.

Sueyoshi, Y., Fukushima, C., and Yoshikawa, M. 2010. Molecularly imprinted nanofiber membranes from cellulose acetate aimed for chiral separation. *Journal of Membrane Science*, 357(1): 90-97.

Su-Hua, W., Bing-zhi, D., and Yu, H. 2010. Adsorption of bisphenol A by polysulphone membrane. *Desalination*, 253(1): 22-29.

Surugiu, I., Ye, L., Yilmaz, E., Dzgoev, A., Danielsson, B., Mosbach, K., and Haupt, K. 2000. An enzyme-linked molecularly imprinted sorbent assay.*Analyst*, 125(1) 13-16.

Takeda, K., and Kobayashi, T. 2005. Bisphenol A imprinted polymer adsorbents with selective recognition and binding characteristics. *Science and Technology of Advanced Materials*, 6(2): 165-171.

Takeda, K., and Kobayashi, T. 2006. Hybrid molecularly imprinted membranes for targeted bisphenol derivatives. *Journal of membrane science*, 275(1): 61-69.

Takeda, K., Uemura, K., and Kobayashi, T. 2007. Hybrid molecular imprinted membranes having selectivity and separation behavior to targeted indole derivatives. *Analytica chimica acta*, 591(1): 40-48.

Tan, C. J., and Tong, Y. W. 2007. Molecularly imprinted beads by surface imprinting. *Analytical and bioanalytical chemistry*, 389(2): 369-376.

Tan, F., Zhao, H., Li, X., Quan, X., Chen, J., Xiang, X., and Zhang, X. 2009. Preparation and evaluation of molecularly imprinted solid-phase microextraction fibers for selective extraction of bisphenol A in complex samples. *Journal of Chromatography A*, 1216(30): 5647-5654.

Tasselli, F., Donato, L., and Drioli, E. 2008. Evaluation of molecularly imprinted membranes based on different acrylic copolymers. *Journal of Membrane Science*, 320(1): 167-172.

Tarley, C. R. T., and Kubota, L. T. 2005. Molecularly-imprinted solid phase extraction of catechol from aqueous effluents for its selective determination by differential pulse voltammetry. *Analytica chimica acta*, 548(1): 11-19.

Tavares, R. S., Martins, F. C., Oliveira, P. J., Ramalho-Santos, J., and Peixoto, F. P. 2009. Parabens in male infertility—Is there a mitochondrial connection? *Reproductive toxicology*, 27(1): 1-7.

Tokonami, S., Shiigi, H., and Nagaoka, T. 2009. Review: Micro-and nanosized molecularly imprinted polymers for high-throughput analytical applications. *Analytica chimica acta*, 641(1): 7-13.

Van Meeuwen, J. A., van Son, O., Piersma, A. H., de Jong, P. C., and van den Berg, M. 2008. Aromatase inhibiting and combined estrogenic effects of parabens and estrogenic effects of other additives in cosmetics. *Toxicology and applied pharmacology*, 230(3): 372-382.

Valero-Navarro, A., Medina-Castillo, A. L., Fernandez-Sanchez, J. F., and Fernández-Gutiérrez, A. 2011. Synthesis of a novel polyurethane-based-magnetic imprinted polymer for the selective optical detection of 1-naphthylamine in drinking water. *Biosensors and Bioelectronics*, 26(11): 4520-4525.

Vieno, N., Tuhkanen, T., and Kronberg, L. 2006. Removal of pharmaceuticals in drinking water treatment: effect of chemical coagulation. *Environmental technology*, 27(2): 183-192.

Vlatakis, G., Andersson, L. I., Müller, R., and Mosbach, K. 1993. Drug assay using antibody mimics made by molecular imprinting.

Vo, T. T., Yoo, Y. M., Choi, K. C., and Jeung, E. B. 2010. Potential estrogenic effect (s) of parabens at the prepubertal stage of a postnatal female rat model. *Reproductive toxicology*, 29(3): 306-316.

Völkel, W., Kiranoglu, M., and Fromme, H. 2010. Determination of free and total bisphenol A in urine of infants. *Environmental research*, 111(1): 143-148.

Wang, Yan-Rang, Ming Zhang, Qian Wang, De-Yi Yang, Chao-Lin Li, Jing Liu, Jian-Guo Li, Hao Li, and Xue-Ying Yang. 2008. Exposure of mother–child and postpartum woman–infant pairs to DDT and its metabolites in Tianjin, China. *Science of the Total Environment* 396(1): 34-41.

Wang, X. J., Xu, Z. L., Feng, J. L., Bing, N. C., and Yang, Z. G. 2008. Molecularly imprinted membranes for the recognition of lovastatin acid in aqueous medium by a template analogue imprinting strategy. *Journal of Membrane Science*, 313(1): 97-105.

Wang, J., Zhang, C., Du, Z., Xiang, A., and Li, H. 2008. Formation of porous epoxy monolith via concentrated emulsion polymerization. *Journal of colloid and interface science*. 325(2): 453-458.

Wang, X., Mao, H., Huang, W., Guan, W., Zou, X., Pan, J., Yan, Y. 2011. Preparation of magnetic imprinted polymer particles via microwave heating initiated polymerization for selective enrichment of 2-amino-4-nitrophenol from aqueous solution, *Chemical Engineering Journal* 178 :85– 92.

Wei, S., Molinelli, A., and Mizaikoff, B. 2006. Molecularly imprinted micro and nanospheres for the selective recognition of 17β-estradiol. *Biosensors and Bioelectronics*, 21(10): 1943-1951.

Wei, S., and Mizaikoff, B. 2007. Recent advances on noncovalent molecular imprints for affinity separations. *Journal of separation science*, 30(11): 1794-1805.

World Health Organization. 1999. Evaluation of national assessment of intake of butylated hydroxyanisole. *WHO Food Additives Series 42.*

Wulff, G. 1995. Molecular imprinting in cross-linked materials with the aid of molecular templates—a way towards artificial antibodies. Angewandte Chemie *International Edition in English*, 34(17): 1812-1832.

Wulff, G., and Sarhan, A. 1972. Use of polymers with enzyme-analogous structures for the resolution of racemates. *Angew. Chem. Int. Ed. Engl*, 11(4): 341-342.

Yan, H., and Row, K. H. 2006. Characteristic and synthetic approach of molecularly imprinted polymer. *International journal of molecular sciences*, 7(5): 155-178.

Yang, H. H., Zhang, S. Q., Yang, W., Chen, X. L., Zhuang, Z. X., Xu, J. G., and Wang, X. R. 2004. Molecularly imprinted sol-gel nanotubes membrane for biochemical separations. *Journal of the American Chemical Society*. 126(13): 4054-4055.

Yang, C. Y., Huang, T. S., Lin, K. C., Kuo, P., Tsai, P. C., and Guo, Y. L. 2011. Menstrual effects among women exposed to polychlorinated biphenyls and dibenzofurans. *Environmental research*, 111(2): 288.

Ye, L., and Mosbach, K. 2001. The technique of molecular imprinting–principle, state of the art, and future aspects. *Journal of Inclusion Phenomena and Macrocyclic Chemistry*, 41(1): 107-113.

Yeum, J. H., and Deng, Y. 2005. Synthesis of high molecular weight poly (methyl methacrylate) microspheres by suspension polymerization in the presence of silver nanoparticles. *Colloid and Polymer Science*, 283(11): 1172-1179.

Yoon, Y., Westerhoff, P., Snyder, S. A., and Wert, E. C. 2006. Nanofiltration and ultrafiltration of endocrine disrupting compounds, pharmaceuticals and personal care products. *Journal of Membrane Science*. 270(1): 88-100.

Yoshimi, Y., Arai, R., and Nakayama, S. 2010. Influence of the solvent on nature of gate effect in molecularly imprinted membrane. *Analytica chimica acta*, 682(1): 110-116.

Yoshimatsu, K., Reimhult, K., Krozer, A., Mosbach, K., Sode, K., and Ye, L. 2007. Uniform molecularly imprinted microspheres and nanoparticles prepared by precipitation polymerization: The control of particle size suitable for different analytical applications. *Analytica chimica acta*, 584(1): 112-121.

Yoshimatsu, K., Ye, L., Lindberg, J., and Chronakis, I. S. 2008. Selective molecular adsorption using electrospun nanofiber affinity membranes. *Biosensors and Bioelectronics*, 23(7): 1208-1215.

Zhang, Jiang-hua, Ming Jiang, Lijun Zou, Dan Shi, Su-rong Mei, Ye-xiang Zhu, Yun Shi, Kang Dai, and Bin Lu. 2006. Selective solid-phase extraction of bisphenol A using molecularly imprinted polymers and its application to biological and environmental samples. *Analytical and bioanalytical chemistry*. 385(4): 780-786.

Zhang, Q., Kusunoki, T., Xu, Q., Wang, H., and Kobayashi, T. 2007. Porous imprinted polymer membranes prepared by phase separation in compressed liquid CO_2. *Analytical and bioanalytical chemistry*, 388(3): 665-673.

Zhang, J., Srivastava, S., Duffadar, R., Davis, J. M., Rotello, V. M., and Santore, M. M. 2008. Manipulating microparticles with single surface-immobilized nanoparticles. *Langmuir*, 24(13): 6404-6408.

Zhang, N. W., Ding, M. X., Liu, G. Y., Song, W. W., and Chai, C. Y. 2008. Molecularly imprinted membrane-based sensor for the detection of chloramphenicol succinate residue in milk. *Chinese Journal of Analytical Chemistry*. 36(10): 1380-1384.

Zhang, B., Wang, Z., and Zhang, X. 2009. Synthesis and properties of a series of cyanate resins based on phenolphthalein and its derivatives. *Polymer*. 50(3): 817-824.

Zhang, Y., Gao, X., Wang, Y., Zhang, Y., and Lu, G. Q. 2009. Study on the build of channels in accurate separation membrane and its selective mechanism. *Journal of Membrane Science*. 339(1): 100-108.

Zhang, Y., Xiang, L., Zhang, Y., and Gao, X. 2009. Study on preparation of composite membrane with molecular recognizing property and its selective permeance mechanism. *Separation and Purification Technology*. 65(2): 130-136.

Zhang, Z., Zhang, Y., Tan, W., Li, G., and Hu, Y. 2010. Preparation of styrene-co-4-vinylpyridine magnetic polymer beads by microwave irradiation for analysis of trace 24-epibrassinolide in plant samples using high performance liquid chromatography. *Journal of Chromatography A*, 1217(42): 6455-6461.

Zhang, L., and Fang, M. 2010. Nanomaterials in pollution trace detection and environmental improvement. *Nano Today*. 5(2): 128-142.

Zhang, Y., Gao, X., Xiang, L., Zhang, Y., and Diniz da Costa, J. C. 2010. Study on composite membranes with high selective permeance properties. *Journal of Membrane Science*. 346(2): 318-326.

Zhang, X., Hu, Q., Sommerfeld, M., Puruhito, E., and Chen, Y. 2010. Harvesting algal biomass for biofuels using ultrafiltration membranes. *Bioresource technology*, 101(14): 5297-5304.

Zhang, M., Huang, J., Yu, P., and Chen, X. 2010. Preparation and characteristics of protein molecularly imprinted membranes on the surface of multiwalled carbon nanotubes. *Talanta*, 81(1): 162-166

Zhang, Z., An, Q., Liu, T., Zhou, Y., Qian, J., and Gao, C. 2011. Fabrication of polysulfone ultrafiltration membranes of a density gradient cross section with good anti-pressure stability and relatively high water flux. *Desalination*, 269(1), 239-248.

Zhao, C., Wei, Q., Yang, K., Liu, X., Nomizu, M., and Nishi, N. 2004. Preparation of porous polysulfone beads for selective removal of endocrine disruptors. *Separation and purification technology*. 40(3): 297-302.

Zularisam, A.W., Ismail, A.F., Salim, M.R., Mimi Sakinah, Matsuura, T. 2009. Application of coagulation–ultrafiltration hybrid process for drinking water treatment: Optimization of operating conditions using experimental design, *Separation and Purification Technology* 65 : 193–210.

APPENDIX A

LIST OF PUBLICATIONS

(a) Proceeding Papers

Shareena, M.S. and Faizal, C.K.M. 2011. The control of bisphenol a molecular imprinted polymers fabrication using factorial design analysis. *Proceedings of the International Conference on Chemical Innovation 2011*, pp. 67-72.

Shareena, M.S. and Faizal, C.K.M. 2011. Application of factorial design analysis to control bisphenol a mip fabrication. *Proceedings of the International Conference of Chemical Engineering and Industrial Biotechnology in conjunction with 25th Symposium of Malaysian Chemical Engineers 2011*, 28 Nov 2011-1 Dec 2011.

Shareena, M.S. and Faizal, C.K.M. 2012. Bisphenol A MIP fabrication using the application of factorial design analysis. *Proceedings of the International Conference on Nanotechnology 2012*, 30 May 2012-1 June 2012.

(b) Journal Papers

Shareena, M.S. and Faizal, C.K.M. 2012. Influence of Factorial Design Analysis on the Performance of Bisphenol A Molecular Imprinted Polymer. *International Journal of Chemical and Environmental Engineering 2012*, **3**(2): 135-139.

(c) Award Winning Papers

Faizal, C.K.M., Shahaidah M.S. and Shareena, M.S. Molecular imprinted membrane for selective separation. *Biomalaysia: Bioinnovation Awards 2012*. Silver Medal.

Faizal, C.K.M., Saufi, S.M. and Shareena, M.S. Molecular imprinted membrane for selective adsoption. *Creation, Innovation, Technology and Research Exposition Competition UMP, 2012*. Silver medal.

(d) Patent Papers

Faizal, C.K.M., Saufi, S.M. and Shareena, M.S. Molecular imprinted membrane for selective separation. *Malaysia patent 2012*. Submitted.

APPENDIX B

CALIBRATION CURVE

B1 Bisphenol A Standard Curve

Table B-1: Bisphenol A standard curve absorbance peak

Bisphenol A concentration (µM)	Absorbance peak
20	0.059
40	0.128
60	0.184
90	0.306
120	0.41
160	0.498
200	0.621
250	0.773
300	0.929
400	1.223
500	1.518

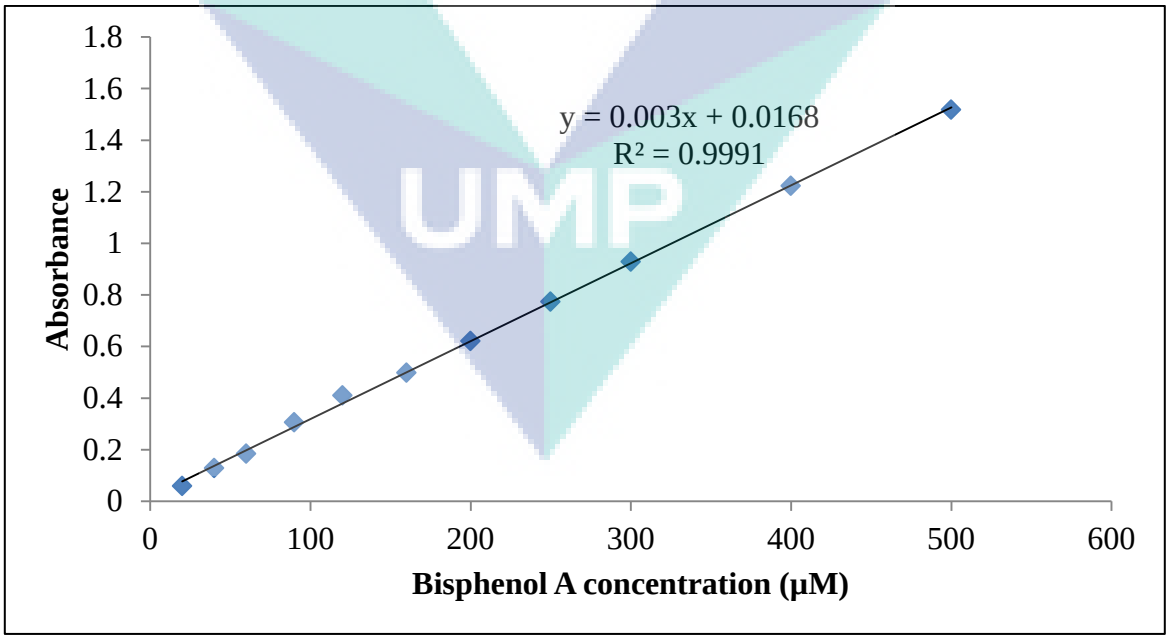

Figure B-1: Bisphenol A standard curve

APPENDIX C

EXPERIMENTAL DATA

C1 Particle Size Distribution

Table C-1: Particle size distribution for MIP 5 (80 ^{o}C) before hydrolysis.

Particle size (nm)	Volume (%)
0.01	0
0.02	0
0.03	0
0.04	0
0.05	0
0.06	0
0.07	0
0.08	0
0.09	1.7
0.10	3.3
0.12	3.3
0.13	28.3
0.14	25.0
0.15	13.3
0.16	16.7
0.18	5.0
0.19	3.3
0.20	0
0.01	0
0.02	0
Total:	100

Table C-2: Particle size distribution for MIP 5 (80 ^{o}C) after hydrolysis.

Particle size (nm)	Volume (%)
0.01	0
0.02	0
0.03	0
0.04	0
0.05	0
0.06	0
0.07	5
0.08	5
0.09	15.0
0.10	18.3
0.11	13.3
0.12	23.3
0.13	15.0
0.14	3.3
0.15	1.7
0.16	0
0.17	0
0.18	0
0.19	0
0.20	0
Total:	100

Table C-3: Particle size distribution for MIP 12 (45 ^{o}C) before hydrolysis.

Particle size (nm)	Volume (%)
0.01	0
0.02	0
0.03	0
0.04	0
0.05	0
0.06	0
0.07	0
0.08	0
0.09	5.0
0.10	0.0
0.11	21.7
0.12	25.0
0.13	23.3
0.14	11.7
0.15	10.0
0.16	3.3
0.16	0.0
0.17	0
0.18	0
0.19	0
Total:	100

Table C-4: Particle size distribution for MIP 12 (45 ^{o}C) after hydrolysis.

Particle size (nm)	Volume (%)
0.01	0
0.02	0
0.03	0
0.04	0
0.05	0
0.06	0
0.07	3.3
0.08	8.3
0.09	18.3
0.1	21.7
0.11	30.0
0.12	13.3
0.13	3.3
0.14	1.7
0.15	0
0.16	0
0.17	0
0.18	0
0.19	0
0.2	0
Total:	100

Table C-5: Degree of hydrolysis.

MIP	Template removal (%)
MIP 4	4.641811
MIP 5	2.126679
MIP12	13.8807
MIP14	10.65804

Table C-6: Data for relative volume of pore distribution MIP 12 and NIP.

Pore diameter range (nm)	MIP 12 relative volume (%)	NIP relative volume (%)
3.16-2.87	0	80.56
2.87-2.61	0	60.85
2.61-2.37	0	99.74
2.37-2.15	0	40.35
2.15-1.96	0	35.96
1.96-1.78	14.75946	15.06
1.78-1.62	38.49857	12.85
1.62-1.47	36.09233	0
1.47-1.33	33.68624	0
1.33-1.78	108.2771	0
1.78-1.62	41.14854	0
1.62-1.47	44.09199	0

Table C-7: Binding capacity of BPA MIPs prepared at different conditions arranged according to their particle size from low to high

Particle size (µm)	Binding capacity (µmol/g)
30 nm (MIP 3)	-
30 nm (MIP 8)	-
30 nm (MIP 13)	-
90 nm (MIP 18)	96.13
90 nm (MIP 19)	93.55
100 nm (MIP 15)	102.26
100 nm (MIP 9)	82.26
100 nm (MIP 16)	77.74
110 nm (MIP 2)	95.81
110 nm (MIP 14)	95.48
110 nm (MIP 11)	95.16
110 nm (MIP 17)	93.23
120 nm (MIP 12)	93.55
120 nm (MIP 7)	90.65
120 nm (MIP 4)	89.68
130 nm (MIP 5)	96.13
160 nm MIP 1)	99.03
2 µm (MIP 10)	96.13
2 µm (MIP 6)	92.9

Table C-8: Binding amount of BPA for HMIP PES and PSf membrane at MIP 15 loading of 2 wt% and 5 wt%

Materials	Binding amount (µmol/g)
BPA-MIP Powder	91.27
PSf membrane	66.8
PSf-MIP membrane	102.3
PES membrane	41.9
PES-MIP membrane	166.g1